Jordan Journal of Mechanical and Industrial Engineering (JJMIE)

JJMIE is a high-quality scientific journal devoted to fields of Mechanical and Industrial Engineering. It is published by The Hashemite University in corporation with the Jordanian Scientific Research Support Fund.

SUBMISSION ADDRESS:

Prof. **Nabil Anagreh** , Editor-in-Chief
Jordan Journal of Mechanical & Industrial Engineering,
Hashemite University,
PO Box 330127, Zarqa, 13133 , Jordan
E-mail: jjmie@hu.edu.jo

Hashemite Kingdom of Jordan

Hashemite University

Jordan Journal of Mechanical and Industrial Engineering

JJMIE

An International Peer-Reviewed Scientific Journal

Financed by Scientific Research Support Fund

http://jjmie.hu.edu.jo/

ISSN 1995-6665

Jordan Journal of Mechanical and Industrial Engineering (JJMIE)

JJMIE is a high-quality scientific journal devoted to fields of Mechanical and Industrial Engineering. It is published by The Jordanian Ministry of Higher Education and Scientific Research in corporation with the Hashemite University.

Introduction: The Editorial Board is very committed to build the Journal as one of the leading international journals in mechanical and industrial engineering sciences in the next few years. With the support of the Ministry of Higher Education and Scientific Research and Jordanian Universities, it is expected that a heavy resource to be channeled into the Journal to establish its international reputation. The Journal's reputation will be enhanced from arrangements with several organizers of international conferences in publishing selected best papers of the conference proceedings.

Aims and Scope: *Jordan Journal of Mechanical and Industrial Engineering* (JJMIE) is a refereed international journal to be of interest and use to all those concerned with research in various fields of, or closely related to, mechanical and industrial engineering disciplines. *Jordan Journal of Mechanical and Industrial Engineering* aims to provide a highly readable and valuable addition to the literature which will serve as an indispensable reference tool for years to come. The coverage of the journal includes all new theoretical and experimental findings in the fields of mechanical and industrial engineering or any closely related fields (Materials, Manufacturing, Management, Design, Thermal and Fluid, Energy, Control, Mechatronics, and Biomedical). The journal also encourages the submission of critical review articles covering advances in recent research of such fields as well as technical notes.

Guide for Authors

Manuscript Submission:
High-quality submissions to this new journal are welcome now and manuscripts may be either submitted online or email.

Online: For online and email submission upload one copy of the full paper including graphics and all figures at the online submission site, accessed via http://jjmie.hu.edu.jo. The manuscript must be written in MS Word 2010 Format. All correspondence, including notification of the Editor's decision and requests for revision, takes place by e-mail and via the Author's homepage, removing the need for a hard-copy paper trail.

Submission address and contact:
Prof. Nabil Anagreh
Editor-in-Chief
Jordan Journal of Mechanical & Industrial Engineering,
Hashemite University,
PO Box 330127, Zarqa, 13115, Jordan
E-mail: jjmie@hu.edu.jo

Types of contributions*:* Original research papers and Technical reports

Corresponding author: Clearly indicate who is responsible for correspondence at all stages of refereeing and publication, including post-publication. Ensure that telephone and fax numbers (with country and area code) are provided in addition to the e-mail address and the complete postal address. Full postal addresses must be given for all co-authors.

Original material: Submission of an article implies that the work described has not been published previously (except in the form of an abstract or as part of a published lecture or academic thesis), that it is not under consideration for publication elsewhere, that its publication is approved by all authors and that, if accepted, it will not be published elsewhere in the same form, in English or in any other language, without the written consent of the Publisher. Authors found to be deliberately contravening the submission guidelines on originality and exclusivity shall not be considered for future publication in this journal.

Withdrawing: If the author chooses to withdraw his article after it has been assessed, he shall reimburse JJMIE with the cost of reviewing the paper.

Manuscript Preparation:

General: Editors reserve the right to adjust style to certain standards of uniformity. Original manuscripts are discarded after publication unless the Publisher is asked to return original material after use. Please use MS Word 2010 for the text of your manuscript.

Structure: Follow this order when typing manuscripts: Title, Authors, Authors title, Affiliations, Abstract, Keywords, Introduction, Main text, Conclusions, Acknowledgements, Appendix, References, Figure Captions, Figures and then Tables. Please supply figures imported into the text AND also separately as original graphics files. Collate acknowledgements in a separate section at the end of the article and do not include them on the title page, as a footnote to the title or otherwise.

Text Layout: Use 1.5 line spacing and wide (3 cm) margins. Ensure that each new paragraph is clearly indicated. Present tables and figure legends on separate pages at the end of the manuscript. If possible, consult a recent issue of the journal to become familiar with layout and conventions. All footnotes (except for table and corresponding author footnotes) should be identified with superscript Arabic numbers. To conserve space, authors are requested to mark the less important parts of the paper (such as records of experimental results) for printing in smaller type. For long papers (more than 4000 words) sections which could be deleted without destroying either the sense or the continuity of the paper should be indicated as a guide for the editor. Nomenclature should conform to that most frequently used in the scientific field concerned. Number all pages consecutively; use 12 or 10 pt font size and standard fonts.

Corresponding author: Clearly indicate who is responsible for correspondence at all stages of refereeing and publication, including post-publication. The corresponding author should be identified with an asterisk and footnote. Ensure that telephone and fax numbers (with country and area code) are provided in addition to the e-mail address and the complete postal address. Full postal addresses must be given for all co-authors. Please consult a recent journal paper for style if possible.

Abstract: A self-contained abstract outlining in a single paragraph the aims, scope and conclusions of the paper must be supplied.

Keywords: Immediately after the abstract, provide a maximum of six keywords (avoid, for example, 'and', 'of'). Be sparing with abbreviations: only abbreviations firmly established in the field may be eligible.

Symbols: All Greek letters and unusual symbols should be identified by name in the margin, the first time they are used.

Units: Follow internationally accepted rules and conventions: use the international system of units (SI). If other quantities are mentioned, give their equivalent in SI.

Maths: Number consecutively any equations that have to be displayed separately from the text (if referred to explicitly in the text).

References: All publications cited in the text should be presented in a list of references following the text of the manuscript.

Text: Indicate references by number(s) in square brackets in line with the text. The actual authors can be referred to, but the reference number(s) must always be given.

List: Number the references (numbers in square brackets) in the list in the order in which they appear in the text.

Examples:

Reference to a journal publication:

[1] M.S. Mohsen, B.A. Akash, "Evaluation of domestic solar water heating system in Jordan using analytic hierarchy process". Energy Conversion & Management, Vol. 38 (1997) No. 9, 1815-1822.

Reference to a book:

[2] Strunk Jr W, White EB. The elements of style. 3rd ed. New York: Macmillan; 1979.

Reference to a conference proceeding:

[3] B. Akash, S. Odeh, S. Nijmeh, "Modeling of solar-assisted double-tube evaporator heat pump system under local climate conditions". 5th Jordanian International Mechanical Engineering Conference, Amman, Jordan, 2004.

Reference to a chapter in an edited book:

[4] Mettam GR, Adams LB. How to prepare an electronic version of your article. In: Jones BS, Smith RZ, editors. Introduction to the electronic age, New York: E-Publishing Inc; 1999, p. 281-304

Free Online Color : If, together with your accepted article, you submit usable color and black/white figures then the journal will ensure that these figures will appear in color on the journal website electronic version.

Tables: Tables should be numbered consecutively and given suitable captions and each table should begin on a new page. No vertical rules should be used. Tables should not unnecessarily duplicate results presented elsewhere in the manuscript (for example, in graphs). Footnotes to tables should be typed below the table and should be referred to by superscript lowercase letters.

Notification: Authors will be notified of the acceptance of their paper by the editor. The Publisher will also send a notification of receipt of the paper in production.

Copyright: All authors must sign the Transfer of Copyright agreement before the article can be published. This transfer agreement enables Jordan Journal of Mechanical and Industrial Engineering to protect the copyrighted material for the authors, but does not relinquish the authors' proprietary rights. The copyright transfer covers the exclusive rights to reproduce and distribute the article, including reprints, photographic reproductions, microfilm or any other reproductions of similar nature and translations.

Proof Reading: One set of page proofs in MS Word 2010 format will be sent by e-mail to the corresponding author, to be checked for typesetting/editing. The corrections should be returned within **48 hours**. No changes in, or additions to, the accepted (and subsequently edited) manuscript will be allowed at this stage. Proofreading is solely the author's responsibility. Any queries should be answered in full. Please correct factual errors only, or errors introduced by typesetting. Please note that once your paper has been proofed we publish the identical paper online as in print.

Author Benefits:

No page charges: Publication in this journal is free of charge.

Free offprints: One journal issues of which the article appears will be supplied free of charge to the corresponding author and additional offprint for each co-author. Corresponding authors will be given the choice to buy extra offprints before printing of the article.

JJMIE

Volume 9 Number 3, June.2015
ISSN 1995-6665

Jordan Journal of Mechanical and Industrial Engineering

JJMIE

Volume 9 Number 3, June.2015
ISSN 1995-6665
Pages 159 - 165

Jordan Journal of Mechanical and Industrial Engineering

Five-Axis CNC Grinding of End-Mills with Generic Revolving Profiles

Mahmoud M. Rababah *

Assistant Prof. Dept. of Mechanical Engineering, The Hashemite University, Zarqa, Jordan

Received 23 March 2015 *Accepted 13 May 2015*

Abstract

Manufacturing end-mill cutting tools of non-traditional revolving profiles have been recently increasing with the increasing demands on smooth and curvy products. Among many tool design features, rake faces are considered the most crucial as they control the cutting forces, guide the tool flutes for smooth chips evacuations, and affect tools vibrations. Thus, the need arose to build a CNC grinding approach to grind the rake faces of end-mills having a generic cutting edge model. A revolving profile of a free-form curve, Non-periodic Uniform Rational Basis Spline (NURBS), is adopted in the present work, and a generic cutting edge model is established. The model can represent the cutting edges of both end-mills with traditional and end-mills with non-traditional revolving profiles. The importance of the model is very obvious in the tools manufacturing, specifically in the rake face grinding. A computer simulation for grinding rake faces of end-mills with free-form revolving profiles using a five-axis CNC grinding approach is conducted. The end-mills are obtained with accurate cutting edges and precise normal rake angles along those edges.

Keywords: *Five-Axis CNC Grinding; End-Mill Cutting Tools; Rake Face Grinding; NURBS Curves*.

1. Introduction

The end-mill cutting tools are commonly used in milling, profiling, plunging, etc. In profiling, the revolving shape of the end-mill is imposed on the side walls of the machined workpiece. With the increasing demands on smooth and curvy products, it becomes necessary to manufacture end-mill cutting tools with free-form revolving profiles. In the present work, the free-form revolving profiles are represented with NURBS curves as they are the most generic. Beside the free-form profiles, NURBS can easily represent the straight lines and the circular arcs [1]. Hence, both traditional and non-traditional end-mills can be modeled using NURBS curves.

The end-mill cutting tools consist of many design features as the side cutting edges, the rake faces, the primary and the secondary relief surfaces, the flute surfaces, the bottom cutting edges, the cores, etc. (Figure 1). Among these features, the rake faces are considered the most crucial and they are the main concern of the present work. The rake faces are always guided by the side cutting edges. Therefore, many researchers were concerned to establish optimal mathematical models for the side cutting edges. The models can be classified into three major categories: side cutting edges with constant helical angles between their tangents and the tool axis [2-4], side cutting edges with constant helical angles between their tangents and the tool generatrix [5-12], side cutting edges with constant pitches [13, 14], and in some situations, a combination of two mathematical models [15]; a ball-end cutter having a side cutting edge with a constant helical angle to its axis will not have a mathematical description at the top of the ball. For the top of the ball, a constant pitch or a constant helical angle to the generatrix should be adopted. At the common point of the two segments of the cutting edge, the continuity and the smoothness should be maintained.

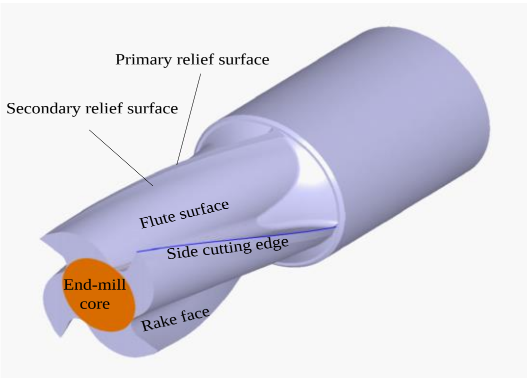

Figure 1. A simple model of an end-mill with its designed features

* Corresponding author. e-mail: : m_rababah@hu.edu.jo.

Figure 2 describes, in more details, the aforementioned definitions of the side cutting edges. For any point **P** on the side cutting edge, the helical angle is measured between the tangent vector **T** and either the tool axis **A** or the generatrix **G**. Thus, modeling cutting edges with a constant helical angle to the generatrix, or to the tool axis, leads to completely two different cutting edges. The cutting edges with a constant helical angle between their tangents and the tool generatrix are adopted in this work.

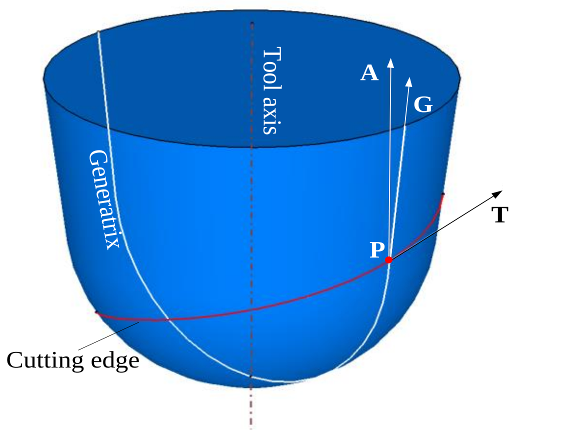

Figure 2. The helical angle definitions of the side cutting edges

Beside the aforementioned models, a mathematical model of the APT cutting edge was first introduced by Engin and Altintas [16]. Cutting edges of many cutters found in industry, such as cylindrical end-mills, fillet end-mills, ball end-mills, can be represented using this model; however, many others cannot. Hence, the present work establishes a generic cutting edge model for end-mill cutters of generic revolving profiles.

After deriving the cutting edge model, the five-axis CNC grinding approach proposed by Rababah *et al*. [17] is extended to grind the rake faces of end-mills with generic revolving profiles. As will be shown, the approach revealed rake faces with constant normal rake angles and accurate cutting edges along the rake faces.

2. The Generic Model of the Side Cutting Edge

In order to derive the cutting edge equation, the end-mill envelope is obtained. However, the revolving profile of the end-mill cutting tool is first established as a free-form curve and is expressed as:

$$\mathbf{C}(u)=\begin{bmatrix} x(u)\\ y(u)\\ z(u)\end{bmatrix}=\sum_{i=0}^{n}\mathbf{P_i}R_{i,k}(u)\,, \tag{1}$$

where

$$R_{i,k}(u)=\frac{w_i N_{i,k}(u)}{\sum_{i=0}^{n} w_i N_{i,k}(u)}\,, \tag{2}$$

and $N_{i,k}$ are the basis functions and are expressed as:

$$N_{i,k}=(u-u_i)\frac{N_{i,k-1}(u)}{u_{i+k-1}-u_i}+(u_{i+k}-u)\frac{N_{i+1,k-1}(u)}{u_{i+k}-u_{i+1}} \tag{3}$$

where

$$N_{i,1}=\begin{cases}1 & u_i\le u\le u_{i+1}\\ 0 & \text{otherwise}\end{cases} \tag{4}$$

The knot vector u can be obtained from the formula:

$$u_i=\begin{cases}0 & i<k\\ i-k+1 & k\le i\le n\\ n-k+2 & i>n\end{cases} \tag{5}$$

where k is the curve order, n+1 is the number of the control points. As the curve is free-form, its shape can be controlled using the control points $\mathbf{P_i}$ and the weighted parameters w_i.

Back to the envelope, the parametric equation is written as:

$$\mathbf{t}(u,\theta)=\begin{bmatrix} r(u)\cdot\cos\theta\\ r(u)\cdot\sin\theta\\ z(u)\end{bmatrix}, \tag{6}$$

where $r(u)=\sqrt{x^2(u)+y^2(u)}$ is the radius of the corresponding circle on the plane with coordinate $z(u)$, and u is the curve parameter (Figure 3). Based on Eq. 6, the first partial derivatives of the envelope $\mathbf{t}(u,\theta)$ in terms of z and θ are derived as:

$$\frac{\partial\mathbf{t}}{\partial z}=\begin{bmatrix} \frac{\partial r/\partial u}{\partial z/\partial u}\cdot\cos\theta\\ \frac{\partial r/\partial u}{\partial z/\partial u}\cdot\sin\theta\\ 1\end{bmatrix}, \tag{7a}$$

and

$$\frac{\partial\mathbf{t}}{\partial\theta}=\begin{bmatrix} -r(u)\cdot\sin\theta\\ r(u)\cdot\cos\theta\\ 0\end{bmatrix}. \tag{7b}$$

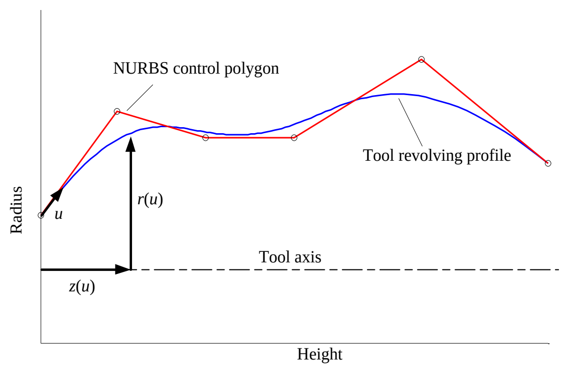

Figure 3. Illustration of the parameters of a generic end-mill revolving profile

In the present work, the differential 1-forms of the tangent vectors of the helical curve and the generatrix are denoted as $d\mathbf{t}$ and $\delta\mathbf{t}$, respectively. They can be obtained with the following equations:

$$d\mathbf{t} =: \frac{\partial \mathbf{t}}{\partial z}\cdot dz + \frac{\partial \mathbf{t}}{\partial \theta}\cdot d\theta \text{, and } \delta\mathbf{t} =: \frac{\partial \mathbf{t}}{\partial z}\cdot \delta z \ . \tag{8}$$

Thus, the relationship between the helical angle ψ and these two vectors can be formulated as:

$$\cos\psi = \frac{d\mathbf{t}\cdot\delta\mathbf{t}}{\|d\mathbf{t}\|\cdot\|\delta\mathbf{t}\|} . \tag{9}$$

By substituting Eq. 8 into Eq. 9 and simplifying, the relationship between the parameters u and θ can be formulated as:

$$d\theta = \int \tan\psi \sqrt{\frac{\left(\frac{\partial r/\partial u}{\partial z/\partial u}\right)^2 + 1}{\left(r(u)\right)^2}}\frac{dz}{du}du \ . \tag{10}$$

Hence, for any value of the curve parameter u, the cutting edge angle θ and the tool axis parameter z are obtained from Eq. 10 and Eq. 6, respectively. As both parameters are correlated, the side cutting edge can now be expressed as:

$$\mathbf{CE}(u) =: \begin{bmatrix} r(u)\cdot\cos\theta(u) \\ r(u)\cdot\sin\theta(u) \\ z(u) \end{bmatrix} . \tag{11}$$

3. Five-Axis CNC Grinding Approach

Due to the complexity of the end-mill profiles, two-axis CNC grinding approaches are unable to grind rake faces with constant normal rake angles and accurate cutting edges [18]. Thus, the approach proposed by Rababah *et al.* is adopted to accomplish the task [17]. The approach is developed on the principle that at any point on the side cutting edge, the normal vector of the rake face and the normal vector of the grinding-wheel lateral surface should be aligned. This principle leads to a complete derivation for the grinding-wheel path (locations and orientations). However, seeking brevity, the approach is not re-elaborated here. Complete details on the approach, the grinding-wheel shapes, and the grinding-wheel path derivations are discussed in literature [17-21].

4. Rake Face Grinding Simulation

Two end-mills with generic revolving profiles are considered for computer simulation. The cutting edges are first established with MATLAB, and then, imported to CATIA to perform the grinding simulation using Boolean operations. The revolving profile of end-mill I is constructed with 6 control points, as shown in Figure 4. Beside the control points' locations, their weights can also alter the shape of the revolving profile. Rotating the revolving profile about the tool axis will generate the end-mill envelope. The side cutting edge of a helical angle of 20 deg. on the end-mill envelope is represented in Figure 5.

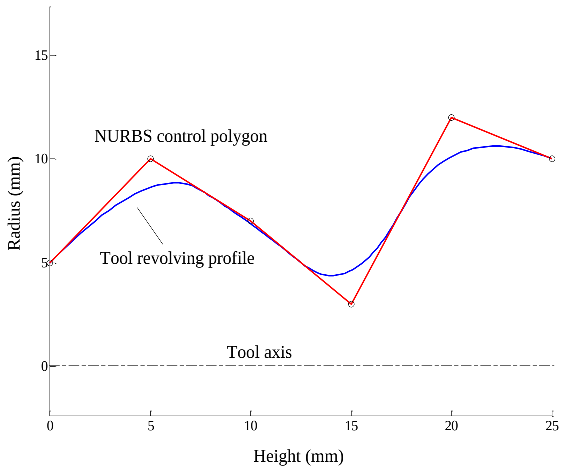

Figure 4. The revolving profile of end-mill I

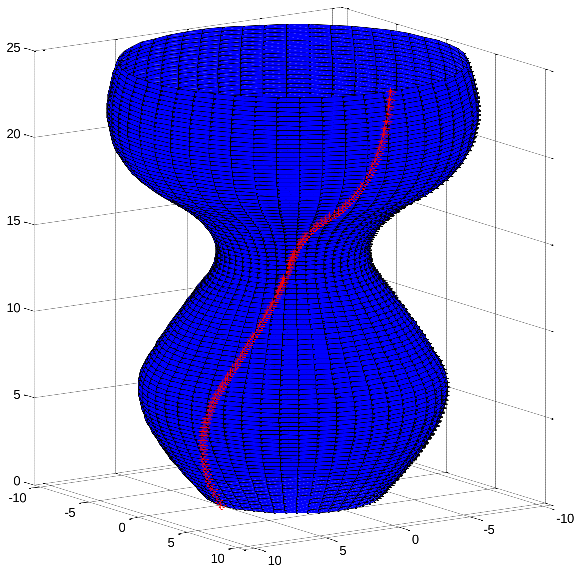

Figure 5. The side cutting edge on end-mill I envelope (mm)

The grinding simulation proved to produce rake faces with accurate side cutting edges as obviously shown in Figure 6, and a constant normal rake angle as will be discussed below.

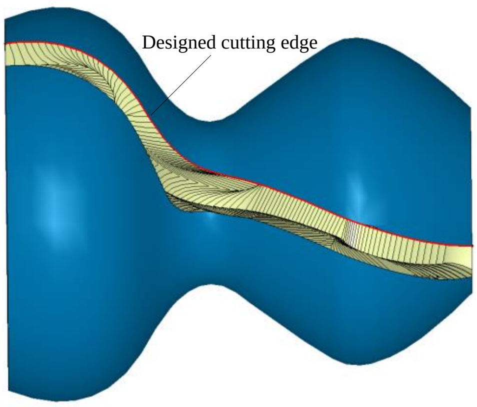

(*a*) view *a*

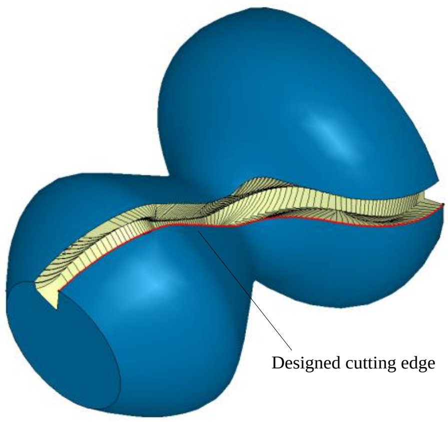

(*b*) view *b*

Figure 6. Rake face grinding of end-mill I with an accurate side cutting edge (different views)

A constant normal rake angle of 10 deg. is adopted in the simulation. Three arbitrary sections normal to the side cutting edge are considered to verify the accuracy of the machined normal rake angle (Figure 7). At any point **P** on the side cutting edge, the normal rake angle is defined as the angle between vectors **M** and **N**, as shown in Figure 8. Vectors **M** and **N** are both laying on a plane normal to the side cutting edge. Vector **M** is aligned with a line connecting point **P** and the tool axis, and vector **N** is the intersection of the rake face with the normal plane. From the Figure, the accuracy of the machined normal rake angle is obvious.

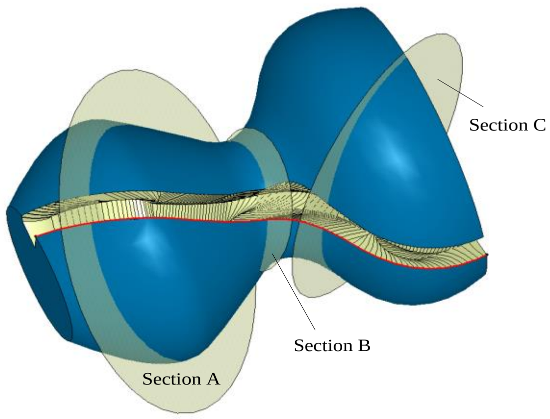

Figure 7. The arbitrary sections normal to the side cutting edge for end-mill I

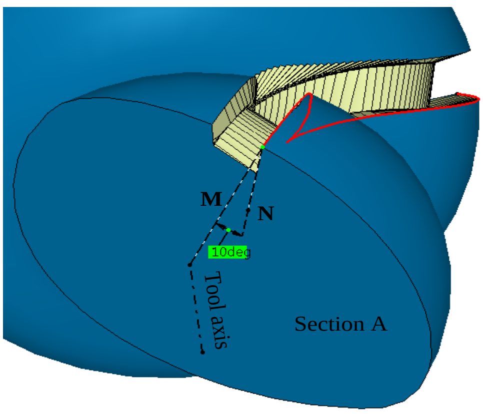

(a) The normal rake angle at section A normal to the cutting edge for end-mill I

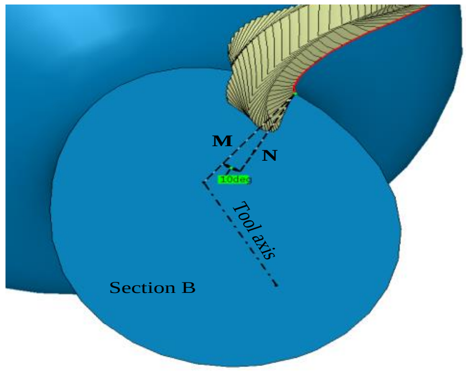

(b) The normal rake angle at section B normal to the cutting edge for end-mill I

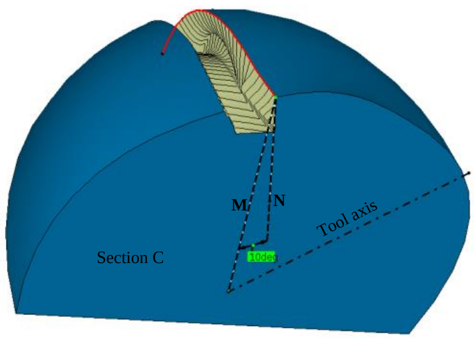

(c) The normal rake angle at section C normal to the cutting edge for end-mill I

Figure 8. The normal rake angle at three arbitrary sections normal to the side cutting edge of end-mill I

As a second grinding simulation example, the revolving profile, used to produce the envelope of end-mill II, consists of 7 control points and is demonstrated in Figure 9. The side cutting edge on the end-mill envelope is shown in Figure. 10 ($\psi = 20^{\circ}$).

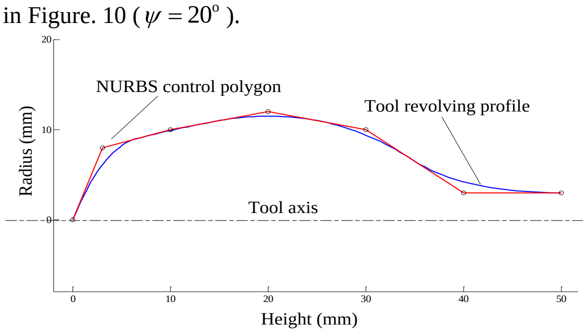

Figure 9. The revolving profile of end-mill II

The grinding simulation of end-mill II is again proved to produce rake faces with accurate side cutting edges (Figure 11), and constant normal rake angles, as shown in Figures 12 and 13.

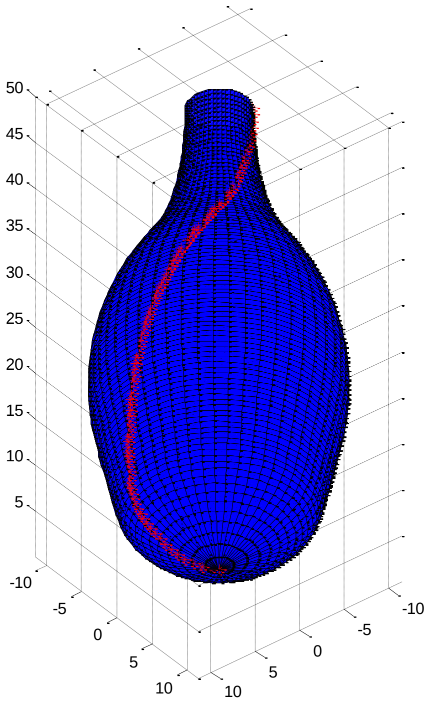

Figure 10. The side cutting edge on the end-mill II envelope (mm)

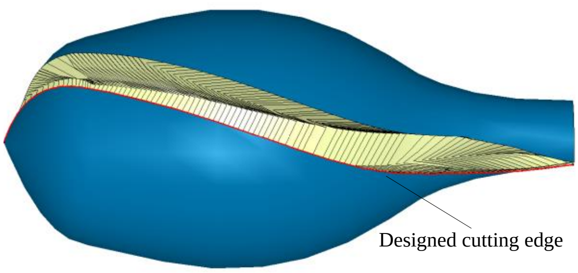

(*a*) View *a*

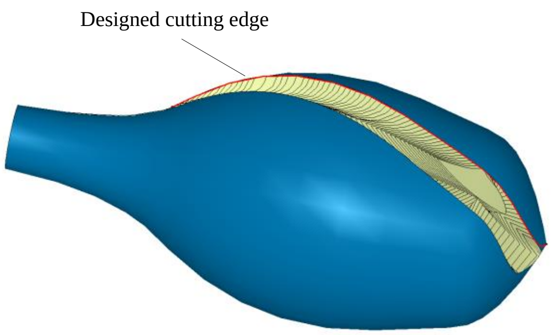

(*b*) View *b*

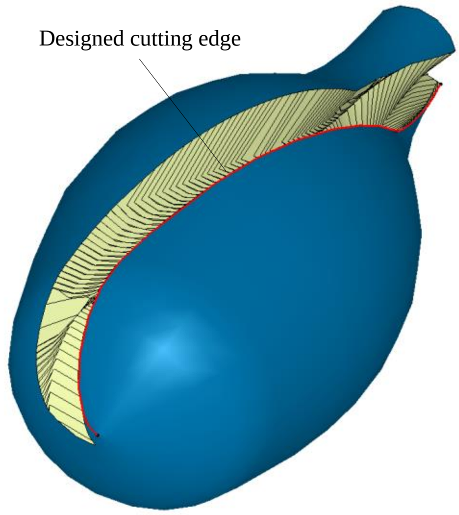

(*c*) View *c*

Figure 11. Rake face grinding of end-mill II with an accurate side cutting edge (different views)

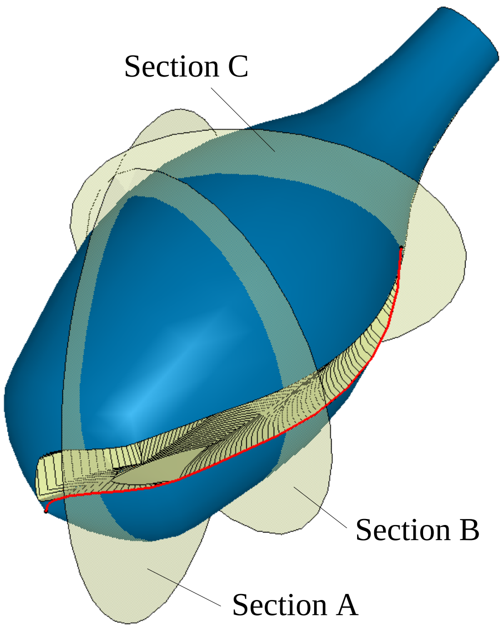

Figure 12. The arbitrary sections normal to the side cutting edge for end-mill II

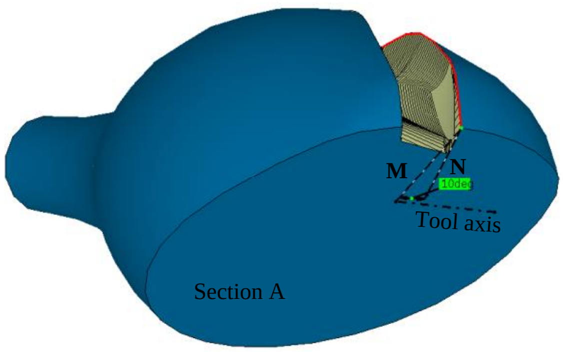

(*a*) The normal rake angle at section A normal to the cutting edge for end-mill II

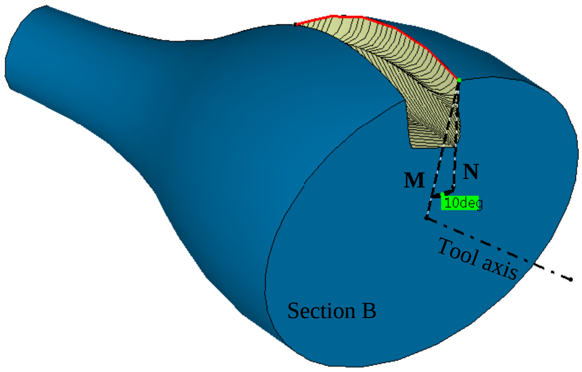

(***b***) The normal rake angle at section B normal to the cutting edge for end-mill II

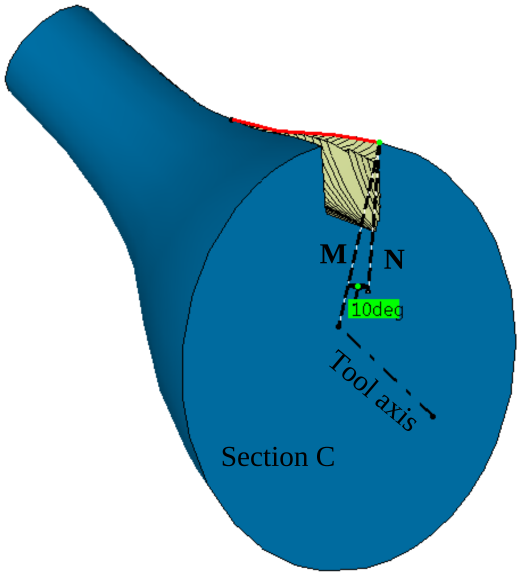

(***c***) The normal rake angle at section C normal to the cutting edge for end-mill II

Figure 13. The normal rake angle at three arbitrary sections normal to the side cutting edge of end-mill II

5. Conclusion

Generic cutting edge models are established using NURBS curves. The generic models facilitated the flutes grinding by adopting a five-axis CNC grinding approach. The approach is proved to produce end-mills flutes with accurate side cutting edges and precise normal rake angles. The approach is considered to be generic five-axis CNC grinding as traditional and non-traditional end-mills can both be built from free-form revolving profiles (NURBS curves).

References

[1] Piegl, L., Tiller, W.: The NURBS book. 2nd ed. Berlin: Mercedesdruck; 1996

[2] Lin S, Lai H, "A mathematical model for manufacturing ball-end cutters using a two-axis NC machine". The International Journal of Advanced Manufacturing Technology, Vol. 17 (2001), 881–888.

[3] Chen WY, Chang PC, Liaw SD, Chen WF, "A study of design and manufacturing models for circular-arc ball-end milling cutters". Journal of Materials Processing Technology, Vol. 161 (2005), 467–77.

[4] Chen C, Wang F, Chang P, Hwang J, Chen W, "A precision design and NC manufacturing model for concave-arc ball-end cutters". The International Journal of Advanced Manufacturing Technology, Vol. 31 (2006), 283–296.

[5] Tsai Y, Hsieh J, "A study of a design and NC manufacturing model of ball-end cutters". Journal of Materials Processing Technology, Vol. 117 (2001), 183–192.

[6] Ren B, Tang Y, Chen C, "The general geometrical models of the design and 2-axis NC machining of a helical end-mill with constant pitch". Journal of Materials Processing Technology, Vol. 115 (2001), 265–270.

[7] Chen W, Lai H, Chen C, "A precision tool model for concave cone-end milling cutters". The International Journal of Advanced Manufacturing Technology, Vol. 18 (2001), 567–578.

[8] Wu C, Chen C, "Manufacturing models for the design and NC grinding of a revolving tool with a circular arc generatrix". Journal of Materials Processing Technology, Vol. 116 (2001), 114–123.

[9] Chen W, Chen W, "Design and NC machining of a toroid-shaped revolving cutter with a concave-arc generator". Journal of Materials Processing Technology, Vol. 121 (2002), 217–225.

[10] Hsieh CM, "Manufacturing models for the design and NC grinding of truncated-cone ball-end cutters". The International Journal of Advanced Manufacturing Technology, Vol. 35 (2008), 1124–1135.

[11] Han C, Tang Y, Dong C, "A research on the non-NC machining of two kinds of revolving cutters". Journal of Materials Processing Technology, Vol. 161 (2005), 485–490.

[12] Hsieh J, Tsai Y, "Geometric modeling and grinder design for toroid-cone shaped cutters". The International Journal of Advanced Manufacturing Technology, Vol. 29 (2006), 912–921.

[13] Chen C, Lin R, "A study of manufacturing models for ball-end type rotating cutters with constant pitch helical grooves". The International Journal of Advanced Manufacturing Technology, Vol. 18 (2001), 157–167.

[14] Lv G, Wang H, Tang Y, Peng L, "Cutting edge curve models for equal pitch cutters and their applications". Journal of Harbin Institute of Technology, Vol. 11 (2004), 46–48.

[15] Chen W, "A mathematical solution to the design and manufacturing problems of ball-end cutters having a cutting edge with constant angle to the axis". Proceedings of the Institution of Mechanical Engineers, Part C, Journal of Mechanical Engineering Science, Vol. 218 (2004), 301–308.

[16] Engin S, Altintas Y, "Mechanics and dynamics of general milling cutters, Part I: Helical end mills". International Journal of Machine Tools and Manufacture, Vol. 41 (2001), 2195–2212.

[17] Rababah M, Aljarrah M, Almagableh A, "Five-axis rake face grinding of end-mills with circular-arc generators". International Journal on Interactive Design and Manufacturing, DOI 10.1007/s12008-013-0198-8.

[18] Rababah M, "A Practical and Optimal Approach to CNC Programming for Five-Axis Grinding of the End-Mill Flutes". PhD dissertation, Concordia University (2011).

[19] Rababah M, Chen C, "Five axis CNC tool grinding, part I: rake face grinding". Proceeding of the ASME 2011, International Manufacturing Science and Engineering, Corvallis, Oregon, USA, June 13-17, 2011.

[20] Rababah M, Chen C, Wang L, "A new approach to five-axis CNC flute grinding of solid end-mills". Materials Science Forum, Vol. 723 (2013), 421-432.

[21] Rababah M, Chen C, "An Automated and Accurate CNC Programming Approach to Five-Axis Flute Grinding of Cylindrical End-Mills using the Direct Method". Journal of Manufacturing Science and Engineering, Transaction of ASME, 135 (2013), 011011.

JJMIE

Volume 9 Number 3, June.2015
ISSN 1995-6665
Pages 167 - 176

Jordan Journal of Mechanical and Industrial Engineering

Partial and Total Productivity Measurement Models for Garment Manufacturing Firms

Amare Matebu[a*], Migibar Shibabaw[b]

[a] Assistant Professor, Industrial Engineering, Institute of Technology, Bahirdar University, Ethiopia
[b] Assistant Lecturer, Industrial Engineering, Institute of Technology, Bahirdar University, Ethiopia

Received 27 Dec 2014 *Accepted 13 May 2015*

Abstract

The main objective of this study is to explore the productivity measures typically used in Ethiopian garment manufacturing firms and its shortcomings. A case study was carried out at NGM manufacturing firm. The analysis of existing productivity measures indicates that the firm does not have proper and systematic productivity measures to monitor its productivity performance. Garment manufacturing firms did not determine the resource (labor, material, machine, energy, etc.) utilization rate and considered productivity as an equivalent to labor productivity. Partial and total productivity measurement models are developed and applied to monitor the productivity status of the firm. The models are tested using the data of five consecutive fiscal years (2007/8 to 2011/12) collected from NGM firm. Accordingly, the partial productivity indices of the firm for current year (2011/12), as compare to base year (2009/10), for each input factor (human, material, capital, energy and miscellaneous input factors) are 2.36, 0.64, 0.51, 2.25 and 1.09, respectively. The total productivity index of the current year is 0.75. Furthermore, the partial and total productivity analysis trends of NGM firm were computed in the same fiscal years. All partial productivity indices of the company during the period of 2008/9 showed a decline as compared to the base period (2009/10) which is the lowest productivity in the specified period. The total productivity index also showed the lowest (a decline by 73%) in the same period. Therefore, the developed partial and total productivity measurement models had the scope to portray the firm's performance in a comprehensive manner.

Keywords: *Productivity Measurement Model, Partial Productivity, Total Productivity, Garment Manufacturing*.

1. Introduction

The productivity measurement has always been an important aspect in manufacturing firms. Nowadays, the issue of productivity improvement, especially in developing countries, has become important for manufacturing firms' managers, strategic planners, government policy makers and it is becoming a key factor affecting the overall performance of firms [11]. Improving organizational productivity is an issue that has been used for some time and will continue to be important. For manufacturing firms characterized by low utilization of their resources (machines/ equipments, human labor, materials, capital, energy, time and others), productivity measurement and improvement is not only desired but is also increasingly becoming a requirement for organizational survival [20].

The productivity measurement is the quantification of both the output and input resources of a production system. It is the pre-requisite for productivity improvement [18]. It shows the gap between the existing and the desired status or the level of productivity in the manufacturing firm. It has been stated that the low level of productivity in manufacturing firms implies a low growth of national as well as organizational economy [17].

Garment manufacturing is one of the labor intensive manufacturing firms that contribute to the economic growth of the country. There are about 39 garment manufacturing firms in Ethiopia. Those manufacturing firms are inadequate in their resource utilization, and low productivity is a common feature for most of them. Almost all of these firms are characterized by low profit due to the high cost of production. Firms do not clearly identify the factors influencing the productivity and the existing productivity status is not known. There is no defined and reliable productivity measurement system. Therefore, the purpose of the present study is to develop productivity measurement models for garment manufacturing firms in Ethiopia.

* Corresponding author. e-mail: amarematebu@yahoo.com.

2. Research Approach

The approaches of the present study include literature review, observations, discussions and a case study. A detailed literature review of productivity measurement approaches and types of productivity measurement are presented. The current productivity measurement practices in manufacturing firms are reviewed.

Researchers have made field observations to see the overall working environment of the garment manufacturing firms, to investigate work processes and procedures, and to observe the productivity tasks practiced in firms. Moreover, a couple of fruitful discussions were held with general managers, production managers and supervisors in the firms.

A case study was carried out at NGM manufacturing firm. NGM firm is selected as a case study because of the data and information availability as well as the interest of managers to do so. The objective of the case study was to study specific productivity problems, to identify the shortcomings of the current productivity measurement method, and to verify and test the proposed productivity measurement models.

3. Development of Productivity Measurement Model

The productivity measurement and analysis should commonly fulfill the criteria that it should provide both aggregate (firm-level) and detailed (operational level) productivity indices, represent the firm productivity, identify or prioritize the problem areas and determine the solutions for improving productivity in such areas, resulting in the identification of potential improvements; it should be complete (completeness refers to the thoroughness with which outputs or results delivered and all inputs or resources consumed are measured and included in the productivity ratio); it should be inclusive, including all activities of the firm; it should show which particular input resources are being utilized inefficiently and it should enable to decide how to reallocate resources; it should determine how well previously established goals were met; it should also point out which operational units are profit making and which are not. The measurement model should offer a way of not only measuring but also evaluating, planning, and improving the overall productivity of an organization as a whole as well as its operational units; it should provide valuable information to strategic planners in making decisions related to diversification and phase outs of products or services.

The development of an effective measurement system is essential for a continuous productivity improvement. What is needed, then, is a productivity measurement system that not only provides a firm-level total productivity index to indicate the productivity health of the firm, but it also points out the growth or the decline in the productivity and the profitability of its products or services. Partial productivities and total productivity were considered in the present study for measuring productivity.

3.1. Computation of Partial Productivities

A. *Partial productivities can be calculated by:*

Partial Productivity:

$$PP_G = \frac{OF}{I_G} \quad (Where\ \ G = H, M, C, E, X) \qquad (1)$$

B. The five basic partial productivity indices can be calculated by:

i. Human Productivity index:

$$PP_{H\text{-}index} = \frac{OP_c}{OP_b} \times \frac{IP_{Hb}}{IP_{Hc}} \qquad (2)$$

ii. Material Productivity index:

$$PP_{M\text{-}index} = \frac{OP_c}{OP_b} \times \frac{IP_{Mb}}{IP_{Mc}} \qquad (3)$$

iii. Capital Productivity index:

$$PP_{C\text{-}index} = \frac{OP_c}{OP_b} \times \frac{IP_{Cb}}{IP_{Cc}} \qquad (4)$$

iv Energy Productivity index:

$$PP_{E\text{-}index} = \frac{OP_c}{OP_b} \times \frac{IP_{Eb}}{IP_{Ec}} \qquad (5)$$

v. Miscellaneous Productivity index:

$$PP_{X\text{-}index} = \frac{OP_c}{OP_b} \times \frac{IP_{Xb}}{IP_{Xc}} \qquad (6)$$

where
OF = Total output of the firm
OP_C = Output of current period
I_G = (H, M, C, E, and X inputs)
OP_b = Output of base period
IP_C = Input of current period
IP_b = Input of base period

3.2.Total Productivity of a Firm: TPF Based on Total Outputs & Inputs

A. *Total productivity of the firm for period t as a function of its total outputs and total inputs is given by:*

$$TPF_t = \frac{OF}{IF} \quad \text{..................................} \qquad (7)$$

where
OF = Total output of the firm and
IF = Total input of the firm

$$TPF_t = \frac{OF}{v.\ of\ I_H + v.\ of\ I_M + v.\ of\ I_C + v.\ of\ I_E + v.\ of\ I_X} \qquad (8)$$

v. : Value

B. *Total productivity index of the firm for period t as a function of its total outputs and total inputs is given by: Total Productivity index of a firm:*

$$TPF_{Index} = \frac{OF_c}{OF_b} \times \frac{IF_{Cb}}{IF_{Cc}} \qquad (9)$$

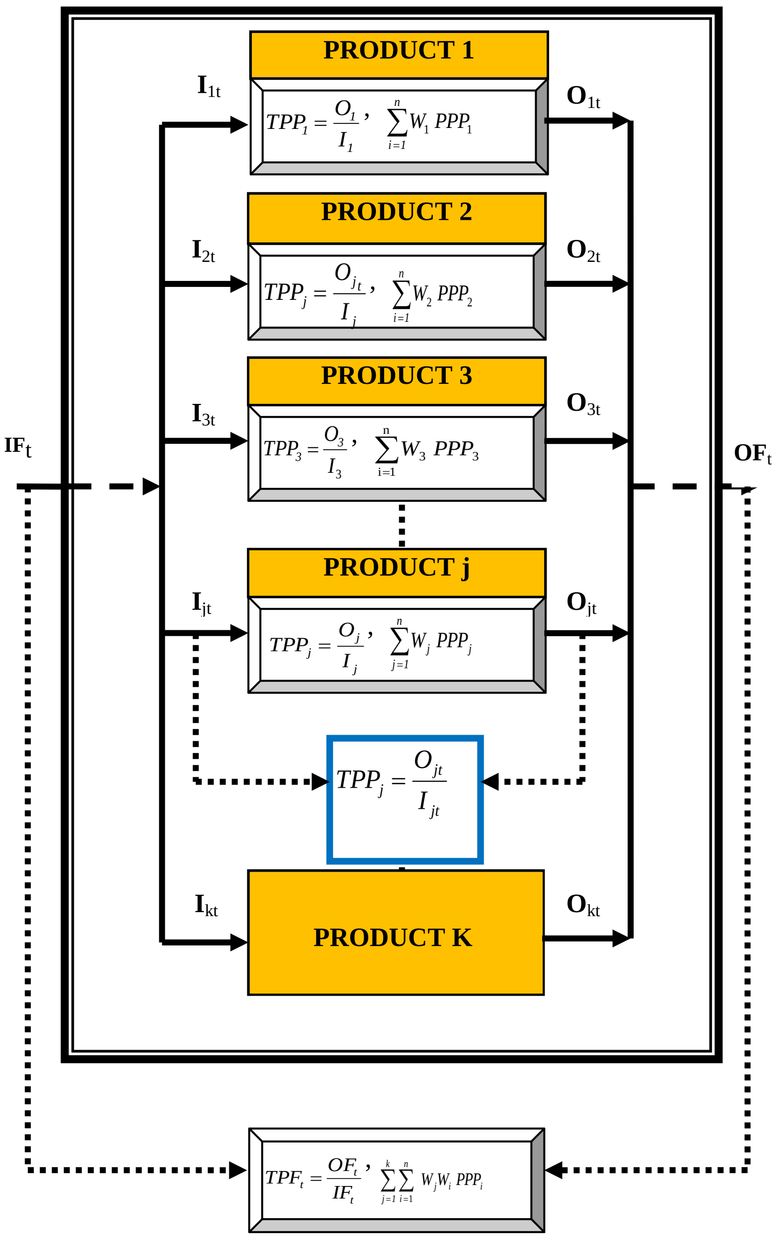

Figure 1. Product-based Productivity Measurement Model at Firm Level

TPF Computation Based on Individual Products: Total productivity of a product in a given period (PP-based):

where

TPP_j = Total productivity of a product j
PPP_{ji} = Partial Productivity of product j for input i
W_{ji} = Weight attached to input factor i & j
j = Designates a type of a product in a firm

C. Partial productivity index of a product:

$$PPP_{ji} = \frac{OP_c}{IP_{ic}} \Big/ \frac{OP_b}{IP_{ib}} \quad (11)$$

PPP_{ji} = Partial Productivity of product j for input i
OP_c = Output value of a product *for* P_c
OP_b = Output value of a product for the P_b
IP_{ic} = An Input factor of a product for P_c
IP_{ib} = An Input factor of a product *for* P_b
I = Designates the type of input factor of a product.

D. *Total productivity of a firm for a given period (PB-Product Based):*

$$TPF = w_j * 1/n\,(w_1 PPP_1 + w_2 PPP_2 .....+ w_j PPP_j)$$

$$= \sum_{j-1}^{K} w_j\, 1/n \left(\sum_{i=1}^{n} w_i PPP_i\right)$$

$$TPF = \sum_{j=1}^{k} w_j TPP_j = \frac{O_1 + O_2 + O_3 + ...O_n}{I_1 + I_2 + I_3 + ...I_n} \quad (12)$$

where

TPF = Total productivity of a Firm
PPP_i = Partial Productivity of a product for input *i*
W_j = Weight attached to a product; & $\Sigma W_j = 1$
W_i = Weight attached to input factor; and
i = Designates the type of input factor of a product
j = Designates type of a product in a Firm
k = Number of products in the firm
n = Number of input factors for a product

E. *Total Productivity of a firm based on its five partial productivities (PB) is given as:*

$$TPF = \frac{1}{5}\left(\sum_j w_{jH} PPP_{jH} + \sum_j w_{jM} PPP_{jM} + \sum_j w_{jC} PPP_{jC} + \sum_j w_{jE} PPP_{jE} + \sum_j w_{jX} PPP_{jX}\right) \quad (13)$$

F. *Total Productivity index of a firm based on its five partial productivities (PB) is given as:*

$$TPF_{Index} = \sum_j w_{jH} PPP_{jH} + \sum_j w_{jM} PPP_{jM} + \sum_j w_{jC} PPP_{jC} + \sum_j w_{jE} PPP_{jE} + \sum_j w_{jX} PPP_{jX} \quad (14)$$

G. *Total Productivity of a firm based on its five partial productivities is given as:*

$$TPF = \frac{1}{5}\left(W_{iH} PP_{iH} + W_{iM} PP_{M} + W_{iC} PP_{iC} + W_{iE} PP_{iE} + W_{iX} PP_{iX}\right) \quad (15)$$

H. *Total Productivity index of a firm based on its five partial productivities is given as:*

$$TPF_{Index} = W_{iH} PP_{H\text{-}index} + W_{iM} PP_{M\text{-}index} + W_{iC} PP_{C\text{-}index} + W_{iE} PP_{E=index} + W_{iX} PP_{X=index} \quad (16)$$

4. Productivity Computation at NGM Firm

The productivity measurement is part of the diagnosis of identifying where the improvement activity should be prioritized. It is important to do measurement as a basis for analysis, and also to track the change and the progress during the improvement program. The basic objectives behind the productivity measurement are to help the practitioners understand their production processes, to ensure that decisions are based on facts, to show where improvements need to be made, to show if improvements actually happened, to identify whether the practitioners are meeting customer requirements or not.

The productivity measurement is not well exercised in NGM firm. To achieve long-term productivity improvements, the present ad-hoc or informal approach has to be replaced by a more systematic and strategic approach to measurement. In particular, it is necessary to analyze the relationship between causes and effects of garment productivity and to quantify the impacts of the different input factors for productivity.

4.1. Computation of Partial Productivities of NGM firm for 2011/2012 Fiscal Year (FY)

NGM firm produces different models of garments (such as Baseball pants, Polo-shirts, T-shirts, etc.). For measuring the partial and total productivity in NGM firm, five-year (i.e., 2007/8 to 2011/12) data were collected.

Base year selection: The base year for the calculation of the productivity growth in the company was defined to be the 2009/2010 fiscal year (FY), because this year got a relatively higher average performance and fully advocated by the interview result from the company's production manager. Implementing the measurement model requires gathering of any two of the quantities, i.e., price or value of each input and output. Accordingly, the data of output and input values of NGM firm for the fiscal years 2007/8 to 2011/12 were compiled as shown in Table 1.

The authors have defined the five partial productivities of NGM firm as follows:

1. ***Human inputs:*** these include the values of salaries and benefits of all employees of the company.
2. ***Material inputs:*** these include major raw materials, such as knitted and woven fabrics; accessories, such as buttons, sewing threads, zippers, bands, etc.
3. ***Capital inputs****:* uniform annual cost of both fixed and working capital.
4. ***Energy Inputs*****:** these include electrical power and water consumption.
5. ***Miscellaneous inputs*****:** these include taxes, professional fees, advertisement cost, insurance, travel and per diem, etc.)

A. *Five Basic Partial Productivities of NGM firm for 2011/2012 FY*

1. The partial productivities of NGM firm for 2011/2012 fiscal year are computed as follows:

$$PP_H = \frac{OF}{I_H} = \frac{12798897}{340650} = 37.57$$

$$PP_M = \frac{OF}{I_M} = \frac{12798897}{2318670} = 5.52$$

$$PP_C = \frac{OF}{I_C} = \frac{12798897}{3012873} = 4.25$$

$$PP_E = \frac{OF}{I_E} = \frac{12798897}{72845} = 175.70$$

$$PP_X = \frac{OF}{I_X} = \frac{12798897}{950236} = 13.47$$

Therefore, the partial productivities of the company for the fiscal year 2011/2012 with respect to each input factor are calculated using equation 1. Accordingly, the partial productivities for human, material, capital, energy and miscellaneous input factors of the process are 37.57, 5.52, 4.25, 175.70 and 13.47, respectively.

Table 1. Data for Computing Partial and Total Productivity. (Source: Authors' computation from NGM firm)

Item	Fiscal Year				
	2007/8	2008/9	2009/10	2010/11	2011/12
Value of Human Inputs	924,372	426,430	549,597	337,993	340,650
Value of Capital Inputs	1,937,522	1,510,843	1,048,983	4,436,026	3,012,873
Value of Material Inputs	1,709,467	1,472,118	1,015,385	3,993,236	2,318,670
Value of Energy Inputs	36,667	45,443	112,044	32,317	72,845
Value of Miscellaneous Inputs	235,777	225,462	708,185	1,181,268	950,236
Value of Total Outputs	4,856,342	2,541,355	8,745,896	11,953,628	12,798,897
Value of Total Inputs	4,843,805	3,680,296	3,434,191	9,980,840	6,695,274

B. *Five Basic Partial Productivity indices of NGM firm for 2011/2012 FY*

2. Using equations (2-6), the partial productivity indices of the different input factors of the NGM firm for fiscal year of 2011/2012 has been computed as follows:

Partial productivity index for human input factors:

$$PP_{H\text{-}index} = \frac{OP_c \times IP_{ib}}{OP_b \times IP_{ic}} = \frac{12798897 \times 549597}{8745896 \times 340650} = 2.36$$

where, $PP_{H\text{-index}}$ is the partial productivity index of the NGM firm for fiscal year of 2011/2012 for human input factor.

Partial productivity index for material input factors:

$$PP_{M\text{-}index} = \frac{OP_c \times IP_{ib}}{OP_b \times IP_{ic}} = \frac{12798897 \times 1015385}{8745896 \times 2318670} = 0.64$$

where, $PP_{M\text{-index}}$ is the partial index of the NGM firm for fiscal year of 2011/2012 for fiscal year of 2011/2012 for material input factor.

Partial productivity index for capital input factors:

$$PP_{C\text{-}index} = \frac{OP_c \times IP_{ib}}{OP_b \times IP_{ic}} = \frac{12798897 \times 1048983}{8745896 \times 3012873} = 0.51$$

where, PPC-index is the partial productivity of the NGM firm for fiscal year of 2011/2012 for capital input factor.

Partial productivity index for energy input factors:

$$PP_{E\text{-}index} = \frac{OP_c \times IP_{ib}}{OP_b \times IP_{ic}} = \frac{12798897 \times 112044}{8745896 \times 72845} = 2.25$$

where, PPE-index is the partial productivity of the NGM firm for fiscal year of 2011/2012 for energy input factor.

Partial productivity index for miscellaneous input factors:

$$PP_{x\text{-}index} = \frac{OP_c \times IP_{ib}}{OP_b \times IP_{ic}} = \frac{12798897 \times 708185}{8745896 \times 950236} = 1.09$$

where, PPx-index is the partial productivity of the NGM firm for fiscal year of 2011/2012 for miscellaneous input factor.

Therefore, the partial productivity indices for the fiscal year 2011/2012 with respect to each input factor (human, material, capital, energy and miscellaneous input factors) of the NGM firm are 2.36, 0.64, 0.51, 2.25 and 1.09, respectively.

4.2. Total Productivity Computation of NGM firm for 2011/2012 FY

In the present study, three basic approaches are developed to calculate the total productivity of the company. Those methods are: Total productivity based on total outputs and total inputs, total productivity based on five basic partial productivities and total productivity based on the individual products of the company. The first and the second approaches were implemented in the company. The third approach was not implemented in the company, because there were no organized data in the form of individual products in the company.

A. *Computation of Total Productivity Based on Total Outputs and Inputs*

The total productivity of the company for fiscal year 2011/2012 as a function of its total outputs and total inputs has computed by using equation (7) as follows:

$$TPF_{2011/2012} = \frac{OF}{IF} = \frac{12798897}{6695274} = 1.912$$

Therefore, the total productivity of NGM firm for fiscal year 2011/2012 based on the function of its total output and total input is 1.912.

B. *Computation of Total Productivity Based on Partial Productivities*

The total productivity of the NGM firm for the fiscal year 2011/2012 was also computed based on five partial productivities by using equation (15) as follows:

$$TPF = \frac{1}{5}(W_{iH}PP_{iH} + W_{iM}PP_M + W_{iC}PP_{iC} + W_{iE}PP_{iE} + W_{iX}PP_{iX})$$

First, the weight factors for each input are computed as follows:

$$W_H = \frac{I_H}{IF} = \frac{340650}{6695274} = 0.051$$

$$W_M = \frac{I_M}{IF} = \frac{2318670}{6695274} = 0.346$$

$$W_C = \frac{I_C}{IF} = \frac{3012873}{6695274} = 0.450$$

$$W_E = \frac{I_E}{IF} = \frac{72845}{6695274} = 0.011$$

$$W_X = \frac{I_X}{IF} = \frac{950236}{6695274} = 0.142$$

$$\therefore TPF = \frac{1}{5}(0.051\ x\ 37.57 + 0.346\ x\ 5.52 + 0.450\ x\ 4.25 + 0.011\ x\ 175.70 + 0.142\ x\ 13.47)$$

$$= 1/5\ (1.91 + 1.910 + 1.913 + 1.933 + 1.913)$$

$$= \underline{\mathbf{1.915}}$$

The total productivity index of the company for the fiscal year 2011/2012, as a function of its total outputs and total inputs, was computed by using equation (9) as follows:

Total Productivity index of firm:

$$TPF_{Index} = \frac{OF_c}{OF_b} \times \frac{IF_{Cb}}{IF_{Cc}}$$

$$TPF_{Index} = \frac{12798897}{8745896}\ x\ \frac{3434191}{6695274} = 0.7506$$

Total Productivity index of a firm based on its five partial productivities has computed using equation (16) as:

$$TPF_{Index} = W_{iH} PP_{H\text{-}index} + W_{iM}\, PP_{M\text{-}index} + W_{iC} PP_{C\text{-}index} + W_{iE} PP_{E\text{-}index} + W_{iX} PP_{X\text{-}index}$$

$$= 0.051 \times 2.360 + 0.346 \times 0.64 + 0.450 \times 0.51 + 0.011 \times 2.25 + 0.142 \times 1.09$$

$$= 0.1204 + 0.2208 + 0.2295 + 0.0248 + 0.1548$$

$$= \underline{0.7504}$$

4.3. Partial & Total Productivity Analysis at NGM

A partial and total productivity analysis was done at NGM firm by comparing the current partial and total productivity with the base period. Based on the data obtained for five consecutive periods (2007/08, 2008/09, 2009/10, 2010/2011, 2011/2012), the status of the current fiscal year 2011/12 was determined with the reference to the base year 2009/10.

A. *Partial Productivities Analysis at NGM Firm*

The partial productivities of the current fiscal year (2011/12) were computed in section 4.1.A. above. Accordingly, the partial productivities of human, energy and miscellaneous inputs showed a growth with an amount of 136 %, 125%, and 9 %, respectively. But the partial productivities of capital and material inputs showed a decline with an amount of 49% and 36%, respectively. Table 2 shows the decline or growth of the partial productivities of the company in 2011/12 fiscal year:

Table 2. Comparison of Current Partial Productivities with P_b

Partial Productivities	Base period (2009/10)	Current period (2011/12)	Change (%)	Status
Human Inputs Productivity	15.91	37.57	136	Growth
Capital Inputs Productivity	8.34	4.25	-49.0	Decline
Material Inputs Productivity	8.61	5.52	-36.0	Decline
Energy Inputs Productivity	78.06	175.7	125.0	Growth
Miscellaneous Inputs Productivity	12.35	13.45	9.0	Growth

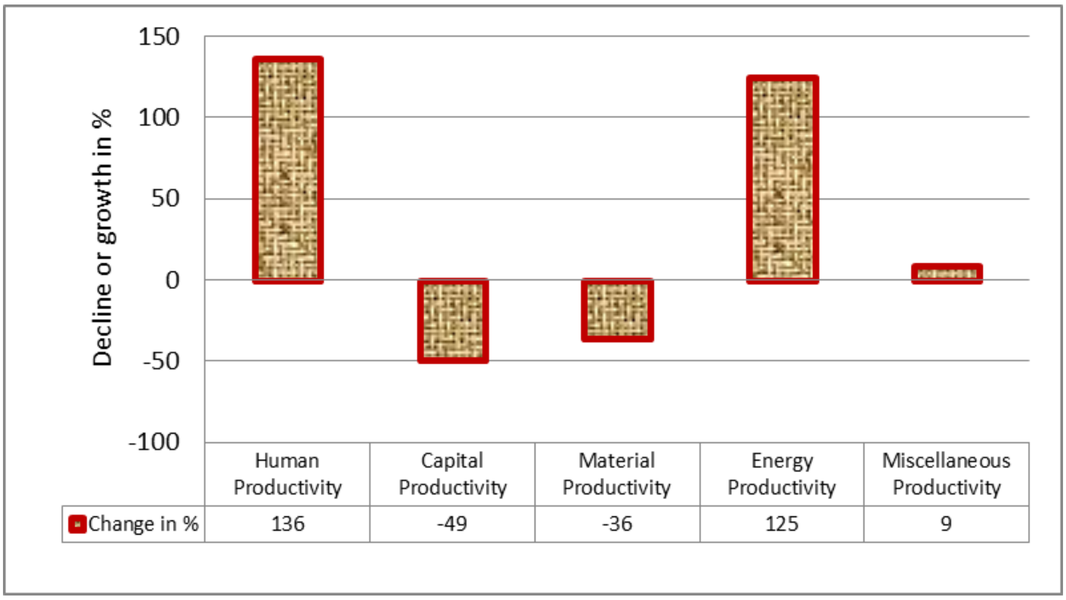

Figure 2. Decline/growth of PP for Year 2011/12 against P_b

B. *Total Productivity Analysis at NGM Firm*

The total productivity index of NGM firm for the current period (2011/12) was computed in section 5.2. and it is 0.75. This indicates that the productivity of the company declined with an amount of 25 %. Hence, it is necessary to investigate the points where primarily poor productivity growth shows and make appropriate improvement initiatives for the firm. The developed productivity measurement methodology indicates not only the productivity growth or the decline of the firm but it also enables to investigate the productivity of the company at firm level, product level, operational level, and even at process input factors or parameters level.

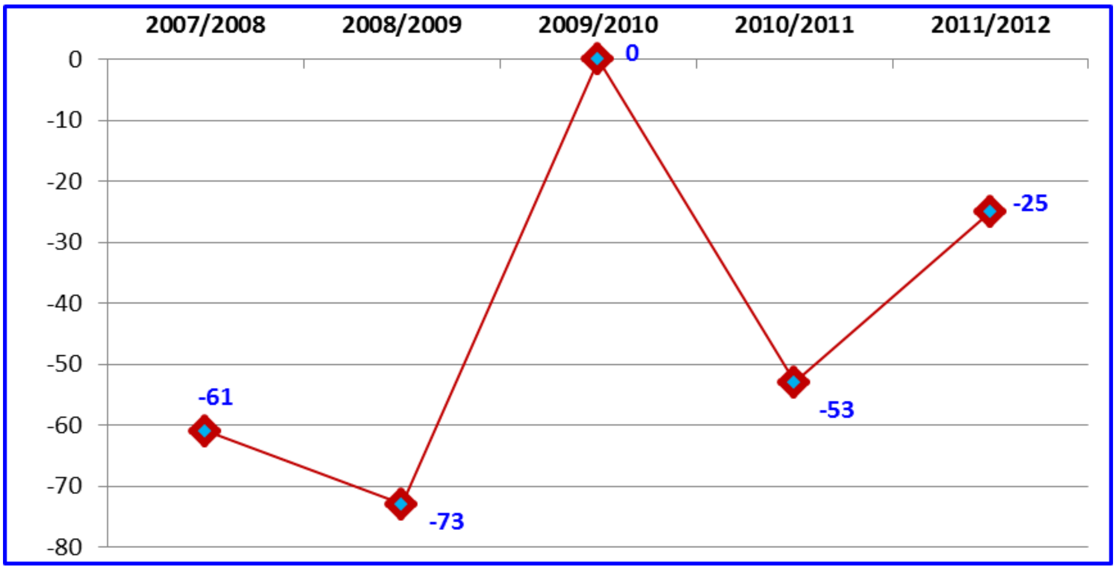

Figure 3. Total Productivity Trends: 2007/8 to 2011/12 against P_b

5. Results and Discussion

5.1. Partial and Total Productivities at NGM Firm (2007/8 – 2011/12)

So far, the partial and total productivities of NGM firm have been computed for fiscal years 2007/8 to 2011/12. The productivity measurement results are helpful for the company to know the status of its performance and to identify the potential areas for improvement. Especially, the productivity index is important to tell the relative position of the current period with respect to the base period, and links to the actual productivity story of the company. Comparison of the productivity index value with the previous productivity history of the company will enable to dig out the critical productivity problems and suggest the appropriate corrective actions that should be taken by the company. The productivity measurement and the analysis result also enable to point out the bottleneck areas where improvement actions that are to be taken at both the operational and the company levels. As stated above, the summarized partial and total productivities and its indices are shown in Table 3.

The productivity of the company for the specified periods (2007/8 to 2011/12) fluctuates from year to year. For instance, the total productivity indices of the company for the fiscal years 2007/8 to 2011/12 were 0.394, 0.271, 1.00, 0.47, and 0.75, respectively. Hence, the productivity of the current year (2011/12) is better than the other fiscal years as compared to the base year. On the other hand, it showed poor productivity during the period 2008/9. Of course there was an interruption of electrical power at a national level during the periods 2007/8 and 2008/9.

5.2. Productivity Trend Analysis at NGM firm (2007/8 – 2011/12)

The productivity trend analysis provides a wealth of information for many other purposes, such as profit planning, short and long-term productivity planning, and productivity evaluation. The productivity trend analysis is probably the most important step in the productivity-measurement stage of a firm's productivity program, because productivity figures are interpreted to trigger action-oriented management strategies. Hence, the productivity indices of NGM firm were compiled in the form of a management summary report to indicate the percent changes in total and partial productivities for the specified periods (2007/8 to 2011/12) as shown in Table 4.

Table 3. Partial and Total Productivity of NGM firm for Five Fiscal Years

Parameters	Fiscal Years					
	2007/2008	2008/2009	2009/2010	2010/2011	2011/2012	Min. value
TPF	1.003	0.691	2.547	1.198	1.912	0.691
TPF_i	0.394	0.271	1.00	0.470	0.751	0.271
PP_H	5.25	5.96	15.91	35.37	37.57	5.25
PP_{H-i}	0.33	0.37	1.00	2.22	2.36	0.33
PP_C	2.51	1.68	8.34	2.69	4.25	1.68
PP_{C-i}	0.30	0.20	1.00	0.32	0.51	0.20
PP_M	2.84	1.73	8.61	2.99	5.52	1.73
PP_{M-i}	0.33	0.20	1.00	0.35	0.64	0.20
PP_E	132.4	55.92	78.06	369.9	175.7	55.92
PP_{E-i}	1.70	0.72	1.00	4.74	2.25	0.72
PP_X	20.60	11.27	12.35	10.12	13.45	10.12
PP_{X-i}	1.67	0.91	1.00	0.82	1.09	0.82

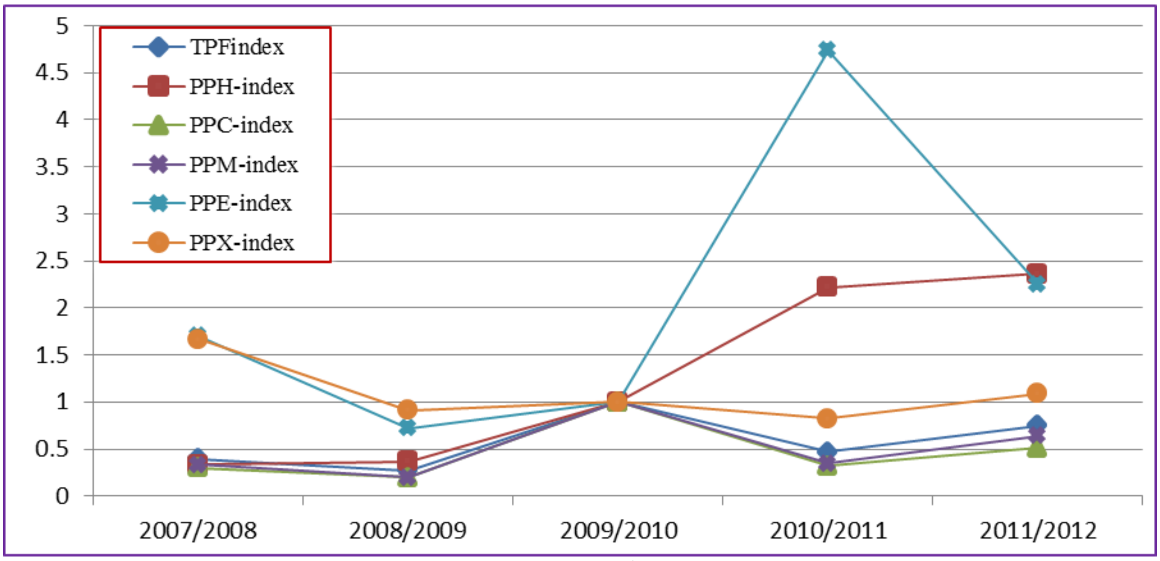

Figure 4. Partial and Total Productivity Indices for Novastar Garment PLC against Base Period

All partial productivity indices of the company during the period 2008/9 showed a decline as compared to the base period 2009/10 which is the lowest productivity in the specified period. The total productivity indices also showed the lowest (a decline by 73%). In general, one can observe the report format of the productivity trend analysis and could easily identify productivity status of the company.

5.3. Productivity Measurement and its Shortfall at NGM firm

NGM firm has been measuring and analyzing its productivity for a long period of time partially (only labor productivity). The company's labor productivity is measured as the ratio of the total number of garment to the total number of employees. It is measured to evaluate the company productivity growth and/or decline. Productivity is expressed in the form of sales volume and used to evaluate the overall performance of company. This productivity measurement model, however, has limitations as: it cannot represent the firm's productivity, it is not complete and inclusive and it does not indicate the areas of productivity problems and opportunities for improvement. The details are discussed as follows:

- *NGM firm uses inappropriate Productivity Measurement Technique*

Currently, the company measures labor productivity only. Moreover, the measurement approach for the labor productivity is inappropriate. It uses Mill's index approach. Mill's index is obtained by dividing the total product output by the total number of employees. Basically, Mill's index approach is used for measuring the productivity index at industry level, such as manufacturing industry, construction industry, service industry, etc. The measured productivity index may be used as an indication of productivity at industry level, not at firm or operational level.

- *Productivity Measurement System of NGM firm Lacks Completeness*

Completeness means the thoroughness with which outputs and all inputs, or resources consumed, are measured and included in the productivity ratio (M. A. Wazed, 2008). With this respect, the productivity measurement is not complete at NGM firm. The company did not consider all factors of production (inputs) of the firm, such as materials, energy, capital and other utilities and facilities, which are used to produce the final products of the company. These input factors have a high impact on the productivity of the organization. Ignoring these factors, while measuring the productivity of the firm, will result in an erroneous effect and will misdirect the company's improvement effort.

- *Productivity Measurement System of NGM firm Lacks Comparability*

The existing productivity measurement system (labor productivity) does not show a comparability result. The company needs to identify its productivity growth by defining a base year. The productivity index will be developed based on the base year and is used to determine whether the company is growing or declining in productivity with time. The current productivity measurement and analysis system, however, measure productivity only as the rate of garments produced per unit of labor utilized in the given period of time.

Table 4. Partial and Total Productivities Trends at NGM firm (2007/8-2011/12)

S.N	Fiscal Years	Partial Productivities Changes, %					Total Productivity Changes, %
		H	**M**	**C**	**E**	**X**	
1	2007/2008	-0.67 ↓(67%)	-0.67 ↓(67%)	-0.70 ↓(70%)	+0.70 ↑(70%)	+ 0.67 ↑(67%)	**-0.61 ↓(61%)**
2	2008/2009	-0.63 ↓(63%)	-0.80 ↓(80%)	-0.80 ↓(80%)	-0.28 ↓(28%)	- 0.09 ↓(9 %)	**-0.73 ↓(73%)**
3	2009/2010	0.00 →(0 %)	0.00 →(0 %)	0.00 →(0 %)	0.00 →(0 %)	0.00 →(0 %)	**0.00 →(0 %)**
4	2010/2011	+1.22 ↑(122%)	-0.65 ↓(65%)	-0.68 ↓(68%)	+3.74 ↑(374%)	- 0.18 ↓(18%)	**-0.53 ↓(53%)**
5	2011/2012	+1.36 ↑(136%)	-0.36 ↓(36%)	-0.49 ↓(49%)	+1.25 ↑(125%)	+ 0.09 ↑(9 %)	**-0.25 ↓(25%)**

6. Conclusion

The present study examined the garment manufacturing firms' productivity measurement and investigated how partial and total productivities could be measured. Basically, the productivity measurement is the pre-requisite for productivity improvement. The garment manufacturing firms are using only one of the partial productivities, i.e., labor productivity. This productivity measurement system, however, has limitations, such as: it could not represent the firm's productivity, or the productivity measurement system lacks completeness, productivity measurement system also lacks comparability (there is no base year selection and the status of productivity growth or decline is unknown), the productivity measurement system in garment manufacturing firms does not include all possible measurement systems (such as partial productivities, total productivity), the existing productivity measurement also has a limitation in identifying and detecting productivity problems as well as productivity improvement opportunities.

A case study was performed at NGM firm. It focused upon the shortcomings of the current productivity measures and the computation of partial and total productivities. Moreover, the proposed partial and total productivity measurement models were tested considering the data of five consecutive fiscal years (2007/8 to 2011/12). Accordingly, the partial productivity indices of the company for the current year (2011/2012) as compared to the base year (2009/10) for each input factor (human, material, capital, energy and miscellaneous input factors) were 2.36, 0.64, 0.51, 2.25 and 1.09, respectively. The total productivity index of the current year was 0.75. Furthermore, the partial and total productivities analysis trends of NGM firm were computed for the fiscal years 2007/8 - 2011/12. All partial productivity indices of the company during the period of 2008/9 showed a decline as compared to the base period (2009/10) which is the lowest productivity in the specified period. The total productivity indices also showed as the lowest (a decline by 73 %) in the same period. Therefore, the developed partial and total productivity measurement models were used for monitoring and measuring the productivity performance of the company that enhances its productivity improvement in the long run.

References

[1] Jamal A. Farooquie, Asit B. Mohapatra, "Japanese manufacturing techniques and practices: An Indian perspective". Jordan journal of mechanical and industrial engineering, Vol. 3 (2009) No. 3, 174 – 181.

[2] Ravikumar Marudhamuthu, Marimuthu Krishnaswamy, Damodaran Moorthy Pillai, "The development and implementation of lean manufacturing techniques in Indian garment industry". Jordan journal of mechanical and industrial engineering, Vol. 5 (2011) No. 6, 527 – 532.

[3] Rajiv Khanduja, P.C Tewari, R.S Chauhan, Dinesh Kumar, "Mathematical Modeling and Performance Optimization for the paper making system of a paper plant". Jordan journal of mechanical and industrial engineering, Vol. 4 (2010) No. 4, 487- 494.

[4] P Verma. Industrial Engineering and Management. 5th edition. New Delhi: Sanjeev Kumar Kataria; 2011.

[5] Aki and Erkki Uusi-Rauva, "Bottom-up approach for productivity measurement in large public organizations". International journal of productivity and performance management, Vol. 60 (2011) No. 3, 252-267.

[6] Alan Robinson. Continuous improvement operations- A systematic approach to waste reduction. Massachusetts: Cambridge - Productivity press; 1991.

[7] Alan stainer, "Capital input and total productivity management". Management decision, Vol.35 (1997) No 3, 224-232.

[8] Alok, Dangayach, Mittal, and Milind." Performance measurement in automated manufacturing". Measuring business excellence, Vol.15 (2011) No.1, 77- 91.

[9] Anna Baines, "Productivity improvement". Work study, Vol. 46 (1997) No.2, 49-51.

[10] Arie Halachmi, "Introduction - Performance measurement is only one way of managing performance". International journal of productivity and performance management, Vol.54 (2005) No.7, 502 - 516.

[11] Arturo L. Tolentino, "New Concepts of Productivity and its Improvement". The European Productivity Network Seminar, Budapest, 2004.

[12] Azusa Tomiura, "Productivity in Japan's manufacturing industry". ELSEVIER, International journal of production economics, Vol. 52 (1997) No 2, 239-246.

[13] B.S. Saha, "Multi-factor productivity measurement model for service organization". International Journal of Productivity and Performance Management, Vol. 54 (2005) No. 1, 7-22.

[14] Bishwanath Goldar, "Productivity trends in Indian manufacturing in the pre-and post-reform periods". Working Paper, No.137, 2004.

[15] Changiz Valmohammadi, "Performance measurement system implementation using Balanced Scorecard and statistical methods". International journal of productivity and performance management, Vol.60 (2011) No.5, 493-511.

[16] Danilo Hisano and Marcel Andreotti,"The use of performance measurement system in logistics change process – proposal of a guide". International journal of productivity and performance management, Vol.60 (2011) No.4, 339-359.

[17] David J. Sumanth. Total productivity management – A systematic and quantitative approach to compete in quality, price, and time. 2nd edition. USA: CRC Press; 2005.

[18] Kanthi M.N and Samuel H. Huang, "A review of literature on manufacturing systems productivity measurement and improvement". International Journal of Industrial and Systems Engineering, Vol. 1 (2006) No. 4, 461- 485.

[19] Kongkiti and Watcharapon, "Productivity/performance measurement- Case application at the government pharmaceutical organization". Industrial management and data systems, Vol. 106 (2006) No. 9, 1272-128.

[20] M.A. Wazed and Shamsuddin Ahmed. Multifactor Productivity Measurements Model (MFPMM) as Effectual Performance Measures in Manufacturing. Malaysia: University of Malaya; 2008.

[21] Mika Hannula, "Total productivity measurement based on partial productivity ratios". International journal of production economics, Vol. 78 (2002) No. 1, 57-67.

JJMIE

Volume 9 Number 3, June.2015
ISSN 1995-6665
Pages 177 - 186

Jordan Journal of Mechanical and Industrial Engineering

A Sustainable Manufacturing Strategy Decision Framework in the Context of Multi-Criteria Decision-Making

Lanndon Ocampo[a *], Eppie Clark[b]

[a] Department of Mechanical Engineering, University of San Carlos, Cebu City, 6000 Cebu, Philippines
[b] Department of Industrial Engineering, De La Salle University, 2401 Taft Avenue, 1004 Manila, Philippines

Received 13 March 2014 Accepted 3 June 2015

Abstract

The present paper proposes a sustainable manufacturing strategy decision framework that integrates classical manufacturing strategy and sustainable manufacturing. Former approaches in these two fields were not inclusive; thus, an integrative decision framework is necessary. Along with this integration, the inclusion of major issues directly associated with manufacturing sustainability, such as firm size, various interests of different stakeholders and strategic responses, becomes a highlight of the proposed framework. Using an appropriate approach, the framework could provide the content of a sustainable manufacturing strategy which is helpful for manufacturing decision-makers in promoting both competitiveness and sustainability. Hypotheses are developed from the proposed framework. A review of a possible methodological approach is shown with a strong emphasis on multi-criteria decision-making. A discussion of a future work, following the decision framework, is also presented. The contribution of the present work lies in the development of a comprehensive decision framework that attempts to integrate a manufacturing strategy and a sustainable manufacturing.

Keywords: *Manufacturing Strategy, Sustainable Manufacturing, Framework, Firm Size, Stakeholders, Strategic Responses*.

1. Introduction

The work of Wickham Skinner in 1969 on Manufacturing Strategy (MS) is considered foundational in its field. Hayes and Wheelwright [1], building on Skinner, defined MS as a consistent pattern of decision-making in the manufacturing function that is directly linked to the business strategy. This link became more pronounced following Skinner's hierarchical top-down strategy framework which highlights the relationships of corporate, business and manufacturing strategies and, thus, indirectly providing the link of MS to corporate strategy. Skinner’s [2] classical framework was remarkable as it, over a span of decades, became a guideline of later approaches in this field. It was agreed by domain scholars and practitioners that MS does not only support business strategy but also translates the strengths and resources of the firm into opportunities in the market [3]. This highlights both the internal and external functions of MS to the manufacturing firm.

Wheelwright [4] emphasized that MS supports business strategy only if a sequence of decisions over structural and infrastructural categories is consistent over long-term planning horizons. Structural decisions, i.e., process technology, facilities, capacity and vertical integration, enable long-term impacts to the firm and they require a huge amount of investments. Infrastructural decisions, i.e., organization, manufacturing planning and control, quality, new product introduction and human resources, on the other hand, are strategic and they require relatively less investment but they are perhaps difficult to subject changes when in place. When the policies over these decision categories are consistent, MS develops a set of manufacturing capabilities or competitiveness determined by the business strategy. This set of competitive priorities is a convergence of both corporate strategy and the position – market or technology-leader – it intends to contest with its competitors. Theories of MS have been established and tested over decades of research and application in this field. Despite the advancements in the manufacturing strategy as a field of study, issues of sustainability have inadequately been studied in the current literature. The struggle of manufacturing firms for competitiveness is insufficient to sustain the manufacturing industry from the perspectives of resource depletion, carbon emissions, human toxicities, land use and environmental degradation. The earlier advances in this field should have been coupled with strategies that address sustainability, which requires a holistic and systems approach.

Due to the increasing concerns about environmental degradation, resource consumption and social equity, the notion of sustainable development has become a focal and

* Corresponding author. e-mail: don_leafriser@yahoo.com.

integral component in the decision-making of various legislative bodies, global economies and several economic sectors. Sustainable development, as defined in the famous report of the United Nations World Commission on Environment and Development (UNWCED) in 1987, is "a development that meets the needs of the present without compromising the ability of future generations to meet their own needs" [5]. A review on how this philosophy came into prominence was detailed by Linnenluecke and Griffiths [6]. One important key to sustainability is the manufacturing sector [7] due to its high volume of resource consumption, increasing annual introduction of new products that relatively require a high amount and a generation of materials, energy and wastes, increasing volume of emissions throughout product life cycles and the collective effect of manufactured products and manufacturing processes to immediate stakeholders [8]. Manufacturing industry is now held responsible for the impact of their products and processes, including waste management and recycling [9]. This gives rise to a growing subfield in sustainability, i.e., sustainable manufacturing which has significantly drawn the attention of domain scholars over the past decade or so.

Sustainable Manufacturing (SM) drives the development of products and processes that simultaneously addresses environmental stewardship, economic growth and social well-being, widely known as the triple-bottom line [10]. With on-going concerns on climate change, destruction of the natural environment, increasing consumption of non-renewable resources, among others, the desire for a sustainable development has gained more attention today than in the past. One enabling and motivating factor to engage manufacturing firms toward sustainability is the presence of stakeholders' interests. Conversely, sustainability is achieved when the interests of different stakeholders, i.e., the government, customers, suppliers, community, competitors, shareholders, employees and consumers, are satisfied [11]. Stakeholders could offer valuable inputs and resources to help firms achieve sustainability. Satisfying stakeholders' interests along with the strategic activities of a manufacturing firm demanded by the manufacturing strategy stimulates the complexity of the decision-making over various decision areas; a relevant framework must be available to provide guidance for addressing this complex condition. This has not been addressed in current literature.

Following this complexity, manufacturing firms are confronted with issues of developing MS, on one hand, and addressing SM, on the other. Recent frameworks provide limited information on how to integrate these two issues. The framework of Hallgren and Olhager [12] provides a quantitative approach for developing MS taking into account the decision categories, manufacturing objectives, market requirements and a recursive guide in improving these components in bridging the gap between the market requirements and the manufacturing objectives. However, Hallgren and Olhager's [12] approach failed to clearly address the issues associated with the sustainability of manufacturing. The conceptual frameworks of Azapagic [13], Reich-Weiser *et al.* [14] and Subic *et al.* [15] on manufacturing sustainability are disintegrated with the competitiveness agenda of the manufacturing function and were merely referenced from the TBL perspective. With emphasis on integration, the work of Johansson and Winroth [16], which explored the impact of stakeholders' concerns for the environment to the MS formulation process, provides a promising starting point of discussion. Their model incorporates the relationships among the decision categories and the competitive priorities described by the works of Wheelwright [3], Hayes and Pisano [17] and Hallgren and Olhager [12] and the stakeholders' interests described in sustainability literature. They emphasized that incorporating environmental issues alters the policy areas of all decision categories and requires an environmental performance as a competitive strategy.

Despite this attempt, the work of Johansson and Winroth [16] fails to consider a number of significant areas. First, the framework considers environmental and economic sustainability only, with no clear guidelines for the specific interests of stakeholders that address the TBL. Second, it does not consider the strategic orientation or responses of manufacturing firms to sustainability [18]. As strategic orientation varies from one firm to another, the strategy to achieve SM also varies. For instance, a compliance-oriented response would be different from market-oriented response as the former is geared towards superficially complying with the minimum requirements set forth by the stakeholders while the latter is geared on setting sustainability as means to attract more interests from the market. Third, the emerging literature in the field of sustainability identified the firm size as a relevant component in decision-making as sustainability approaches require, relatively, high investment [19-20] and a shortage of resources, such as time, manpower and money characterize small and medium enterprises [21]. Lastly, the framework does not consider various interrelationships of corporate, business and MS as these constitute a more cohesive framework. Thus, an integrative framework is required to serve as a guide for developing a SMS.

The major concern of the present paper is the holistic integration of the competitiveness perspectives of manufacturing strategy and the issues associated with sustainability. This has not been addressed in current literature to a plausible level of details. The present work attempts to link together in a single framework the demands of manufacturing strategy and sustainability, so that the resulting decisions at firm level can address these two issues. This paper aims to propose an integrated decision framework in the development of a sustainable manufacturing strategy. This framework attempts to integrate two seemingly independent theories of MS and SM. The objective of the present work is to develop the content of MS which bases itself on sustainability, incorporating significant issues associated in it such as firm size, firm's competitive strategy, and the firm's strategic responses along with the persuading role of different stakeholders' interests. The framework intends to develop quantitative models that are able to address such conditions. The contribution of the present work is two-fold: (1) the development of a sustainable manufacturing strategy (SMS) that integrates MS and SM, and (2) the development of a framework used to guide decision-makers in SMS with relevant issues such as firm size, competitive priority, strategic response and stakeholders' sustainability interests.

The remainder of the present work is provided as follows: Section 2 elaborates a literature review on firm size, interests of stakeholders and strategic responses. A holistic decision framework is presented in Section 3. Section 4 highlights the hypotheses from the proposed framework and a discussion of the possible solution approaches. Finally, Section 5 presents a conclusion and future work.

2. Relevant Issues in Sustainable Manufacturing Strategy (SMS)

This section attempts to establish the major issues associated with the sustainability of manufacturing firms. These are firm size, stakeholders' interests and strategic responses.

2.1. Firm Size

This review focuses primarily on how firms respond to sustainability issues in relation to their sizes. The arguments of Ageron *et al.* [19] and Law and Gunasekaran [21] rely on the idea that the firm size promotes differences on the responses of firms on the basis that the sustainability approaches require a relatively high amount of investment and as the firm size shrinks, time, human and financial resources are limited in SMEs [21]. This central idea is widely shared in literature [22-23].

Traditional discussion on this domain is centered on the size-innovation relationship of firms [24-25] and later evolves into size-eco-innovation issues [26-28] as the result of the continuous effort in addressing the sustainability concerns. There are opposing stances regarding the firm size and innovation. Symeonidis [24] contends that innovation increases with the firm size proportionately. However, Laforet [25] argues that the organizational innovation has relatively greater impacts on small firms as it is positively associated with small firm's profit margin, competitiveness, market leadership and the improvement of the design of products and processes. Laforet [25] also claims that smaller firms yield more cost-efficient in innovation and they are also more innovative and adaptable and have quicker response times to implement new technologies and to meet specific customer needs. This discussion on firm size-innovation relationship has been extended to challenge the link of firm size to sustainability issues such as eco-innovation [27], corporate social responsibility [29-30], small business social responsibility [22], corporate giving [31] and employment share distribution [32]. Bos-Brouwers [26] emphasized that companies with a sustainability in their orientation and innovation processes create value by introducing new products to the market and by a close cooperation with different stakeholders. Explicitly, Schrettle *et al.* [33] reported that the firm size is a crucial factor in linking sustainability drivers to strategic decisions of manufacturing firms. They found out that the firm size moderates the differences in the level of the sustainability efforts a firm undertakes. The firm size curbs the relationship between the drivers of sustainability and the sustainability efforts as large firms can engage in sufficiently a large number of sustainability programs over longer duration of time. These works establish a common argument that the firm size plays a significant role in forging the sustainability of manufacturing firms.

Various studies explored the differences between different firm sizes based on their capability to respond to sustainability issues and related domains. Bourlakis *et al.* [34] observed the relationship between firm size and sustainable performance in food supply chains in Greece. Bronchain [29] discussed the role of firm size on Corporate Social Responsibility (CSR) and pointed out that the firm size increases the capability to act on CSR initiatives. Howard and Jaffee [35] elaborated the tensions between the firm size and the sustainability goals, taking a rigorous look not just at the resources of firms as an impediment to sustainability but also at the ethical stances each firm size has on addressing sustainability issues. As a counterpart of CSR on SMEs, Lepoutre and Heene [22] provided a critical review of the impact of the firm size on Small Business Social Responsibility (SBSR). Their findings suggest that small business would likely experience more difficulties in engaging "socially responsible action" than larger counterparts. Similarly, Amato and Amato [31] examined the effects of firm size on corporate giving and found out that charitable giving rises with firm size up to a certain threshold and falls in medium-sized firms and rises up again at the upper end of large firm distribution. This implies that small and "upper end" large firms contribute to social programs on ethical stances as opposed to "brand image view" of other firm sizes. Nisim and Benjamin [36], on the other hand, discussed the public visibility as one of the key differences of firm sizes. This means that unlike large firms with high public exposure, CSR and sustainability related activities of SMEs tend to be out of sight from the public.

While previous studies established relationships between firm sizes and sustainability agenda and their differences, however, there is a significant gap in identifying the content of an MS that conforms to sustainability in relation to firm size. Such gap advances the link of firm size and sustainability by following a careful identification of strategy content. However, the current literature provides a limited help in critically evaluating the content of an MS for SMEs and large firms. This provides a possible direction to managers and policy-makers as decision support in critical and complex decision areas in manufacturing.

2.2. Stakeholders' Interests

The classical model of Skinner [2] and Wheelwright [3] on MS was mostly motivated by market requirements and behavior. As a result of buying experiences, dynamic needs, etc., the market creates a priority set of the four widely accepted competitive priorities, namely cost, quality, dependability and flexibility [1, 4, 17, 37]. This prioritization process of the market motivates the priority set of competitive priorities of a business unit which in turn directs the manufacturing function accordingly. This network of influences from the market to the business unit and to the manufacturing function and back to the business unit and market seems to function only when the market is solely the focal point of interest. However, this network could not cope with the conditions that demand simultaneous considerations of several stakeholders. The best example of these conditions is the demand of sustainability. Thus, an update of this network becomes necessary for addressing the complex interests of several stakeholders.

Recent studies have placed a great emphasis on the role of stakeholders in forging sustainability of manufacturing organizations [11, 16, 39-40]. Pham and Thomas [40] argue that traditional organizations tend to focus only on a handful, limited number of stakeholders with a special attention to shareholders, such as board of directors and investors. Griffiths and Petrick [39] contend that such an approach fails to develop stakeholder integration for firms. A widely accepted notion is that when stakeholders are managed well, they are capable of offering invaluable assistance and resources beyond simply exerting pressures on firms [41]. For instance, customers can possibly exert pressure on suppliers to establish corporate social responsibility practices either as a precondition for tendering to supply or as a complementary variable in their considerations of different suppliers [42]. On the other hand, employees can provide recommendations for advancing the firm's responsibility for the community by pointing out inputs related to the current socio-economic conditions of the local community. Suppliers play a critical role in providing insights which are associated with technology, materials and processes that could be helpful in strengthening firm's environmental efforts [43]. Harrison *et al.* [44] claim that manufacturing firms are likely to build trusting relations across several stakeholders when the firms include them in their key decision-making processes. With stronger relations with stakeholders, necessary insights for deciding how to allocate limited resources towards efforts that satisfy stakeholders could be certainly gained.

A growing body of literature claims that stakeholders play a significant role in the firm's sustainability efforts [42, 45]. Aside from exerting pressures on manufacturing firms, stakeholders could assist firms in deciding which environmental and social programs or initiatives to adopt because stakeholders have already established some forms of perspectives, experiences and resources vital in addressing sustainability issues. Creating programs that enhance close relations with employees and suppliers advances the capability of the firms in integrating the environmental aspects into key organizational processes. With the emerging issues on sustainability confronted by manufacturing firms, manufacturing organizations must proactively create value through investment in customers, suppliers, employees, processes, technology and innovation [40]. While these claims are significant, current studies are still leaning to a descriptive stance on the relationships between stakeholders and sustainability. Prescriptive approaches on how to evaluate strategies that address stakeholders along with the competitiveness agenda of MS are still lacking in current literature. These approaches are crucial in providing possible directions of manufacturing firms towards competitiveness and sustainability and at the same time serve as decision support tools for manufacturing decision-making.

2.3. Strategic Responses

The first work that attempts to group MS comprehensively was done by Sweeney [46]. The groupings were termed by Sweeney [46] as "generic manufacturing strategies" which include caretaker, marketeer, reorganizer and innovator strategies. Aside from this, Sweeney [46] also recognized transition routes from one strategy type to another strategy type. The idea was that manufacturing organizations tend to brand themselves into a particular stance on key decisions in developing MS. For instance, the environmental regulations being placed today by several institutional bodies eventually become a gauge in identifying the type of strategy manufacturing organizations engage. Some organizations become responsive to these regulations and take initiatives to further its responsibility for protecting the environment and the society. Others take a stance by merely complying with the minimum requirements being stipulated by a particular regulation. And, regretfully, some become irresponsive to these regulations.

In a similar argument, this discussion of generic manufacturing strategies was further refined by Miller and Roth [47]. Building upon this work, Frohlich and Dixon [48] supported the previous report on manufacturing taxonomies using different types of samples. However, with slight modifications, Frohlich and Dixon [48] identified three types of manufacturing strategies which are caretakers, marketeers and innovators. Aside from classifying MS types, Sweeney [46] provided this notion of transition paths or routes for firms to achieve the most positive form of strategy, which is an innovator strategy. This transition would guide firms to the manufacturing policies and competitive advantages they must place to support a particular route.

The discussion on this research domain became prominent following several works published in literature. Interestingly, there is a consistency in the types of strategic responses of manufacturing organizations as identified by the literature. With the influx of interests in sustainability, the former taxonomies were paralleled by the reactions or stances of firms toward the sustainability issues as described by the works of de Ron [49] and Heikkurinen and Bonnedahl [18]. Their works highlighted the three strategic responses that firms engage in embracing sustainability issues. These are stakeholder-oriented, market-oriented and sustainability-oriented. The proposed idea is that the concept of transition could similarly be applied to the transition of the strategic responses of manufacturing toward sustainability. This implies that firms are initially stakeholder-oriented and their policies are addressed at satisfying stakeholders' requirements. As they evolve around meeting these requirements, they transform their responses from stakeholder-orientation to market-orientation, developing strategies that extend stakeholder requirements into exploiting sustainability to create a competitive advantage. At this stage, firms view sustainability from a marketing perspective as a way to enhance market leadership in the industry. As firms enhance this, they evolve by achieving the sustainability-oriented stage wherein the goal extends from merely complying stakeholder requirements and attaining market leadership into a genuine care for the environment, the economy and the society. Despite these observations, the current literature fails to examine the impact of these strategic responses on developing a strategy that addresses sustainability and competitiveness.

3. Sustainable Manufacturing Strategy Decision Framework

Following the issues relevant to SMS, a proposed decision framework is presented in this section as shown in Figure 1. The framework consists of models that, by using appropriate methodology, are able to identify the content of SMS. The first decision model explores the impact of firm size on SMS development. This model consists of five decision components: goal, firm size, manufacturing decision categories, policy areas and policy options. The goal component comprises one single element which is the development of a SMS. Firm size has two elements: Small-Medium Enterprise (SME) and large firms. SMEs are those firms that have no more than 250 employees with annual sales of less than US$50 million [50]. Otherwise, firms are considered large firms. Manufacturing decision categories are those nine categories discussed in section 1. However, due to sustainability issues similar to those described by Johansson and Winroth [16] policy areas are revised to address these sustainability issues. Each policy area has policy options which constitute the SMS of the firm. These decision components are linked together in a decision network allowing interrelationships and interdependencies to take place. The model is expected to provide priorities of SMEs and large firms on their capability to develop SMS.

The second model explores the impact of competitive priority to SMS development. Unlike the former approach which considers only the market requirements as the main reference in attaching priorities in competitive dimensions, this model explores the integration of different stakeholders' interests as an influencing component to competitive priorities. This competitive priority set influences the kind of strategic response a firm would take in addressing sustainability. Then, the kind of strategic response a firm considers determines its SMS. The competitive priorities component consists of four elements: cost, quality, dependability and flexibility. The model is expected to provide priorities of each competitive priority in developing SMS. The significance of this model lies in its providing some guidelines on policy options when a specific competitive priority is chosen.

The third model is expected to draw some insights on the impact of strategic responses to manufacturing policy options. Developed from the previous two models, this model incorporates the hierarchical flow of strategy from a corporate strategy through strategic responses as described in the operational framework. A corporate strategy has one element which is the sustainability at a corporate level. The business strategy has two components: technology-oriented and market-oriented. MS has one element. Strategic responses have three elements: stakeholder-oriented, market-oriented and sustainability-oriented. The model is expected to provide priorities for each strategic response on the degree of its influence on developing an SMS. This model is significant as it provides guidelines to policy options for each strategic response.

Integrating the three models constitutes a quantitative unifying framework used to explore the integration of MS and SM fields in developing SMS.

4. Hypotheses and the Multi-Criteria Decision-Making Approach

Based on the proposed decision framework, the following hypotheses are set forth:

H1: Different firm sizes yield different configurations of sustainable manufacturing strategy.

H2: Manufacturing decision priority focus varies with different firm sizes.

H3: Government is the most influential stakeholder in developing a sustainable manufacturing strategy.

H4: Quality is the most important competitive priority in forging a sustainable manufacturing strategy.

H5: A technology-oriented business strategy enforces the development of a sustainable manufacturing strategy.

H6: A sustainability-oriented manufacturing strategy embodies a sustainable manufacturing strategy.

The integration of MS and SM in developing an SMS requires a decision framework that operates on manufacturing decision categories with components that share complex relationships. A Multi-Criteria Decision Analysis (MCDA) is relevant to this framework due to the following reasons: (1) the qualitative structure of the decision framework involving interests of different stakeholders, generic SM strategies, firm size, manufacturing capabilities, business and corporate strategies, (2) the complexity of decision components of the decision framework, (3) the interdependencies of the decision components, (4) uncertainty of the measurements of decision components, and (5) the inherent structure of assessment involving value judgments, assumptions and scenarios [51]. MCDA involves determining the overall preferences for several alternatives and choosing the best alternative subject to different criteria that may be tangible or intangible [52-53]. When the number of alternatives is finite, MCDA introduces Multi-Criteria Evaluation Methods (MCEM); otherwise, if it is infinite, it focuses on Multi-Criteria Design Methods (MCDM) [52]. MCEM has ELECTRE, ORESTE, PROMETHEE, Multi-Attribute Utility Theory (MAUT), AHP/ANP, regime method, convex cone approach, hierarchical interactive approach, fuzzy set theory and Bayesian analysis while MCDM has goal programming, data envelopment analysis, method of Geoffrion, Dyer and Feinberg, method of Zionts and Wallenius, reference point method, Pareto race, interactive weighted Tchebycheff procedure [52-53]. A survey of literature on MCDA applications implies that AHP/ANP and outranking methods are commonly used in industry-related applications [53].

Previous studies embarked on the use of MCDA methods in environmental or sustainability assessment. For instance, the widely-used AHP [54] is used in computing the product sustainability index [55], computing the sustainability index with time as an element [56], developing the sustainability index for a manufacturing enterprise [57], developing multi-actor multi-criteria approach in complex sustainability project evaluation [58], evaluating industrial competitiveness [59], evaluating energy sources [60], developing an AHP-based impact matrix and sustainability-cost benefit analysis [61] and developing a reverse logistics model [62]. This leaves AHP as the most prominent MCDA method in the sustainability assessment [63] especially in product and process design [54].

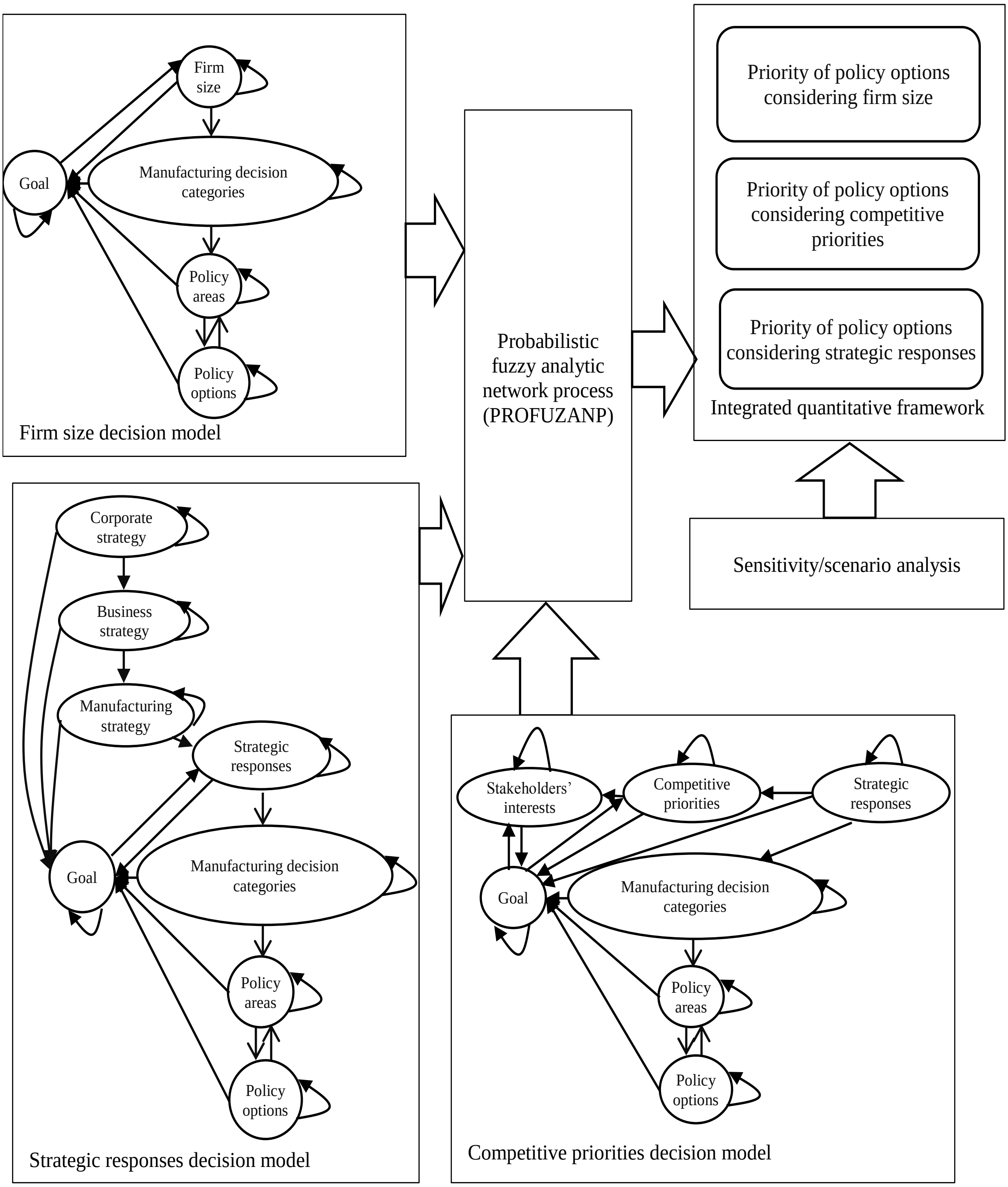

Figure 1. A sustainable manufacturing strategy decision framework

Some previous studies involving strategy selection and development used the MCDM methods. Barad and Gien [64] proposed a two-phased deployment process based on QFD and competitive priorities. Tsai and Chou [21] presented a hybrid approach combining DEMATEL, ANP and Zero-One Goal Programming (ZOGP) in the selection of management systems for phased implementation. Yu and Hu [65] proposed a fuzzy TOPSIS for evaluating the performance of manufacturing plants with productivity, production amount, production cost, inventory amount and quality cost as performance indicators for capability. Vinodh *et al.* [66] utilized fuzzy association rules mining used to evaluate the sustainability in the presence of attributes such as cost, market share performance, profitability, quality, toxicity, legislative factors, social cohesion, trade opportunities and flexibility. Vinodh and Girubha [67] proposed PROMETHEE based MCDM methodology in the selection of the best sustainable concept from the triple-bottom line wherein the sustainable concept is classified as material-oriented, product-oriented and manufacturing process-oriented. Al-Hawari *et al.* [68] applied AHP to select the best temperature measuring sensor for a certain industrial application. Dalalah *et al.* [69] explored AHP in crane selection for construction operations. Jajimoggala *et al.* [70] show the integration of AHP and TOPSIS for supplier selection problem under uncertainty. Chen *et al.* [71] explored a business strategy selection for green supply chain management using ANP. They agreed that AHP and ANP are appropriate analytical tools for addressing locations, programs or strategy selection problems. Zhou *et al.* [72] utilized mixed-integer programming and simulation models in the selection and evaluation of green production strategies. The model is able to provide trade-offs between green improvement and economic performance. With the same problem on the selection of Green Production (GP) strategies, Zhou *et al.* [73] proposed a hybrid approach of combining discrete-event simulation, multi-objective genetic algorithm to search for Pareto optimal values in the selection of GP strategies. Following these literatures, strategy development and selection fairly adopted MCDM methods particularly AHP/ANP.

For the proposed decision framework which is described in three different models, the hybrid methodological approach developed by Ocampo and Clark [74], as shown in Figure 2, especially for the conditions required to holistically address uncertainty in a group decision-making. A probabilistic fuzzy analytic network process is proposed by Ocampo and Clark [74], which is a hybrid approach that integrates Fuzzy Set Theory (FST), simulation and Analytic Network Process (ANP). The use of ANP is motivated from the complexity of the decision problems under consideration. It offers a flexible and viable approach in modelling the decision problem with various components and elements that are inherently connected in complex relationships. From a complex decision structure, ANP has the capability to measure the objective and the subjective elements of the decision problem based on a ratio-scale and then to synthesize them based on its supermatrix approach. Eventually, the ANP facilitates identification of the content of SMS which is the core problem of the present work.

A probabilistic fuzzy analytic network (PROFUZANP) approach is highly appropriate in the present work due to the following motivations:

1. the decision problem of developing SMS consists of several components with complex interrelationships
2. judgment elicitation must be done in linguistic variables to address uncertainty due to incomplete and imprecise information
3. the group of expert decision-makers could possibly be a quasi-collaborative group where the resulting group decision is also uncertain.

5. Conclusion

The present work expands the knowledge concerning: (1) the development of a sustainable manufacturing strategy and design of sustainability program based on consideration of both manufacturing strategy and sustainable manufacturing fields, and (2) the development of a framework used to guide decision-makers in sustainable manufacturing strategy development with relevant issues, such as firm size, competitive priority, strategic response and stakeholders' interests. Specifically, the interesting insights are: (1) the sustainable manufacturing strategy supports the competitive advantage of the firm, (2) the framework extends the traditionally market-perspective of strategy to a holistic approach which incorporates the interests of stakeholders to address sustainability, (3) stakeholders' interests are not independent but are allowed to interact with each other which happens in actual cases, (4) the framework explores the impact of firm size which other researchers failed to consider, (5) it also explores the impact of strategic responses of manufacturing on sustainability, (6) it also provides an opportunity to explore the relationship between the competitive strategies and decision areas, (7) the conceptual framework relates a sustainable manufacturing strategy to the best practices developed today. Several studies may be extended from this framework: (i) empirical studies using factor analysis or Structural Equation Modelling (SEM) could be conducted to test the validity of the proposed framework, (ii) development of a content sustainable manufacturing strategy using Multi-Criteria Decision Methods (MCDM) is seen as a fruitful work which creates a set of decisions on key manufacturing decision areas, (iii) optimization studies using multi-objective techniques of allocating firm's resources on the resulting manufacturing decisions, (iv) sequencing of firm's strategic decisions using artificial neural networks or meta-heuristic algorithms, and (v) identifying Key Performance Indicators (KPIs) of the sustainable manufacturing strategy.

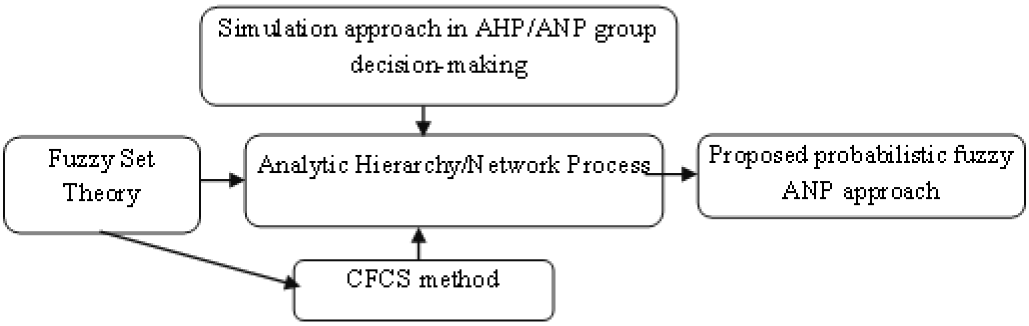

Figure 2. Proposed methodological framework (adopted from Ocampo and Clark [74])

6. Acknowledgement

The present work was part of the dissertation of L. Ocampo who expresses appreciation to the dissertation technical panel, especially to Dr. Anthony Chiu, Dr. Ma. Victoria Tibon, Dr. Michael Promentilla and Dr. Kathleen Aviso for the constructive comments on the proposed framework. The dissertation is funded by DOST Engineering Research and Development for Technology (ERDT) scholarship of the Department of Science and Technology, Republic of the Philippines. We thank the two anonymous reviewers for their insightful comments that improved the content of this work.

References

[1] Hayes RH, Wheelwright SC. Restoring our competitive edge: competing through manufacturing. John Wiley and Sons, New York; 1984.

[2] W. Skinner, "Manufacturing-missing link in corporate strategy". Harvard Business Review, Vol. 47 (1969), 136-145.

[3] S.C. Wheelwright, "Manufacturing strategy: defining the missing link". Strategic Management Journal, Vol. 5 (1984) No. 1, 1984, 77-91.

[4] S.C. Wheelwright, "Reflecting corporate strategy in manufacturing decisions". Business Horizons, Vol. 21 (1978) No. 1, 57-66.

[5] Brundtland, GH. Report of the world commission on environment and development: Our common future. Oxford, UK: Oxford University Press; 1987.

[6] M.K. Linnenluecke, A. Griffiths, "Corporate sustainability and organizational culture". Journal of World Business, Vol. 45 (2010) No. 4, 357-366.

[7] C.B. Joung, J. Carrell, P. Sarkar, S.C. Feng, "Categorization of indicators for sustainable manufacturing". Ecological Indicators, Vol. 24 (2013), 148-157.

[8] L.A. Ocampo, E.E. Clark, "Developing a framework for sustainable manufacturing strategies selection". DLSU Business & Economics Review, Vol. 23 (2014) No. 2, 115-131.

[9] A. Azab, A. Ziout, W. ElMaraghy, "Modeling and optimization for disassembly planning". Jordan Journal of Mechanical and Industrial Engineering, Vol. 5 (2011) No. 1, 1-8.

[10] Elkington, J. Cannibals with Forks: The Triple Bottom Line of 21st Century Business. Oxford: Capstone; 1997.

[11] G. Theyel, K. Hofmann, "Stakeholder relations and sustainability practices of US small and medium-sized manufacturers". Management Research Review, Vol. 35 (2012) No. 12, 1110-1133.

[12] M. Hallgren, J. Olhager, "Quantification in manufacturing strategy: a methodology and illustration". International Journal of Production Economics, Vol. 104 (2006) No. 1, 113-124.

[13] A. Azapagic, "Systems approach to corporate sustainability: a general management framework". Process Safety and Environmental Protection, Vol. 81 (2003) 5, 303-316.

[14] C. Reich-Weiser, A. Vijayaraghavan, D. Dornfeld, "Metrics for sustainable manufacturing". International Manufacturing Science and Engineering Conference, Illinois, 2008.

[15] A. Subic, B. Shabani, M. Hedayati, E. Crossin, "Capability framework for sustainable manufacturing of sports apparel and footwear". Sustainability, Vol. 4 (2012) No. 9, 2127-2145.

[16] G. Johansson, M. Winroth, "Introducing environmental concern in manufacturing strategies: implications for the decision criteria". Management Research Review, Vol. 33 (2010) No. 9, 877-899.

[17] R.H. Hayes, G.P. Pisano, "Manufacturing strategy: at the intersection of two paradigm shifts". Production and Operations Management, Vol. 5 (1996) No. 1, 25-41.

[18] P. Heikkurinen, K.J. Bonnedahl, "Corporate responsibility for sustainable development: a review and conceptual comparison of market-and-stakeholder-oriented strategies". Journal of Cleaner Production, Vol. 43 (2013), 191-198.

[19] B. Ageron, A. Gunasekaran, A. Spalanzani, "Sustainable supply chain management. An empirical study". International Journal of Production Economics, Vol. 140 (2012) No. 1, 168-182.

[20] K.M.Y. Law, A. Gunasekaran, "Sustainability development in high-tech manufacturing firms in Hongkong: motivators and readiness". International Journal of Production Research, Vol. 137 (2012) No. 1, 116-125.

[21] W.H. Tsai, W.C. Chou, "Selecting management systems for sustainable development in SMEs: A novel hybrid model based on DEMATEL, ANP, and ZOGP". Expert Systems with Applications, Vol. 36 (2009) No. 2, 1444-1458.

[22] J. Lepoutre, A. Heene, "Investigating the impact of firm size on small business social responsibility: a critical review". Journal of Business Ethics, Vol. 67 (2006) No. 3, 257-273.

[23] R. Banomyong, N. Supatn, "Developing a supply chain performance tool for SMEs in Thailand". Supply Chain Management: An International Journal, Vol. 16 (2011) No. 1, 20 – 31.

[24] Symeonidis G. Innovation, firm size and market structure: Schumpeterian hypotheses and some new themes. Economics Department Working Papers No. 161. Paris: OECD; 1996.

[25] S. Laforet, "Organizational innovation outcomes in SMEs: Effects of age, size, and sector". Journal of World Business, Vol. 48 (2013) No. 4, 490-502.

[26] H.E.J. Bos-Brouwers, "Corporate sustainability and innovation in SMEs: Evidence of themes and activities in practice". Business Strategy and the Environment, Vol. 19 (2010) No. 17, 417–435.

[27] A. Triguero, L. Moreno-Mondéjar, M.A. Davia, "Drivers of different types of eco-innovation in European SMEs". Ecological Economics, Vol. 92 (2013), 25-33

[28] J. Klewitz, E.G. Hansen, "Sustainability-oriented innovation of SMEs: a systematic review". Journal of Cleaner Production, Vol. 65 (2014), 57-75.

[29] Bronchain, P. Towards a sustainable corporate social responsibility. European Foundation for the Improvement of Living and Working Conditions, Luxembourg: Office for Official Publications of the European Communities; 2003.

[30] R. Vázquez-Carrasco, M.E. López-Pérez, "Small & medium-sized enterprises and Corporate Social Responsibility: a systematic review of the literature". Quality & Quantity, Vol. 47 (2013) No. 6, 3205-3218.

[31] L.H. Amato, C.H. Amato, "The effects of firm size and industry on corporate giving". Journal of Business Ethics, Vol. 72 (2007) No. 3, 229-241.

[32] N. Doi, M. Cowling, "The evolution of firm size and employment share distribution in Japanese and UK manufacturing: a study of small business presence". Small Business Economics, Vol. 10 (1998), 283-292.

[33] S. Schrettle, A. Hinz, M. Scherrer –Rathje, T. Friedli, "Turning sustainability into action: Explaining firms' sustainability efforts and their impact on firm performance". International Journal of Production Economics, Vol. 147 (2014), 73-84.

[34] M. Bourlakis, G. Maglaras, E. Aktas, D. Gallear, C. Fotopoulos, "Firm size and sustainable performance in food supply chains: Insights from Greek SMEs". International Journal of Production Economics, Vol. 152 (2014), 112-130.

[35] P.H. Howard, D. Jaffee, "Tensions between firm size and sustainability goals: fair trade coffee in the United States". Sustainability, Vol. 5 (2013) No. 1, 72-89.

[36] S. Nisim, O. Benjamin, "Power and size of firms as reflected in cleaning subcontractors' practices of social responsibility". Journal of Business Ethics, Vol. 83 (2008) No. 4, 673-683.

[37] C.H. Fine, A.C. Hax, "Manufacturing strategy: a methodology and an illustration". Interfaces, Vol. 15 (1985) No. 6, 28-46.

[38] P.T. Ward, D.J. Bickford, G.K. Leong, "Configurations of manufacturing strategy, business strategy, environment and structure". Journal of Management, Vol. 22 (1996) No. 4, 597-626.

[39] A. Griffiths, J.A. Petrick, "Corporate architectures for sustainability". International Journal of Operations and Production Management, Vol. 21 (2001) No. 12, 1573-1585.

[40] D.T. Pham, A.J. Thomas, "Fit manufacturing: a framework for sustainability". Journal of Manufacturing Technology Management, Vol. 23 (2012) No. 1, 103-123.

[41] N. Misani, "The convergence of corporate social responsibility practices". Management Research Review, Vol. 33 (2010) No. 7, 734-748.

[42] D. Baden, I. Harwood, D. Woodward, "The effect of buyer pressure on suppliers in SMEs to demonstrate CSR practices: an added incentive or counterproductive?". European Management Journal, Vol. 27 (2009) No. 6, 429-441.

[43] M. Cheung, M.B. Myers, J.T. Mentzer, "The value of relational learning in global buyer-supplier exchanges: a dyadic perspective and test of the pie-sharing premise". Strategic Management Journal, Vol. 32 (2011) No. 10, 1061-1082.

[44] J. Harrison, D. Bosse, R. Philips, "Managing for stakeholders, stakeholder utility functions, and competitive advantage". Strategic Management Journal, Vol. 31 (2010) No. 1, 58-74.

[45] A. Paloviita, V. Luoma-aho, "Recognizing definitive stakeholders in corporate environmental management". Management Research Review, Vol. 33 (2010) No. 4, 306-316.

[46] M.T. Sweeney, "Towards a unified theory of strategic manufacturing management". International Journal of Operations and Production Management, Vol. 11 (1991) No. 8, 6-23.

[47] J.G. Miller, A.V. Roth, "A taxonomy of manufacturing strategies". Management Science, Vol. 40 (1994) No. 3, 285-304.

[48] M.T. Frohlich, J.R. Dixon, "A taxonomy of manufacturing strategies revisited". Journal of Operations Management, Vol. 19 (2001) No. 5, 541-558.

[49] A.J. de Ron, "Sustainable production: the ultimate result of a continuous improvement". International Journal of Production Economics, Vol. 56-57 (1998), 99-110.

[50] M.E. Gonzalez, G. Quesada, C. Mora-Monge, "An international study on manufacturing competitive priorities". Journal of Management Policy and Practice, Vol. 13 (2012) No. 3, 116-128.

[51] R. Heijungs, G. Huppes, J.B. Guinee, "Life cycle assessment and sustainability analysis of products, materials and technologies: toward a scientific framework for sustainability life cycle analysis". Polymer Degradation and Stability, Vol. 95 (2010) No. 3, 422-428.

[52] K.T. Cho, "Multicriteria decision methods: an attempt to evaluate and unify". Mathematical and Computer Modeling, Vol. 37 (2003) No. 9-10, 1099-1119.

[53] M. Herva, E. Roca, "Review of combined approaches and multi-criteria analysis for corporate environmental evaluation". Journal of Cleaner Production, Vol. 39 (2013), 355-371.

[54] N. Subramanian, R. Ramanathan, "A review of applications of analytic hierarchy process in operations management". International Journal of Production Economics, Vol. 138 (2012) No. 2, 215-241.

[55] Gupta A, Vangari R, Jayal AD, Jawahir IS. Priority evaluation of product metrics for sustainable manufacturing. In: Bernard A, editor. Global Product Development, 2011, pp. 631-641.

[56] D. Krajnc, P. Glavic, "A model for integrated assessment of sustainable development". Resources, Conservation and Recycling, Vol. 43 (2005) No. 2, 189-208.

[57] I.H. Garbie, "Framework of manufacturing enterprises sustainability incorporating globalization issues". 41st International Conference on Computers and Industrial Engineering, Los Angeles, California, 2011.

[58] K. de Brucker, C. Macharis, A. Verbeke, "Multi-criteria analysis and the resolution of sustainable development dilemmas: a stakeholder management approach". European Journal of Operational Research, Vol. 224 (2013) No. 1, 122-131.

[59] S.B. Sirikrai, J.C.S. Tang, "Industrial competitiveness analysis: using the analytic hierarchy process". Journal of High Technology Management Research, Vol. 17 (2006) No. 1, 71-83.

[60] A.I. Chatzimouratidis, P.A. Pilavachi, "Technological, economic and sustainability evaluation of power plants using the analytic hierarchy process". Energy Policy, Vol. 37 (2009) No. 3, 778-787.

[61] M.S. Chiacchio, "Early impact assessment for sustainable development of enabling technologies". Total Quality Management and Excellence, Vol. 39 (2011) No. 3, 1-6.

[62] T.J. Barker, Z.B. Zabinsky, "A multicriteria decision-making model for reverse logistics using analytical hierarchy process". Omega, Vol. 39 (2011) No. 5, 558-573.

[63] S. Seuring, "A review of modeling approaches for sustainable supply chain management". Decision Support Systems, Vol. 54 (2013) No. 4, 1513-1520.

[64] M. Barad, D. Gien, "Linking improvement models to manufacturing strategies–a methodology for SMEs and other enterprises". International Journal of Production Research, Vol. 39 (2001) No. 12, 2675-2695.

[65] V.F. Yu, K. Hu, "An integrated fuzzy multi-criteria approach for the performance evaluation of multiple manufacturing plants". Computers & Industrial Engineering, Vol. 58 (2010) No. 2, 269-277.

[66] S. Vinodh, K.E. Selvan, N.H. Prakash, "Evaluation of sustainability using fuzzy association rules mining". Clean Technology and Environmental Policy, Vol. 13 (2011) No. 6, 809-819.

[67] S. Vinodh, R. Girubha, "PROMETHEE based sustainable concept selection". Applied Mathematical Modelling, Vol. 36 (2012) No. 11, 5301-5308.

[68] T. Al-Hawari, S. Al-Bo'ol, A. Momani, "Selection of temperature measuring sensors using the analytic hierarchy process". Jordan Journal of Mechanical and Industrial Engineering, Vol. 5 (2011) No. 5, 451-459.

[69] D. Dalalah, F. AL-Oqla, M. Hayajneh, "Application of the analytic hierarchy process (AHP) in multi-criteria analysis of the selection of cranes". Jordan Journal of Mechanical and Industrial Engineering, Vol. 4 (2010) No. 5, 567-578.

[70] S. Jajimoggala, V.V.S.K. Rao, S. Beela, "Supplier evaluation using fuzzy analytical network process and fussy TOPSIS". Jordan Journal of Mechanical and Industrial Engineering, Vol. 5 (2011) No. 6, 543-551.

[71] C.C. Chen, H.S. Shih, H.J. Shyur, K.S. Wu, "A business strategy selection of green supply chain management via an analytic network process". Computers and Mathematics with Applications, Vol. 64 (2012) No. 8, 2544-2557.

[72] M. Zhou, Y. Pan, Z. Chen, W. Yang, B. Li, "Selection and evaluation of green production strategies: analytic and simulation models". Journal of Cleaner Production, Vol. 26 (2012), 9-17.

[73] M. Zhou, Y. Pan, Z. Chen, W. Yang, "Optimizing green production strategies: an integrated approach". Computers and Industrial Engineering, Vol. 65 (2013) No. 3, 517-528.

[74] L.A. Ocampo, E.E. Clark, "A framework for capturing uncertainty of group decision-making in the context of the Analytic Hierarchy/Network Process". Advances in Industrial Engineering and Management, Vol. 3 (2014) No. 3, 7-16.

JJMIE

Volume 9 Number 3, June.2015
ISSN 1995-6665
Pages 187 - 193

Jordan Journal of Mechanical and Industrial Engineering

Determining the Optimum Tilt Angle for Solar Applications in Northern Jordan

Qais Azzam Khasawneh [a*], Qatada Abdullah Damra[b], Omaymah Husni Bany Salman[b]

[a] Assistant Prof., Chairman of Mechanical Engineering Dept. ,Jordan University of Science and Technology, P.O. Box 3030, Irbid, Jordan
[b]Masters Students at Mechanical Engineering Dept. Jordan University of Science and Technology, P.O. Box 3030, Irbid, Jordan

Received 31 Dec 2014 Accepted 31 May 2015

Abstract

Determining the optimum tilt angle for PV system based power plants is crucial to be considered when fixing the PV systems. Although the optimum tilt angle is normally close to the latitude value of the location, lots of other factors affect this. So when designing a power plant, it is necessary to take these factors into consideration to maximize the output of those plants. The present paper reviews the main scientific concepts related to solar radiation, the models used to describe the solar radiation properties, and the methods of calculating the optimum tilt angle. The optimum tilt angle for northern Jordan and, as a case study, Jordan University of Science and Technology (JUST) Campus is then calculated by applying the appropriate methods and models. In addition to that, simulation software is used to calculate the optimum tilt angle and the yield of the power station. Other factors affecting the tilt angle of a PV array are reported and relevant recommendations are given.

Keywords: *Solar Radiation, Tilt Angle, Photovoltaic, Optimum Tilt, PV Power Plants*.

1. Introduction

The lack of energy resources is one of the most challenging problems that face the economic development in Jordan; the situations are worsened even by the overall regional political disturbances around Jordan, which resulted in cutting the energy supply lines (Egyptian gas and Iraqi oil), raising the fears of energy security and causing tremendous losses in the sector of electricity generation.

Renewable energy is widely looked at as a sustainable solution that can push the wheel of development; Jordan has a good potential for renewable and solar resources in particular [1-13]. It has plans to increase the share of renewable energy in its energy mix up to 15% by 2020. Solar energy and, particularly, photovoltaics are among the main technologies that Jordan relies on to achieve its renewable energy targets [14] and to meet the increasing demand on electrical energy, especially at the northern part of Jordan.

Jordan University of Science and Technology (JUST) is located near to Irbid, north of Jordan, at (32°29' N 35°59' E). It is one of the leading universities in Jordan and the Middle East in academic and technology transfer fields. It was ranked 49th by UI Green Metric World University Ranking in 2013[18] and the 1st among the Arab universities. JUST is planning to build a 5 MWp PV power station as part of its continuous efforts toward a sustainable and green campus, besides lowering the electricity bill bought from the national grid. The station will serve the educational purposes of the university by providing practical training to the students on actual utility scale PV systems. [20]

There are many factors that affect the Levelized Cost of Electricity (LCE) that is generated from PV source; some of these factors are installation conditions, including the orientation of the PV array, distance between strings, and, most importantly, the tilt angle. [16,17,19]

The tilt angle of the solar panel affects the output of the PV array as it changes the amount of solar radiation incident on the panel; therefore, installing PV panels at an optimum angle helps reducing the LCE by increasing the energy production for the same installation. Furthermore, understanding the effect of the tilt angle and the orientation helps in predicting the yield of a specific system where the panel's tilt angle or orientation is fixed, such as rooftops applications in which the orientation and slope of the roof determine the tilt angle and the orientation of the panel.

The present paper reviews the main scientific concepts related to solar radiation, in addition to the methods used in predicting the solar radiation to be applied for obtaining the optimum tilt angle. Finally, some recommendations

* Corresponding author. e-mail: qakhasawneh@just.edu.jo.

will be suggested regarding the optimum tilt angle for northern part of Jordan.

2. Solar Radiation

Solar radiation can best be approximated to the radiation of a black body with a temperature of 5780 K in both intensity and spectrum. Taking this into consideration, the extraterrestrial solar radiation falling on a surface normal to the sun's rays at the mean sun earth distance, which is also called the solar constant, can be calculated using equation 1:

$$G_{sc} = \sigma T^4 . \frac{r_s^2}{r_{se}^2} \qquad (1)$$

The solar constant is approximately equal to 1367 W/m2; this value is an approximation based on the distance between the earth and the sun, which is equal to 1AU. And since the earth's orbit around the sun is elliptical, then the Gsc value may change slightly (about +3.3%) due to the change in the distance between the earth and the sun. This value was verified experimentally and the World Meteorological Organization (WMO) chose the average value 1367 W/m2 as the solar constant.

2.1. Diffusion of Solar Radiation

The solar radiation is subjected to several radiation attenuating effects when it travels across the atmosphere. There are two general cases of attenuating effects: absorption and scattering (reflection is a special case of scattering). The radiation that is neither scattered nor absorbed and reaches the surface directly from the sun disk is called direct radiation, while the scattered radiation that reaches the ground is called diffused radiation.

The radiation extinction depends on different factors, such as: humidity, cloud coverage, other residual particles; those factors can only be determined by measurements, while others can be calculated (such as the path length of the solar beam from the top of the atmosphere to a given location on the earth's surface, which is called the air mass), and it is a function of the geographic altitude of a certain location and the solar zenith angle Θ_z at that location, but it can be simplified using Eq. 2. [21]:

$$AM = \frac{1}{\cos\theta_z} \qquad (2)$$

2.2. Solar Radiation on Tilted Surfaces and Radiance Distribution over the Sky

In order to determine the incident radiation on a tilted surface, the measured value of radiation on a horizontal surface can be used in addition to the direction of the beam and the diffused radiation component.

The distribution of the solar diffused radiance over the sky is shown in Figure 1. It consists of three components: isotropic dome, where the diffused radiation is uniform over the sky dome, circumsolar brightening [22], which is concentrated at the center of the sun, and horizon brightening, which is assumed to be a line source concentrated at the horizon; the latter results from radiation reflected from the ground, thus the horizontal brightening is a function of ground reflection (albedo). Clear sky diffused radiation is maximized at the horizon and decreases when moving away from the horizon and the radiance increases away from the horizon at the overcast skies, specific solar angles on tilted surfaces are shown in Figure 2.

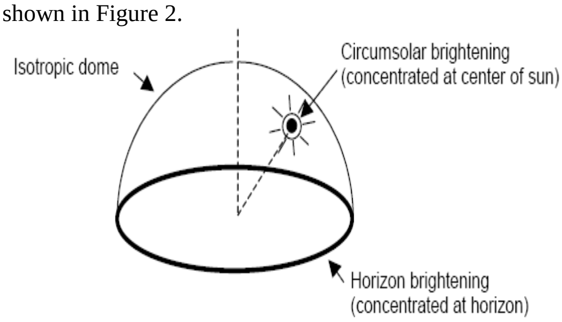

Figure 1. Distribution of diffused radiance [22]

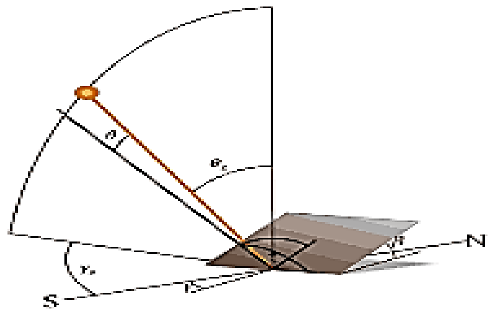

Figure 2. Solar radiation angles [21]

The isotropic model, which assumes that the diffused radiation is uniform over the sky dome, can describe the overcast or cloudy sky, while the anisotropic model, which includes diffused sky radiation in the circumsolar and horizon brightening components of the solar radiation, is more accurate in describing clear sky. Isotropic diffused solar radiation can be obtained by the following equations:

$$G_T = G_{T,b} + G_{T,d} + G_{T,ref} \qquad (3)$$

$$G_{T,d} = G_d \left(\frac{1+\cos\beta}{2}\right) \qquad (4)$$

$$G_{T,ref} = G_{ref} \left(\frac{1-\cos\beta}{2}\right) \qquad (5)$$

$$G_{T,b} = G_b . R_b \qquad (6)$$

$$R_b = \frac{\cos(\varphi-\beta)\cos\delta\sin\omega_s + \left(\frac{\pi}{180}\right)\omega_s'\sin(\varphi-\beta)\sin\delta}{\cos(\varphi)\cos\delta\sin\omega_s + \left(\frac{\pi}{180}\right)\omega_s\sin(\varphi)\sin\delta} \qquad (7)$$

$$\omega_s' = \cos^{-1}(-tan(\varphi-\beta).tan\delta) \qquad (8)$$

The previous equations are based on Liu and Jordan model which is one of the simplest and earliest models. Anisotropic models should take into consideration two more components, as the following equation shows:

$$G_T = G_{T,b} + G_{T,d,iso} + G_{T,d,os} + G_{T,d,hc} + G_{T,ref} \qquad (9)$$

where,
G_T is the global radiation
$G_{T,b}$ is the beam radiation
$G_{T,d,iso}$ is the isotropic component
$G_{T,d,cs}$ is the circumsolar component

$G_{T,d,hz}$ is the Horizontal brightening component

$G_{T,d,ref}$ is the reflected radiation component

Researchers have introduced a variety of isotropic and anisotropic models, suggesting relations to determine the ratio of the average daily diffused radiation incident on an inclined surface to that on a horizontal surface (R_d). A. K. Yadav and S. S. Chandel conducted a review of the solar radiation models, where each model had its own limitations and conditions [23]. Nooriana *et al.* made an evaluation in which 12 models where investigated to estimate the hourly diffused radiation on inclined surfaces and compared the results to actual measured data [24]. If one of those models can be validated for a certain place and atmospheric conditions, an optimum tilting angle can be reached by varying tilt angle (β) from 0 to 90 until the solar radiation on the tilted surface is maximized.

3. Optimum Tilt Angle Calculation

Failing to install PV panels at its optimum tilt angle leads to the loss of the potential solar power. The optimum tilt angle calculations are based on maximizing the solar radiation falling on a sloped surface using different optimization techniques. In [23], the authors summarized some of the relations between the latitude and the optimum tilt angle.

This section shows the work of different researchers who have determined optimum tilt angles analytically or experimentally for a number of locations.

Skeiker [26] used a mathematical model to estimate the daily optimum tilt angle according to equation (10), and a monthly optimum tilt angle according to equation (11) for many locations in Syria, and, in addition to that, the seasonal and annual optimum tilts angles. The annual optimum tilt angle for Daraa (on the northern border of Jordan – 32°37′N 36°6′E) was *ß* = 30.13°, monthly, and the seasonal tilt angles energy gains were 28% and 26%, respectively. A major concern regarding this model was that it took into consideration the varying tilt angle to the maximize extraterrestrial radiation but disregarded the attenuation effects that changes the properties of the solar radiation. Soulayman [27] commented on Skeiker work and set all the negative values of the tilt angles to zero, identifying some other errors in his methodology.

$$\beta_{opt,d} = \emptyset - \tan^{-1}\left[\frac{h_{ss}}{\sin(h_{ss})}\tan(\delta)\right] \tag{10}$$

$$\beta_{opt,m} = \emptyset - \tan^{-1}\frac{X}{Y}$$

$$X = \sum_{n=n1}^{n=n2}\frac{24}{\pi}I_0\left[1+0.034\cos\left(\frac{2\pi n}{365}\right)\right]\sin(\delta)h_{ss} \tag{11}$$

$$Y = \sum_{n=n1}^{n=n2}\frac{24}{\pi}I_0\left[1+0.034\cos\left(\frac{2\pi n}{365}\right)\right]\cos(\delta)\sin(h_{ss})$$

Agha and Sbita [28] conducted a study for four different locations in Libya to determine the optimum tilt angle for the solar systems using an accurate simple sizing method rather than numerical methods. The selection criterion for the optimum tilt angle was based on an optimization factor (F_{opt}) as shown in equation (12):

$$F_{opt}(\beta) = H_{avg}(\beta)/SDEV(\beta) \tag{12}$$

where H_{avg} is the monthly average of the daily total of the solar irradiation (kWh/m^2.day), SDEV is the standard deviation of the curve that represents the divergence between the normalized load curve and normalized solar irradiation curve at a certain angle.

One of the cities, included in this study, is Tripoli, *Lat.*=32.87° which is close to that of the northern part of Jordan. The optimum tilt angle for Tripoli is about 25°. One of the assumptions of the present study is, excluding the cloudy days, even though Tripoli is a coastal city, both Tripoli and Jordan have a near latitude but concerning other factors, like the weather conditions and temperature variation, solar radiation, etc., which affect the optimum tilt angle, they are different.

Moghadam *et al.* [29] conducted a study to determine the optimum tilt angle of the solar collectors in Iran by making a simulation using MATLAB program. Iran is located on the sun belt of the world and has a high value of solar radiation; it is mostly sunny all year around. Moghadam *et al.* [29] calculated the monthly, seasonal, semi-annual and annual optimum tilt angles for Zahedan city (*latitude* = 29.49°). The annual optimum tilt angle for Zahedan was equal to 28°. The study also found that the tilt angle was equal to 5° in the first half of the year and 50° in the second half and if the tilt angle is adjusted two times in a year, the total annual extra received energy will be more than 8% .

Talebizadeh [30] developed new correlations to calculate the monthly, seasonal, and yearly optimum slope angles for latitudes of 20° to 40° north, suggesting that the annual optimum tilt angle was $\beta_{opt} = 0.6804\emptyset + 7.203$. Therefore, the optimum for locations in northern Jordan equals 29.17°. The correlations were obtained according to the optimum slope angles predicted by the researcher and using the optimum slope angles achieved by other researchers at locations out of Iran but in the same range of latitudes; the results showed that the optimum azimuth angle is zero for receiving maximum solar energy.

It can be noticed that the previous results are consistent with the simple and general correlations to determine the optimum tilt angle depending only on the latitude that can be used as a rule of thumb, such as Heywood [31] who came up with the following equation:

$$\beta_{opt} = \emptyset - 10^{\circ} \tag{13}$$

According to equation 13, the optimum tilt angle in the northern part of Jordan is equal to 22.29 degree. Or Lunde [32] suggested the following equation:

$$\beta_{opt} = \emptyset \pm 15^{\circ} \tag{14}$$

The optimum tilt angle for the northern part of Jordan, according to equation 14, is equal to 17.5 in summer, 47.5 in winter, where the plus and minus signs are used for the winter and summer seasons.

Duffie and Beckman [33] suggested that the optimum tilt is in the range of the latitude plus 10° to the latitude plus 20°, and the variation of 10° either way outside of this range, so, accordingly, the optimum tilt angle (*ß*) is equal to 52.29° - 62.29°, in winter, and from 32.29° to 42.29°, in summer. That was determined to insure the visibility of a thermal system recommendation but is not expected to be accurate within the view of a PV system.

4. PV System Simulation

PVSYST is a simulation tool that can be used to calculate all the design parameters for a PV system; it uses an anisotropic model (transposition: Perez, Diffuse: Erbs) and uses Meteonorm solar radiation data with long-term solar radiation measured values. Figure 3 represents the main parameters that are entered into the simulation software. The simulation is based on hourly values, using PVSYST, the optimum tilt angle all over the year is about 30°, as shown in Figure 4. Meanwhile, the seasonal tilt angle is about 10°, in summer, and 50°, in winter, as shown in Figure 5 and 6.

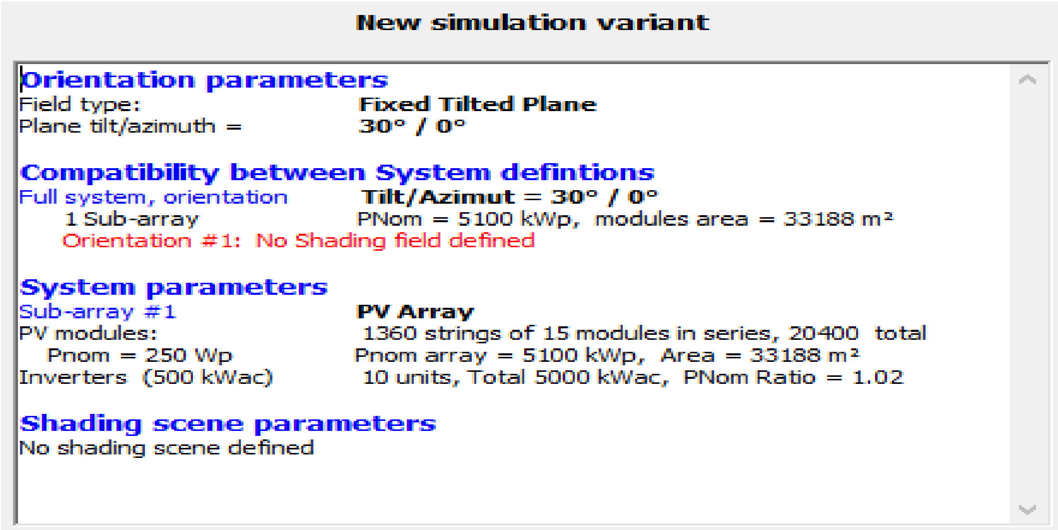

Figure 3. Parameters of the Simulation

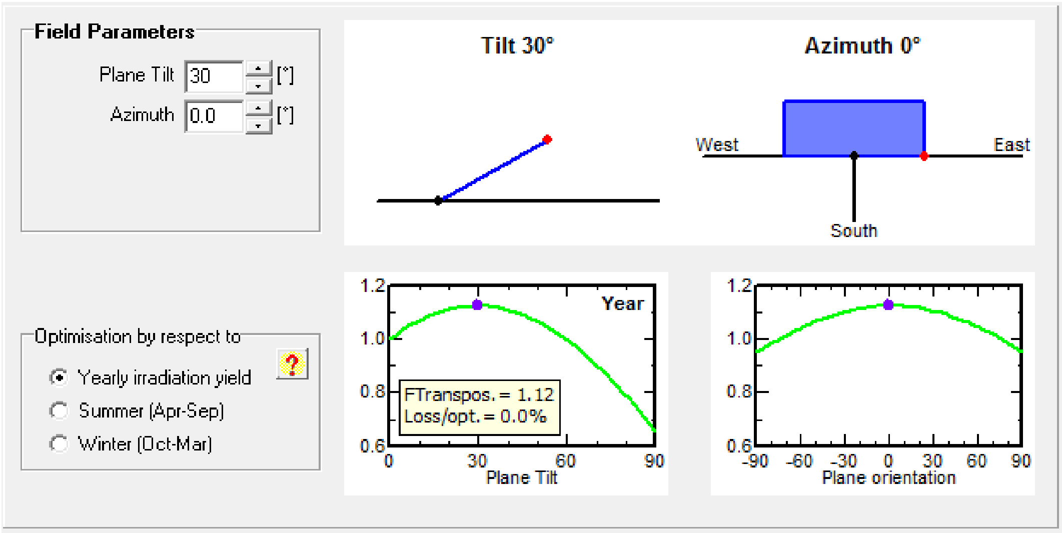

Figure 4. Year optimized angle

The yield of the 5 MWh PV solar system was also simulated using the software and meteorological data of Jerusalem city (31.8°N , 35.2°E). The main simulation results are shown in the Figure 7:

5. Applying Results to JUST Station

Most of the relations from the literature lead to an optimum angle between 22° and 30°, though other factors should be taken into consideration in order to get a practical result. Those factors can be summarized as follows:

- The above relations do not take the altitude into consideration.
- The above relations rely only on the idea of maximizing radiation, that might be the general case, but in winter the threshold of the inverter might not be satisfied in a few days due to small radiation; if such days are excluded from the calculations, the result may shift toward the summer optimum angle.
- There might be some weather conditions occurring over parts of the day during the year, such as a summer cloud cover in the afternoon, which might change the results depending on its frequency.
- Some geographic features may play a role in determining the optimum tilt angle and the orientation of the array.
- Land usage and the PV array shading losses are also important issues in a multi-line array.

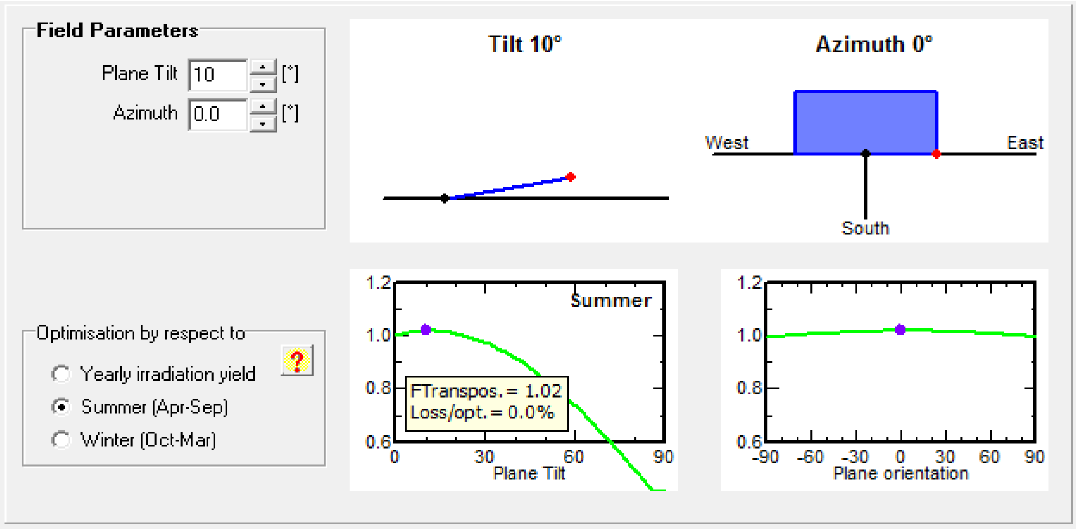

Figure 5. Summer optimized angle

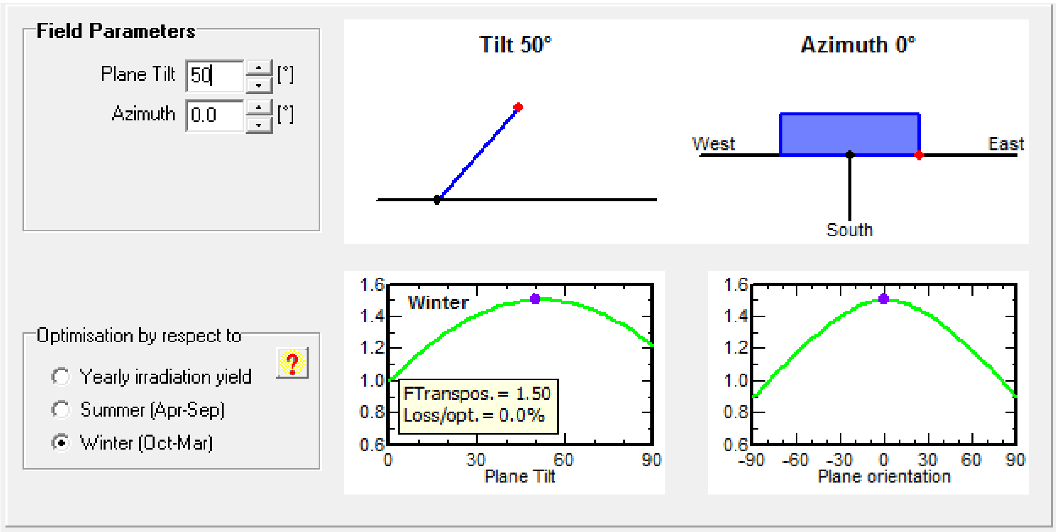

Figure 6. Winter optimized angle

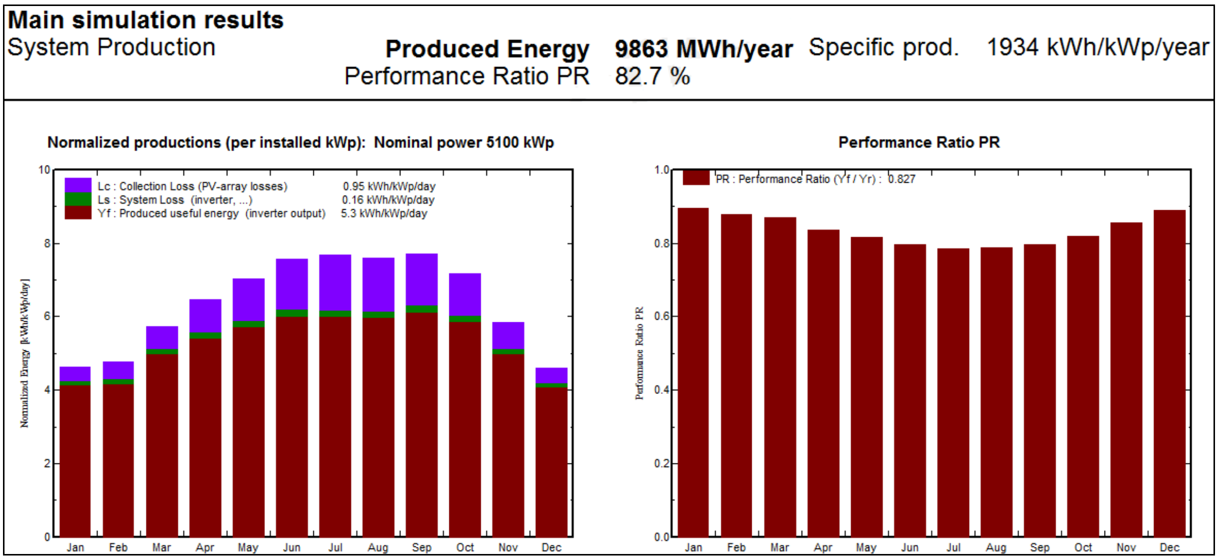

Figure 7. Main simulation results

Table 1. The different results based on references

Author	Result for JUST (32.29oN)
Etier [4]	30° @ 32.05°N
Skeiker[26]	30.56o @32.37oN
Agha and Sbita[27]	25o @32.87oN
Moghadam [28]	28o @29.49N
Talebizadeh [29]	29.17o
Heywood [30]	22.29o
Lunde[31]	32.29o
PVSYST	@ 31.8N

Based on the result of the simulation of the optimum tilt angle is 30° and Summer optimum tilt angle 10° and winter optimum tilt angle 50° as Table 2 shows:

Table 2. The yield of the 5MWp System in MWh per deferent tilt angle

Month	tilt=10°	tilt=30°	tilt=50°	best tilt	best value
January	527	655.8	714.7	50	714.7
February	517	596.4	617.7	50	617.7
March	735	788.3	769.8	30	788.3
April	830	829.2	755.7	10	830
May	965	904.5	766.1	10	965
June	1024	920.2	738.1	10	1024
July	1040	949.6	775.5	10	1040
August	974	944.9	831.5	10	974
September	892	938	897.6	30	938
October	804	926.7	957.9	50	957.9
November	617	764	829.6	50	829.6
December	508	645.7	731.5	50	731.5
Year	9433	9863.3	9385.7	30	10410.7

The simulation shows that if the variable tilt angle is adopted the yield of the system will increase decently; Table 3 demonstrates the cases simulated and provides a summary of the results. The result is consistent with other results obtained by other researchers in the literature; though the results are not identical due to the different location [15, 26 and 27]. The result obtained by 26 and 27 are the yield solar radiation, not the electric yield. And the value of the additional yield was calculated based on 0.20 JD/kWh.

Table 3. The yield of the 5MWp System with different cases

Case	Year optimum tilt	Simi annually tilt	quarter annually tilt	Monthly tilt
Yield (MWh)	9863.3	10328	10410.7	10465.8
Increment (%)	0	4.71	5.55	6.11
Value of the Additional energy (JD)	0	92940	109480	120500

6. Conclusions

Using the correlation and data available in the literature, an optimum angle was found to be around 30°; this result was verified by PV SYS software. To get an accurate and a confirmed value, we need to study the different radiation models and decide which one applies best to JUST site and, then, run our own simulation based on an hourly measured direct and diffused solar radiation. A system with a changeable tilt angle, on a monthly basis or seasonal basis, may increase the yield of the system to about 6%, 5.5%, respectively. For the case of the monthly optimum angle that can be about 600 MWh per year for JUST site, this result is consistent with other results from the literature with a small difference due to the variance in latitude [15].

References

[1] Ministry of Energy and Mineral Resources, Energy Statistics, Amman Jordan 2013.

[2] Y. Anagreh, A. Bataineh, “Renewable energy potential assessment in Jordan”. Renewable and Sustainable Energy Reviews, Vol. 15 (2011) No. 5, 2232–2239.

[3] F. Abdulla, M. Widyan, Z. Al-Ghazawi, S. Kiwan, H. Abu-Qdais, M. Hayajneh, A. Harb, M. Al-Nimr, “Status of Jordan Renewable Energy Sector: Problems, Needs and Challenges” , School of Engineering, Jordan University of Science and Technology, Irbid 2004.

[4] I. Etier, A. Al Tarabsheh , and M. Ababne, “Analysis of Solar Radiation in Jordan”. Jordan Journal of Mechanical and Industrial Engineering”, Vol. 4 (2010) No. 6, 733 – 738.

[5] Mohsen, Mousa, “Potential for Wind-Powered Desalination Systems in Jordan”. International Journal of Thermal & Environmental Engineering, Vol. 1 (2010) No. 2, 109 – 123.

[6] K. Bataineh, D. Dalalah, “Assessment of wind energy potential for selected areas in Jordan”. Renewable Energy, Vol. 59 (2013), 75-81.

[7] M.A. Alsaad,“Wind energy potential in selected areas in Jordan”. Energy Conversion and Management, Vol. 65 (2013), 704–708.

[8] J. Hojstrup,"Wind Atlas for Jordan". Riso National Laboratory, Roskilde, Denmark, (1989).

[9] M. Al Zou'bi, “Renewable Energy Potential and Characteristics in Jordan”. Jordan Journal of Mechanical and Industrial Engineering, Vol. 4 (2010) No. 1, 45 – 48.

[10] M. Ababneh, W. Kakish, O. Abu Mohareb, I. Etier, “Investigation of Wind Energy in Jordan”. International Conference and Exhibition on Green Energy and Sustainability for Arid Regions and Mediterranean Countries ICEGES, Amman, Jordan, 2009.

[11] G. Halas, “Wind-Solar Hybrid Electrical Power Generation in Jordan”. Jordan Journal of Mechanical and Industrial Engineering , Vol. 4 (2010) No. 1, 205 – 209.

[12] R. Al-Sayed, “Status of Renewable Energy in Jordan”. IEEE 1st International Conference & Exhibition on the Applications of Information Technology in the Development of Renewable Energy processes & System IT-DREPS, Amman, Jordan 2013.

[13] O. Badran, E. Abdulhadi, R. Mamlook, “Evaluation of Solar Electric Power Technologies in Jordan”, Jordan Journal of Mechanical and Industrial Engineering, Vol. 4 (2010) No. 1, 121 – 128.

[14] Ministry of Energy and Mineral Resources, Updated Master Strategy of Energy Sector in Jordan for the period (2007-2020). http://www.memr.gov.jo/LinkClick.aspx?fileticket=ZtYRN7m6wYU%3d&tabid=255

[15] M. Despotovic, V. Nedic, “Comparison of optimum tilt angles of solar collectors determined at yearly, seasonal and monthly levels”. Energy Conversion and Management, Vol. 97 (2015), 121-131.

[16] A. El-Sebaii, F. Al-Hazmi, A. Al-Ghamdi, S. Yaghmour, “Global, direct and diffuse solar radiation on horizontal and

tilted surfaces in Jeddah, Saudi Arabia", Applied Energy, Vol. 87 (2010) No. 2, 568-576.

[17] C. Demain, M. Journee, C. Bertrand. "Evaluation of different models to estimate the global solar radiation on inclined surfaces". Renewable Energy, Vol. 50 (2013), 710-721.

[18] UI GreenMetric World University Ranking, World Ranking 2014, http://greenmetric.ui.ac.id/ranking/detailUniv/2014/just.edu.jo

[19] Z. Al-Hammouri, "JUST Ranked 49 World Wide and the First among Arab Universities in UI Green Metric", JUST news center, 2015 http://www.just.edu.jo/NewsCenter/Lists/JustNews/DisplayItem.aspx?ID=484

[20] Tender Documents for the Project Photovoltaic Power Station(s) at Jordan University of Science and Technology (JUST) http://www.just.edu.jo/News/Documents/N-2012/%D8%B9%D8%B7%D8%A7%D8%A1%20%D8%B1%D9%82%D9%85%2059-2012.pdf

[21] Günther, M., Joemann, M., & Csambor, S. "Advanced CSP Teaching Materials," Parabolic Trough Technology". In Deutsches Zentrum fuer Luft- und Raumfahrt eV MENA Teaching Materials Implementation Workshop. (2011)

[22] The methods used in calculation of solar radiation in Energy Plus http://www.designbuilder.co.uk/

[23] A. K. Yadav, S.S. Chande, "Tilt angle optimization to maximize incident solar radiation: A review". Renewable and Sustainable Energy Reviews, Vol. 23 (2013), 503–513.

[24] A. M. Noorian, I. Moradi, G. A. Kamali, "Evaluation of 12 models to estimate hourly diffuse irradiation on inclined surfaces". Renewable Energy, Vol. 33 (2008) No. 6, 1406–1412.

[25] Y. Q. Tian, R. J. Davies-Colley, P. Gong, B. W. Thorrold, "Estimating solar radiation on slopes of arbitrary aspect". Agricultural and Forest Meteorology, Vol. 109 (2001) No. 1, 67–77.

[26] K. Skeiker "Optimum tilt angle and orientation for solar collectors in Syria". Energy Conversion and Management, Vol. 50 (2009), 2439–2448.

[27] S. Soulayman, W. Sabbagh, "Comment on 'Optimum tilt angle and orientation for solar collectors in Syria' by Skeiker". Energy Conversion and Management, Vol. 89 (2015), 1001–1002.

[28] K. R. Agha, M. N. Sbita, "On the sizing parameters for stand-alone solar-energy systems". Applied Energy, Vol. 65 (2000) No. 1, 73–84.

[29] H. Moghadam, F. F. Tabrizi, A. Z. Sharak, "Optimization of solar flat collector inclination". Desalination, Vol. 265 (2011) No. 1, 107–111.

[30] P. Talebizadeh, M. A. Mehrabian, M. Abdolzadeh, "Determination of optimum slope angles of solar collectors based on new correlations". Energy Sources, Part A: Recovery, Utilization, and Environmental Effects, Vol. 33 (2011) No. 17, 1567-1580.

[31] H. Heywood, "Operating experience with solar water heating". JIHV, Vol. 39 (1971), 63–69.

[32] Lunde PJ. Solar thermal engineering. New York: Wiley; 1980.

[33] Duffie JA, Beckman WA. Solar engineering of thermal processes. New York: Wiley; 1991.

JJMIE

Volume 9 Number 3, June.2015
ISSN 1995-6665
Pages 195 - 207

Jordan Journal of Mechanical and Industrial Engineering

Free Vibration of an Axially Preloaded Laminated Composite Beam Carrying a Spring-Mass-Damper System with a Non-Ideal Support

Majid Ghadiri [a] *, Keramat Malekzadeh [b] , Faramarz Ashenai Ghasemi[c]

[a] Faculty of Engineering, Department of Mechanics, Imam Khomeini International University, Qazvin, Iran.
[b] Department of Mechanical Engineering, Malek Ashtar University of Technology 4th Kilometer, Makhsous RD, Tehran, Iran
[c] Department of Mechanical Engineering, Shahid Rajaee Teacher Training University (SRTTU) Lavizan, Tehran, Iran

Received 28 May 2014 Accepted 28 May 2015

Abstract

This paper investigates the effect of a non-ideal support on free vibration of an Euler-Bernoulli composite beam carrying a mass-spring-damper system under an axial force. The beam simply supported boundary conditions and it is assumed that one of its supports is non-ideal. Therefore, it has a small non-zero deflection and a small non-zero moment. The governing equations of the problem constitute a coupled system including a PDE and an ODE. To solve the problem, the Galerkin method is employed in the displacement field in conjunction with the average acceleration method in the time domain. The effect of a non-ideal support of composite beam, under axial force on natural frequencies and mode shapes of the system, is studied in details. For the validation of the performed solution and the obtained results, in a special case, the fundamental frequency was compared with those cited in the literature. The obtained results show that with increasing the perturbation parameter, the fundamental frequency decreases. This behavior is independent of the fiber directions of the beam. Also, the beams having fully-ideal supports will be buckled sooner than the beams with semi-ideal supports.

Keywords: *Beam; Free Vibration; Axial Load; Non-Ideal Support; Spring-Mass-Damper System.*

1. Introduction

Although the beams are still used as a design model for the vibration analysis of various realistic systems, most of the research studies are conducted on the vibration analysis of the beams with ideal supports and there are very few studies related to the ones having non-ideal supports.

Rayleigh [1] determined the fundamental frequency of a uniform cantilever beam carrying a tip mass. He used the static deflection curve of the beam acted upon concentrated tip load as a good estimation of fundamental mode shape estimate. Timoshenko [2] developed a series of formulae corresponding to various beam-point mass configurations. Turhan [3] studied the beams with various ideal end conditions. He presented an exact frequency equation for each case and compared the results in a broad range of relevant parameters. Matsunaga [4] analyzed the natural frequencies and buckling loads of a simply supported beam to initial axial tensile and/ or compressive forces. He applied Hamilton's principle to derive the equations of dynamic equilibrium and natural boundary conditions of a beam. He presented a one-dimensional higher order theory of thin rectangular beams to take into account the effects of both shear deformations and depth changes. He showed that with the help of his method, the natural frequencies and buckling loads of such beams could be evaluated more accurately than the previous methods. Banerjee [5] studied the free vibrations of axially loaded composite Timoshenko beams using the dynamic stiffness method. The solution technique, which he used to yield the natural frequencies, was that of the Wittrick-Williams algorithm. The effects of axial force, shear deformation and rotatory inertia on the natural frequencies were demonstrated. He showed that the shear deformation and rotatory inertia are seen to have a relatively marginal effect on the natural frequencies of this particular composite beam. However, the axial force was seen to have quite a significant effect on the fundamental natural frequency of the beam whereas it was seen to have a relatively lesser effect on other natural frequencies. He demonstrated that the natural frequency diminishes when the axial load changes from tensile to compressive, as expected. Naguleswaran [6] studied the transverse vibration of uniform Euler–Bernoulli beams linearly varying fully tensile, partly tensile or fully compressive

* Corresponding author. e-mail: ghadiri@eng.ikiu.ac.ir.

axial force distribution. He derived the general solution, expressed as the super-position of four independent power series solution functions. He showed that an increase in the values of one or both of the system parameters stiffens the system and results in an increase in the frequency parameter. He also presented that if one or both of the system parameters are negative; combinations exist for which a frequency parameter is zero. He stated that a necessary (but not sufficient) condition for the onset of buckling is when one or both system parameters are negative.

Naguleswaran [7] also studied the vibration of beams with up to three-step changes in cross-section and in which the axial force in each portion is constant but different. He showed that the Euler buckling occurs for certain combinations of the axial forces for which a frequency parameter is zero. A necessary (but not sufficient) condition for this to occur is at least one of the axial forces must be compressive.

Yesilce *et al.* [8] presented an extensive literature review of the beams carrying simply spring-mass systems and additional complexities. He also studied the effect of axial force on free vibration of Timoshenko multi-span beam with multiple attached spring-mass systems. He showed that an increase in the value of axial force causes a decrease in the frequency values; however, the amount of this decrease due to the modes is related to the number of spring-mass systems attached to the model. He also demonstrated that the frequency values show a very high decrease as a spring-mass system is attached to the bare beam; the amount of this decrease considerably increases as the number of spring-mass attachments is increased.

It is normally assumed that the ideal conditions are satisfied exactly. However, small deviations from ideal conditions in real systems occur. Pakdemirli *et al.* [9] studied the effect of non-ideal boundary conditions on the vibrations of the beams. He considered two different beam vibration problems and an axially moving string problem. He treated them using the Lindstedt-Poincare technique and the method of multiple scales. He showed that non-ideal boundary conditions may affect the frequencies as well as amplitudes of vibration. He also demonstrated that, depending on the location of non-ideal support conditions and their small variations in time, frequencies may increase or decrease. Pakdemirli *et al.* [10] also studied the non-linear vibrations of a simple-simple beam with a non-ideal support in between. He presented the approximate analytical solution of the problem using the method of multiple scales. He showed that depending on the mode shape numbers and locations, the frequencies may increase or decrease or remain unchanged. He also demonstrated that derivations from the ideal conditions lead to a drift in frequency-response curves which may be positive, negative or zero, depending on the mode number and locations.

Boyaci [11] widened the idea of non-ideal supports to a damped forced non-linear simple-simple beam vibration problem in which the nonlinearity was due to stretch effects. He combined the effects of non-linearity and non-ideal boundary conditions on the natural frequencies and mode shapes and examined them using the method of multiple scales. He stated that the stretching effect may increase the frequency while the non-ideal boundary conditions may increase or decrease them. Malekzadeh *et al.* [12] investigated the effect of non-ideal boundary conditions and initial stresses on the vibration of laminated plates on Pasternak foundation studied. The plate had simply supported boundary conditions and it was assumed that one of the edges of the plate allowed a small non-zero deflection and moment. The vibration problem was solved analytically using the Lindstedt-Poincare perturbation technique. So the frequencies and mode shapes of the plate, with a non-ideal boundary condition, was extracted by considering the Pasternak foundation and in-plane stresses. The results of the finite element simulation, using ANSYS software, were presented and compared with the analytical solution. The effect of various parameters, like stiffness of foundation, boundary conditions and inplane stresses on the vibration of the plate, was discussed. The Lindstedt-Poincare perturbation technique was used to study the effect of non-ideal boundary conditions on buckling load of laminated plates on elastic foundations by Khalili *et al.* [13]. The plate was simply supported and it was assumed that one of the edges of the plate allowed a small non-zero deflection and a small non-zero moment. The cross-ply rectangular plate rested on Pasternak foundation. The results of finite element simulations, using ANSYS FE code were presented and compared with the analytical solution. After determining the buckling load, the effect of various parameters, like stiffness of the foundation and in-plane pre-loads on the buckling load, was discussed. The proposed non-ideal boundary model was applied to the free vibration analyses of Euler-Bernoulli beam and Timoshenko beam by Jinhee [14]. The free vibration analysis of the Euler-Bernoulli beam was carried out analytically and the pseudospectral method was employed to accommodate the non-ideal boundary conditions in the analysis of the free vibration of Timoshenko beam. It was found that when the non-ideal boundary conditions are close to the ideal clamped boundary conditions, the natural frequencies are reduced noticeably as k increases. When the non-ideal boundary conditions are close to the ideal simply supported boundary conditions, however, the natural frequencies hardly change as k varies, which indicates that the proposed boundary condition model is more suitable for the non-ideal boundary condition close to the ideal clamped boundary condition. Ghadiri *et al.* [15] investigated the vibration analysis of an Euler-bernouli composite beam subjected to axial loading. The boundaries are assumed to allow small deflections and moments. So, the boundary conditions of the beam were considered as non-ideal. The governing equation of the system was solved by Lindstedt-Poincare technique. Finally, the effects of the non-ideal boundary conditions on the amplitude and frequency of vibration as well as the critical buckling load were studied.

The present paper investigates the effect of non-ideal simply supported boundary conditions under axial force on the vibration of laminated composite beams. Effect of non-ideal boundary condition on the natural frequencies and mode shapes are examined. An Euler-Bernoulli composite beam having fully-ideal (both ideal) and semi-ideal (one ideal and one non-ideal) boundary conditions under axial force is studied with the presence of an attached mass-spring-damper system. The governing equations of the beam are derived using the D'Alembert's principle. The Galerkin method is employed in the displacement field in conjunction with the average acceleration method in the time domain to solve the problem. The effect of ideal and non-ideal support of the composite beam under axial force on natural frequencies and mode shapes of the system is investigated. In order to validate the performed solution and the obtained results, in a special case, the fundamental frequency is compared with those cited in literature.

2. The Mathematical Model and Formulation

A laminated composite beam is considered, as shown in Figure 1. The governing equations of the uniform beam with an attached spring-mass system could be derived with the help of equilibrium of the dynamic forces by the D'Alembert's principle as follows [16]:

$$D\frac{\partial^4 w}{\partial x^4}+\rho A\frac{\partial^2 w}{\partial t^2}-P\frac{\partial^2 w}{\partial x^2}=f(x) \tag{1}$$

Considering Eq. (1) and Figure 1, $f(x)$ could be defined as follow as:

$$f(x)=[F+mg]\delta(x-x_o) \tag{2}$$

Therefore, Eq. (1) could be written as:

$$D\frac{\partial^4 w}{\partial x^4}+\rho A\frac{\partial^2 w}{\partial t^2}-P\frac{\partial^2 w}{\partial x^2}= \tag{3}$$
$$[mg-m\,\ddot{y}(t)]\,\delta(x-x_0) \qquad t>0$$

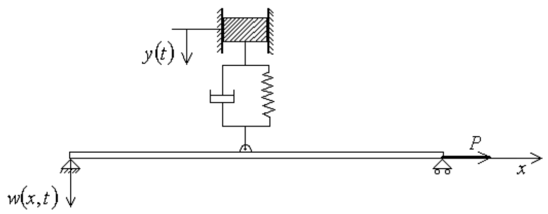

Figure 1. A schematic view of an Euler-Bernoulli laminated beam

where D is the reduced bending stiffness and $w(x,t)$ is the transverse displacement of the beam. $y(t)$ is the displacement of the attached mass relative to base level, ρ, A, L and m are density, cross section, length and amount of the attached mass to the beam, respectively. Also $\delta(x\text{-}x_0)$ is the Dirac delta function.

The reduced bending stiffness is as follows [17]:

$$D=D_{11}-\frac{(B_{11})^2}{A_{11}} \tag{4}$$

where:

$$A_{11}=b\sum_{k=1}^{n}\left(\bar{Q}_{11}^{k}\right)_k\left(z_k-z_{k-1}\right), \tag{5}$$

$$B_{11}=\left(\frac{b}{2}\right)\sum_{k=1}^{n}\left(\bar{Q}_{11}^{k}\right)_k\left(z_k^2-z_{k-1}^2\right), \tag{6}$$

$$D_{11}=\left(\frac{b}{3}\right)\sum_{k=1}^{n}\left(\bar{Q}_{11}^{k}\right)_k\left(z_k^3-z_{k-1}^3\right) \tag{7}$$

$$\bar{Q}_{11}^{k}=Q_{11}^{k}\cos^4\phi+Q_{22}^{k}\sin^4\phi+2\left(Q_{11}^{k}+2Q_{66}^{k}\right)\cos^2\phi\sin^2\phi \tag{8}$$

$$Q_{11}=\frac{E_{11}}{1-\upsilon_{12}\upsilon_{21}} \tag{9}$$

$$Q_{22}=\frac{E_{22}}{1-\upsilon_{12}\upsilon_{21}} \tag{10}$$

$$Q_{66}=G_{12} \tag{11}$$

$$\upsilon_{21}=\frac{\upsilon_{12}E_{22}}{E_{11}} \tag{12}$$

where A_{11} is the extensional stiffness, B_{11} is the coupling stiffness, D_{11} is the bending stiffness, $\bar{Q}_{11}^{k}$ is the coefficient of reduced stiffness of the lamina, b is the width, H is the height, n_i is the number of plies, E_{11} and E_{22} are the longitudinal and transverse Young's moduli, respectively, G_{12} is the in-plane shear modulus, υ_{12} and υ_{21} are the longitudinal and transverse Poisson's ratio, respectively, ϕ is the angle of the k^{th} lamina orientation and z_k and z_{k-1} are the locations of the k^{th} lamina with respect to the midplane of beam (Figure 2) [17,18]:

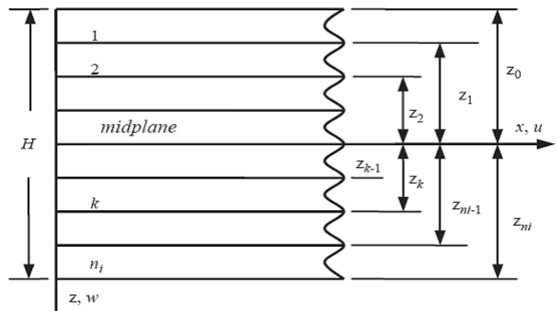

Figure 2. A schematic view of the stacking sequence of the laminated beam.

From Figure 1, the governing equation of the attached mass could be written as follows:

$$k\,y+c\dot{y}+m\ddot{y}=k\,w+c\,\dot{w} \tag{13}$$

For writing the governing equations of the problem, i.e., Eqs. (3) and (13), in their dimensionless forms, the relations between the dimensional and dimensionless (denoted by "‾") quantities are defined:

$$\bar{x}=\frac{x}{L}\ ;\quad \bar{t}=\Omega\,t\ ;\quad \Omega=\frac{1}{L^2}\sqrt{\frac{D}{\rho A}}\ ;\quad \bar{w}=\frac{\Omega^2\,w}{g}\ ;$$
$$\bar{y}=\frac{\Omega^2\,y}{g}\ ;\ \bar{k}=\frac{k\,L^3}{D}\ ;\ \bar{m}=\frac{m}{\rho L}\ ;\ \bar{\delta}(0)=L\,\delta(0)\ ; \tag{14}$$
$$\bar{c}=\frac{c\,L^3}{D}\Omega\ ;\quad \bar{p}=\frac{p}{\rho\,\Omega^2\,L^2}\ ;$$

Substituting the above dimensionless quantities into Eqs. (3) and (13), the dimensionless defining equations of the behavior of the beam and its attached mass could be written as:

$$\frac{\partial^4 \bar{w}}{\partial \bar{x}^4} + \frac{\partial^2 \bar{w}}{\partial \bar{t}^2} - \bar{p}\frac{\partial^2 \bar{w}}{\partial \bar{x}^2} = \bar{m}\left(1-\ddot{\bar{y}}\right)\bar{\delta}\left(\bar{x}-\bar{x}_o\right); \quad \bar{t} > 0 \tag{15}$$

$$\bar{k}\,\bar{y} + \bar{c}\,\dot{\bar{y}} + \bar{m}\,\ddot{\bar{y}} = \bar{k}\,\bar{w} + \bar{c}\,\dot{\bar{w}}; \quad \bar{x} = \bar{x}_o, \quad \bar{t} > 0 \tag{16}$$

Hereinafter, we simplify the above equations by removing the "‾" symbol.

In general form, the dimensionless governing equations of an Euler-Bernoulli composite beam with an attached spring-mass-damper system could be written as:

$$\frac{\partial^4 w}{\partial x^4} + \frac{\partial^2 w}{\partial t^2} - p\frac{\partial^2 w}{\partial x^2} = m\left(1-\ddot{y}\right)\delta\left(x-x_o\right); \quad t > 0 \tag{17}$$

$$k\,y + c\,\dot{y} + m\ddot{y} = kw + c\dot{w}; \quad x = x_o, \quad t > 0 \tag{18}$$

The boundary condition of the problem is as:

$$w(0,t) = 0; \qquad \frac{\partial^2 w(0,t)}{\partial^2 x} = 0;$$
$$w(1,t) = \varepsilon a(t); \qquad \frac{\partial^2 w(1,t)}{\partial^2 x} = \varepsilon b(t) \tag{19}$$

ε is small perturbation parameter denoting that the variations in deflections and moments are not zero but small at the end of the beam (here, at the right end of the beam). The symbol "1" in (1,*t*) shows this non-ideal condition at the right end of the beam.

Having the same time variations in the boundaries, the following equations must be satisfied:

$$w(1,t) = \varepsilon a; \qquad \frac{\partial^2 w(1,t)}{\partial^2 x} = \varepsilon b \tag{20}$$

where a and b are constant amplitudes and are: a=b=1 [9].

3. The Solution Method

To solve the coupled Eqs. (17) and (18), the Galerkin's method in coordinate domain and the method of average acceleration to time discretizing are employed. The test function should be predicted in a proper way to satisfy the boundary conditions of the problem. It must be noted that in ideal support condition (ε = 0), the test function must satisfy the boundary conditions of the problem too. Therefore,

$$\phi_n(x) = \sin(n\pi x) + \varepsilon\left(cx^3 + dx^2\right); \quad 0 < x < 1 \tag{21}$$

where c and d could be determined with the help of boundary conditions. Therefore, the test function is:

$$\phi_n(x) = sin(n\pi\, x) + \varepsilon\left(\frac{11}{6}x^3 - \frac{5}{6}x^4\right); \quad 0 < x < 1 \tag{22}$$

It is seen that for ε = 0 (ideal boundary conditions), $\phi_n(x)$ could satisfy the boundary conditions of the problem too.

Finding the test function, *w(x,t)* is considered as follows:

$$w(x,t) = \sum_{n=1}^{\infty} \phi_n(x)\,\alpha_n(t) \tag{23}$$

where $\alpha_n(t)$ is the time dependent functions.

Substituting the above equations into Eqs. (17) and (18):

$$\sum_{n=1}^{\infty} \phi_n''''(x)\,\alpha_n(t) + \sum_{n=1}^{\infty} \phi_n(x)\,\ddot{\alpha}_n(t) - p\sum_{n=1}^{\infty} \phi_n''(x)\,\alpha_n(t) = m\left(1-\ddot{y}\right)\delta\left(x-x_o\right); \quad t > 0 \tag{24}$$

$$k\,y + c\,\dot{y} + m\ddot{y} = k\sum_{n=1}^{\infty} \phi_n(x)\,\alpha_n(t) + c\sum_{n=1}^{\infty} \phi_n(x)\,\dot{\alpha}_n(t); \quad x = x_o, \ t > 0 \tag{25}$$

Considering the Galerkin's method, the weight function could be chosen as:

$$\phi_m(x) = sin(m\pi\, x) + \varepsilon\left(\frac{11}{6}x^3 - \frac{5}{6}x^4\right); \quad 0 < x < 1 \tag{26}$$

Multiplying the above equation in Eq. (24) and integrating on 0<*x*<1:

$$\int_0^1 \phi_m(x)\sum_{n=1}^{\infty} \phi_n''''(x)\,\alpha_n(t)dx + \int_0^1 \phi_m(x)\sum_{n=1}^{\infty} \phi_n(x)\,\ddot{\alpha}_n(t)dx - p\int_0^1 \phi_m(x)\sum_{n=1}^{\infty} \phi_n''(x)\,\alpha_n(t)dx = \int_0^1 \phi_m(x) m\left(1-\ddot{y}\right)\delta\left(x-x_o\right)dx; \quad t > 0 \tag{27}$$

The above equations could be simplified with the help of orthogonality condition.

The method of average acceleration is employed for discretizing the time. This method is mostly used in finite element analysis of time discretized dynamic equations. In this method, estimations of finite differences for displacement and velocity could be found using of Taylor's series as follows [19]:

$$\dot{w}^{t+\Delta t} = \dot{w}^{t} + \ddot{w}^{t}\,\Delta t \tag{28}$$

$$w^{t+\Delta t} = w^{t} + \dot{w}^{t}\,\Delta t + \ddot{w}^{t}\,\frac{\Delta t}{2} \tag{29}$$

where w is a time dependent variable, Δt is the time step size and the superscripts show the time in which the proposed expression must be calculated.

In average acceleration method, the additional assumption is:

$$\ddot{w}^{t} \Rightarrow \frac{\ddot{w}^{t+\Delta t} + \ddot{w}^{t}}{2} \tag{30}$$

where $\Rightarrow$ denotes substituting. Therefore, substituting Eq. (30) in Eqs. (28) and (29):

$$\dot{w}^{t+\Delta t} = \dot{w}^{t} + a_1 \ddot{w}^{t} + a_2 \ddot{w}^{t+\Delta t} = c1w\left(\dot{w}^{t}, \ddot{w}^{t}\right) + a_2 \ddot{w}^{t+\Delta t} \tag{31}$$

$$w^{t+\Delta t} = w^{t} + a_3 \dot{w}^{t} + a_4 \ddot{w}^{t} + a_5 \ddot{w}^{t+\Delta t} = c2w\left(w, \dot{w}^{t}, \ddot{w}^{t}\right) + a_5 \ddot{w}^{t+\Delta t} \tag{32}$$

where a_i is equal to:

$$a_1 = \frac{\Delta t}{2} \; ; \; a_2 = \frac{\Delta t}{2} \; ; \; a_3 = \Delta t \; ; \; a_4 = \frac{\Delta t^2}{4} \; ; \; a_5 = \frac{\Delta t^2}{4} \tag{33}$$

and $c1w$ and $c2w$ show the expressions which are as follows:

$$c1w\left(\dot{w}^{t}, \ddot{w}^{t}\right) = \dot{w}^{t} + a_1 \ddot{w}^{t} \tag{34}$$

$$c2w\left(w^{t}, \dot{w}^{t}, \ddot{w}^{t}\right) = w^{t} + a_3 \dot{w}^{t} + a_4 \ddot{w}^{t} \tag{35}$$

With this method, the linear differential equations would be reduced to a system of linear algebraic equations including acceleration in time $t+\Delta t$, displacement, velocity and acceleration in time t [19].

Noticing Eqs. (31) and (32), variables of the system of equations could be defined as:

$$\dot{\alpha}_n^{t+\Delta t} = \dot{\alpha}_n^{t} + a_1 \ddot{\alpha}_n^{t} + a_2 \ddot{\alpha}_n^{t+\Delta t} = c1\alpha\left(\dot{\alpha}_n^{t}, \ddot{\alpha}_n^{t}\right) + a_2 \ddot{\alpha}_n^{t+\Delta t} \tag{36}$$

$$\alpha_n^{t+\Delta t} = \alpha_n^{t} + a_3 \dot{\alpha}_n^{t} + a_4 \ddot{\alpha}_n^{t} + a_5 \ddot{\alpha}_n^{t+\Delta t} = c2\alpha\left(\alpha_n, \dot{\alpha}_n^{t}, \ddot{\alpha}_n^{t}\right) + a_5 \ddot{\alpha}_n^{t+\Delta t} \tag{37}$$

Substituting the above equations in the motion equations of the system, linear partial differential equations would be changed to linear algebraic equations. The above equations could be defined as time discretized equations that $\alpha(t)$ is its unknown parameter. In order to avoid lengthy explanations, the motion equations are not shown after the above-mentioned substitution. Solving the resulted system of algebraic equations simultaneously, having the value of variables in time t, the corresponding values could be easily determined in time $t+\Delta t$.

4. Calculation of Fundamental Natural Frequency

The equation of fundamental natural frequency of a simply supported beam with one non ideal boundary condition and carrying a spring-mass system is derived using Rayleigh's method as follow as [16]:

$$T_{\max} = V_{\max} \tag{38}$$

where V_{max} is maximum potential energy and T_{max} is maximum kinematics energy of the total system. Assuming identical phase for beam and the attached mass oscillations, the maximum kinetic energy can be calculated as follows:

$$T_{\max} = T_{beam} + T_{mass}$$

$$T_{\max} = \frac{1}{2} \rho A \omega^2 \int_0^l W(x)^2 \, dx + \frac{1}{2} m \omega^2 Y^2 \tag{39}$$

which ω is a fundamental natural frequency of the system, $W(x)$ and Y are transverse deflections of beam and the attached mass to it, respectively. Using Eq. (26), the first mode shape can be considered as:

$$W(x) = \phi_1(x) = \sin(\pi x) + \varepsilon\left(\frac{11}{6} x^3 - \frac{5}{6} x^4\right) ; \tag{40}$$

The beam and the mass attached to it are supposed to oscillate with the same phase and fundamental frequency.

The maximum potential energy can be calculated as follows:

$$V_{\max} = V_{beam} + V_{mass} \tag{41}$$

and

$$V_{\max} = \frac{1}{2} k (Y - W(x_0))^2 + D \int_0^l W(x)'' \, dx \tag{42}$$

where,

$$mg = k(Y - W(x_0)) \tag{43}$$

Therefore, the fundamental natural frequency of a simply supported beam with one non ideal boundary condition and carrying spring-mass system is given as follows:

5. Model Verification

The fundamental frequency of the composite beam with ideal supports, which is derived with the help of Eq. (44), is compared to the calculated one by [3] for a concentrated mass without a spring. To model the present spring-mass system with a system consisting of one concentrated mass only, the spring constant k is tended to infinity. The first, second and third rows of Table 1 show that a good verification is reached for the case of ideal supports. Table 1 also demonstrates that with the increase of ε, the fundamental natural frequency decreases.

$$\omega_1^2 = \frac{\frac{(mg)^2}{k} + D\int_0^1 [-\pi^2 \sin(\pi x) + \varepsilon(-10 x^2 + 11 x)]^2 \, dx}{m\left[\frac{mg}{k} + \sin(\pi x_0) + \varepsilon\left(\frac{11}{6} x_0^3 - \frac{5}{6} x_0^4\right)\right]^2 + \rho A \int_0^1 \left[\sin(\pi x) + \varepsilon\left(\frac{11}{6} x^3 - \frac{5}{6} x^4\right)\right]^2 \, dx} \tag{44}$$

Table1. Verification of the present method with [3], in comparison with first fundamental frequency of beam

Distance of the concentrated mass from the left side of beam support	$x_0 = 0.1$	$x_0 = 0.2$	$x_0 = 0.3$	$x_0 = 0.4$	$x_0 = 0.5$
Ideal supports ($\varepsilon = 0.0$) [3]	120.628	80.869	64.204	56.978	54.901
Ideal supports ($\varepsilon = 0.0$) [Present method (Eq. (44))]	122.726	82.384	65.335	57.722	55.218
Non-Ideal support ($\varepsilon = 0.1$) [Present method (Eq. (44))]	118.841	82.039	63.707	55.199	52.418
Non-Ideal Support ($\varepsilon = 0.2$) [Present Method (Eq. (44))]	113.083	80.869	64.204	56.978	49.770

6. Numerical Analysis and Discussions

All numerical analyses of the present paper are obtained based on the following data [17]:

$m = 2\,kg$; $L = 1\,m$; $A = 2.4\times10^{-4}\,m^2$;

$\rho = 1480 kg/m^3$; $x_o = 0.5\,m$;

$E_{11} = 134\times10^9\ N/m^2$;

$E_{22} = 10.3\times10^9\ N/m^2$;

$G_{12} = 5\times10^9\ N/m^2$; $\upsilon_{12} = 0.33$;

$b = 30\times10^{-3}\,m$; $\Delta t = 0.005$;

$H = 8\times10^{-3}\,m$; $k = 5\times10^3\ N/m$;

$y(t=0) = 0.144$;

In all of the presented results, in form of time dependent curves, the oscillation amplitude of the beam is determined and drawn at the point: $x=x_0$.

It is worth mentioning that for the sake of the facility of the calculations, Matlab software is used to get the results.

7. Effect of Non-Ideal Support

Figure 3 illustrates a comparison of the first four mode shapes of the composite beam with different perturbation parameters. The layer sequence of the laminated composite beam is [90 60 30 0]$_s$. It is observed that the mode shapes of the beam with two ideal supports are different from the mode shapes of the beam with non-ideal support. It means that as one of the supports is non ideal (ε = 0.1), the amplitude of mode shape is higher.

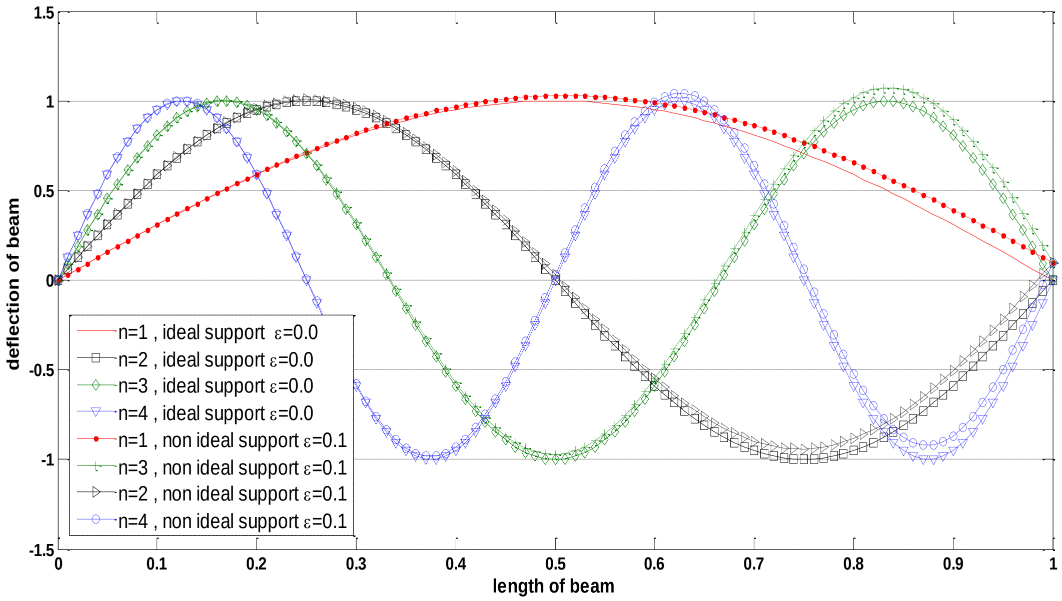

Figure 3. Comparison of mode shapes of the beam in the cases of two ideal supports and one non-ideal and one ideal support

The oscillation amplitude of the middle point of the beam and its attached mass for different perturbation parameter are shown in Figures 4 and 5, respectively. The beam is considered as a composite laminate having 8 plies which its layer sequence is: $[90\ 60\ 30\ 0]_s$. The mass oscillation is begun from point $y\ (t = 0) = 0.144$ that is given to the mass as an initial condition.

Figure 4 shows that the increase in ε causes an increase in the oscillation amplitude and the phase difference between the oscillations amplitudes.

Figure 5 shows that with increasing the perturbation parameter, the oscillations amplitude of the attached mass to the beam decreases.

The oscillations amplitude of the middle point of the beam and its attached mass with two ideal supports are shown in Figures 6 and 7, respectively. The effect of fiber directions on the oscillation of the beam and its attached mass could be seen in these figures, respectively. It is seen that in some fiber directions, the oscillation amplitude of the middle point of beam decreases. For instance, the oscillation amplitude of the middle point of the beam decreases in unsymmetrical fiber directions. Whereas the effect of the fiber directions on the oscillation amplitude of the attached mass is only a phase difference.

The effect of the fiber directions on the oscillation amplitude of the beam and its attached mass with a non-ideal support ($\varepsilon = 0.1$) are shown in Figures 8 and 9, respectively.

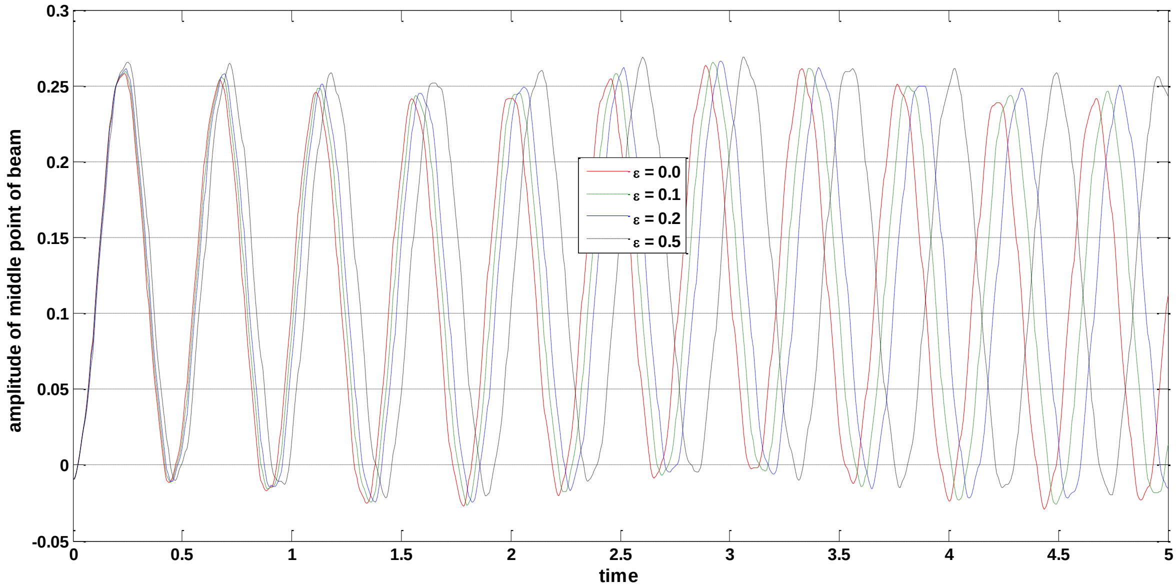

Figure 4. Comparison of vibrations of middle point of beam for different perturbation parameter

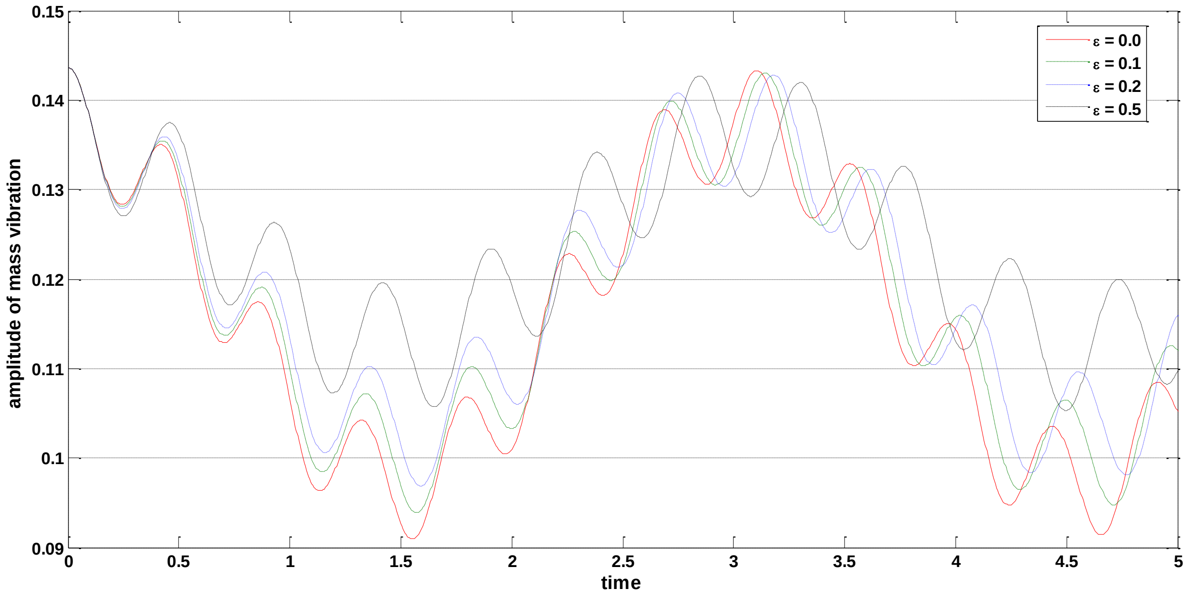

Figure 5. Comparison of vibrations of the attached mass to beam for different perturbation parameter.

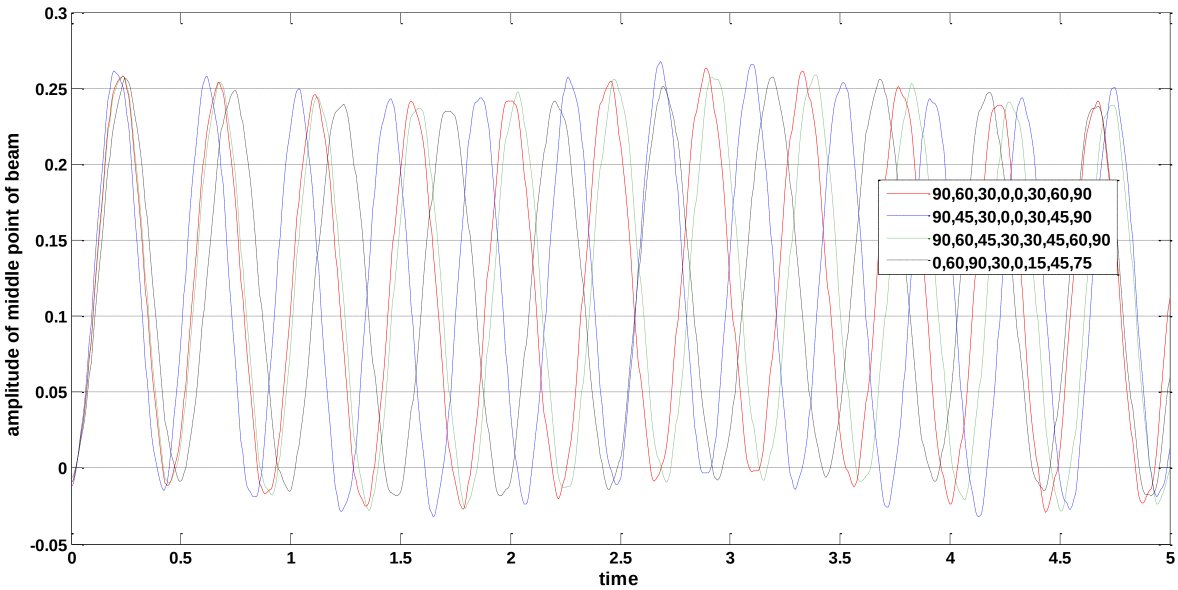

Figure 6. Comparison of vibration of the middle point of beam with two ideal supports for different fiber directions

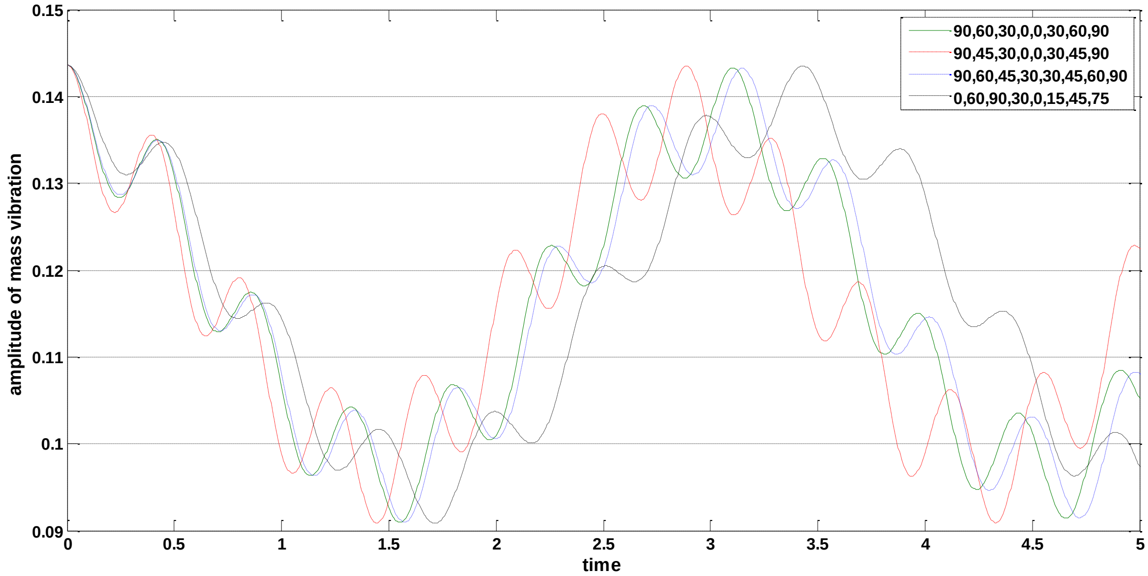

Figure 7. Comparison of vibration of the attached mass to beam with two ideal supports for different fiber directions

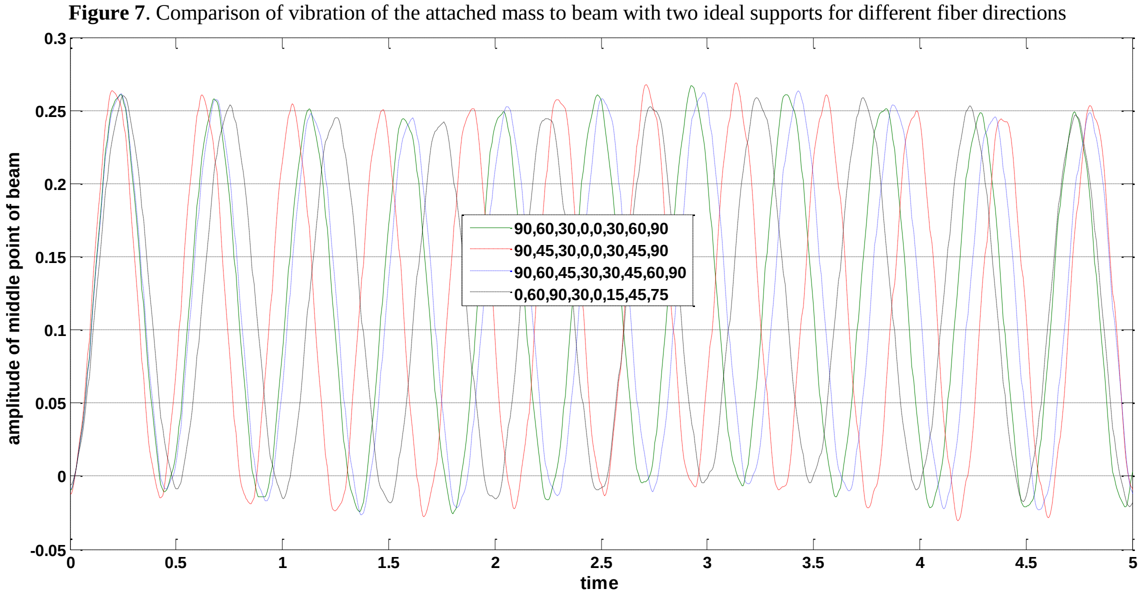

Figure 8. Comparison of vibration of the middle point of beam with one non-ideal support ($\varepsilon = 0.1$) for different fiber directions

Table 2. The effect of fiber directions of beam on its bending stiffness (*D*).

Fiber Directions	Bending Stiffness of the Beam (D)
$[90,60,30,0]_s$	100.03
$[90,45,30,0]_s$	76.47
$[90,60,45,30]_s$	105.64
[0,60,90,30,0,15,45,75]	153.56

Considering Table 2 and figures 8 and 9, it is visible that the bending stiffness of the beam with the unsymmetrical fiber directions is more than the symmetric ones. This leads to a reduction in the oscillation amplitude of the beam. Figures 8 and 9 also show that the effect of the different bending stiffness on the oscillation amplitude of the attached mass is only a phase difference.

Figure 10 shows the behavior of the fundamental frequency of the whole system (including the beam and its attached mass) with respect to the perturbation parameter (ε) for the different fiber directions.

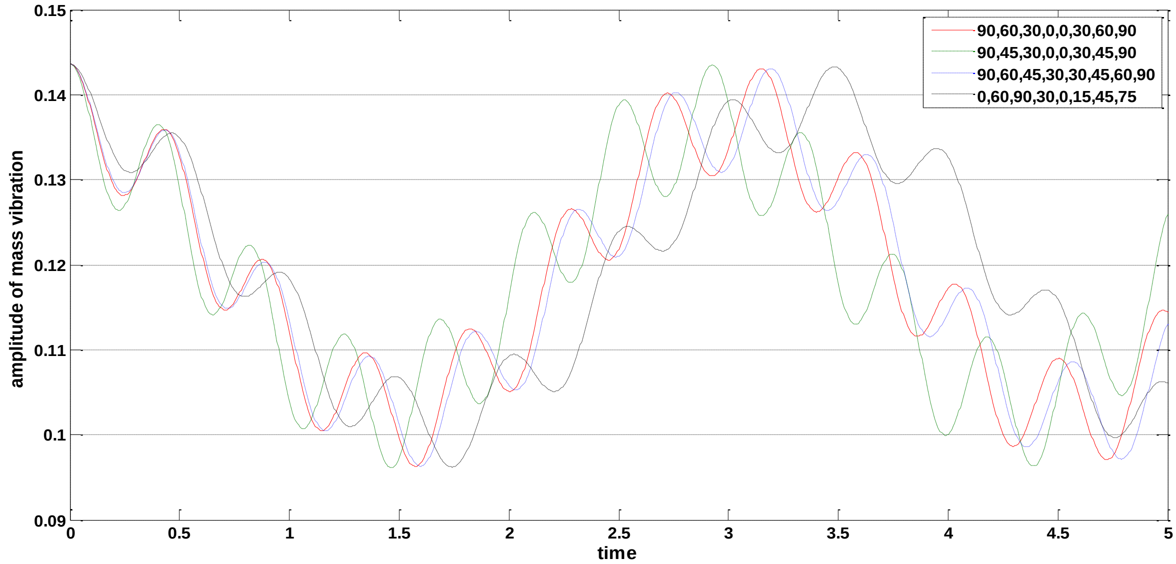

Figure 9. Comparison of vibration of the attached mass to beam with one non-ideal support ($\varepsilon = 0.1$) for different fiber directions

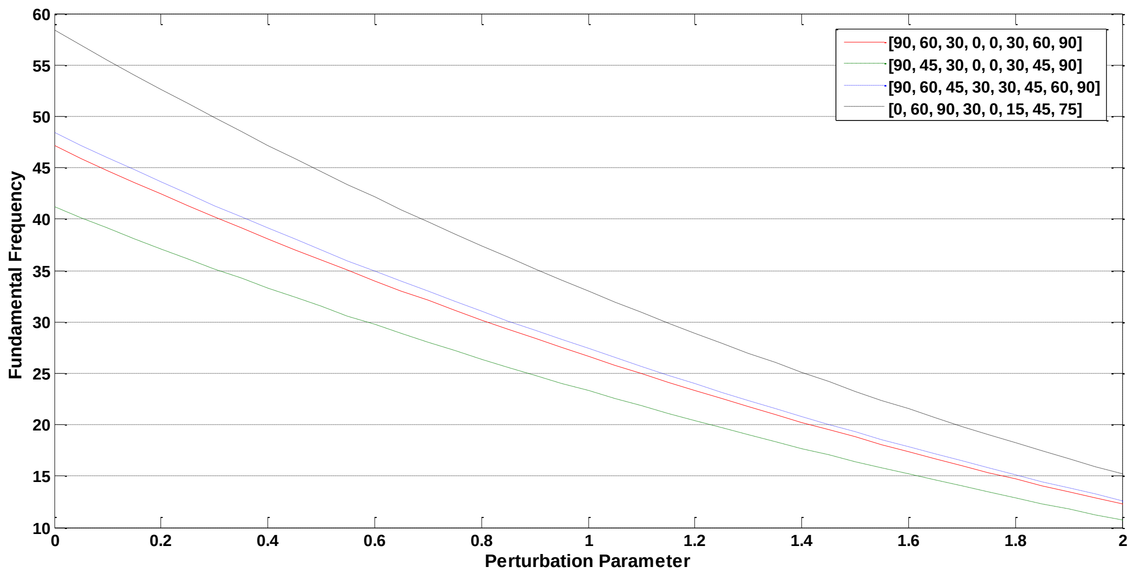

Figure 10. Comparison of vibration of the whole system with respect to perturbation parameter (ε) for different fiber directions

It is seen that for the unsymmetrical fiber directions, the fundamental is the most frequency. The more perturbation parameter is, the less fundamental frequency (no matter whether the fiber directions are symmetric or unsymmetrical).

The effect of the tensile and the compressive force on dimensionless oscillation amplitude of a laminated beam with constant fiber directions $[90\ 60\ 30\ 0]_s$ for fully-ideal and semi-ideal (having one support with ε= 0.1) supports is shown in Figures 11 and 12, respectively. The more tensile axial force, the less oscillation amplitude of the beam. Figures 11 and 12 show that increasing the compressive axial force (smaller than the axial force of the first buckling mode of the beam), increases the average of dimensionless oscillation amplitude of the middle point of beam. Because the compressive axial force decreases the bending stiffness of the beam, therefore, the average of dimensionless oscillation amplitude of the beam increases.

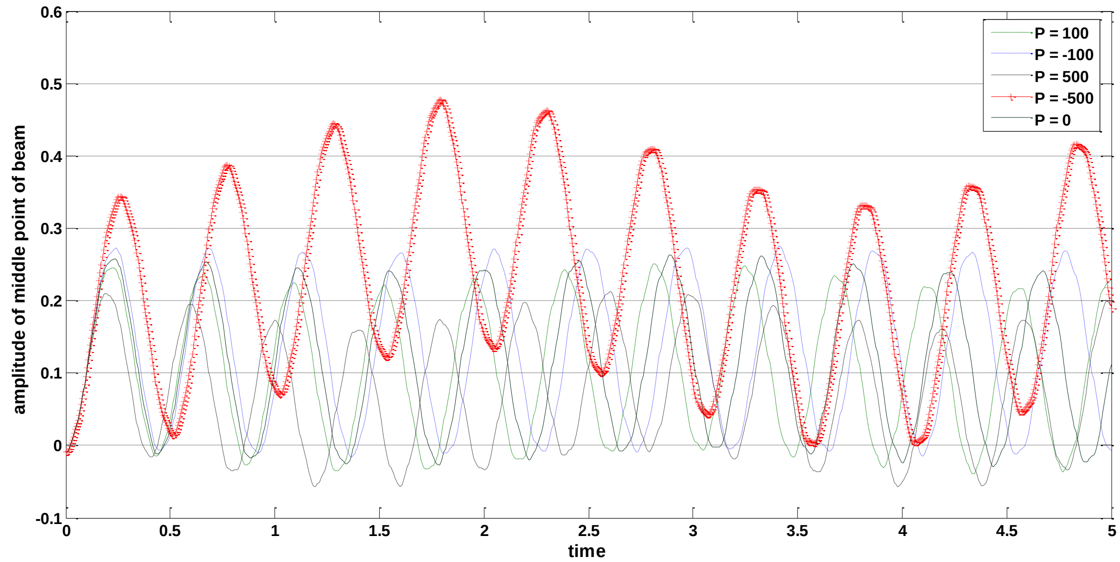

Figure 11. Comparison of vibration of the mid-point of the beam with fully-ideal supports for different axial forces

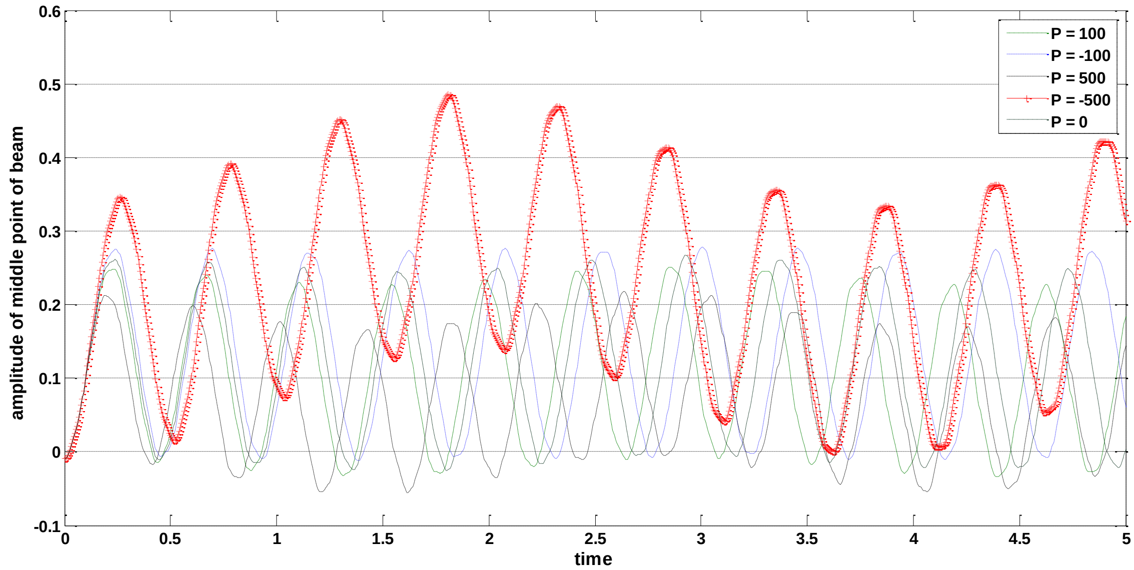

Figure 12. Comparison of vibration of the mid-point of the beam with semi-ideal supports (ε= 0.1) for different axial forces

The effect of the tensile and the compressive axial forces on dimensionless oscillation amplitude of the attached mass to the composite beam with constant fiber directions $[90\ 60\ 30\ 0]_s$ for fully-ideal and semi-ideal (ε = 0.1) supports is shown in Figures 13 and 14, respectively. No matter whether the axial force is tensile or compressive, for the case of semi ideal supports (ε = 0.1), it leads to an increase in the oscillation motion of the attached mass to the beam. When the axial force is tensile, the oscillation amplitude tends to the equilibrium point (i.e., the point that amplitude is equal to zero). The mass begins its oscillation from the point $y(t = 0) = 0.144$ that is given initial condition. Also, the compressive axial force increases the oscillation amplitude of the attached mass. This is because of the variation of the bending stiffness of the beam due to axial force.

The effect of the non-ideal supports in the reduction of the buckling probability of a laminated composite beam with the constant symmetric fiber directions [90 60 30 0]s under a compressive axial force (P = -2000 N), near the first mode of the buckling load is shown in Figure 15. It is seen that having a non-ideal support postpones the buckling of a beam under compressive forces near the first mode of the buckling load. Therefore, a beam with fully-ideal supports will be buckled sooner than with semi-ideal ones at the same loading condition.

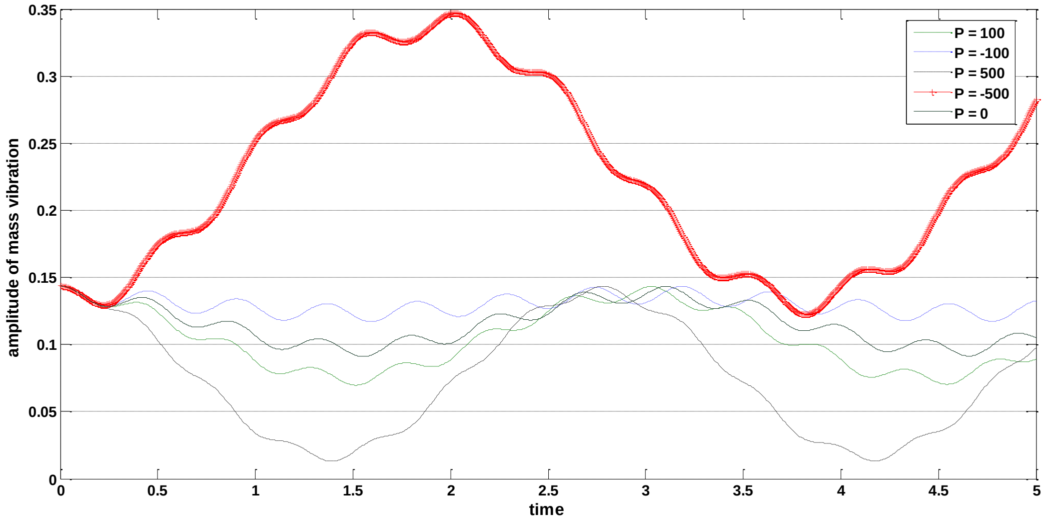

Figure 13. Comparison of vibration of the attached mass to beam with fully-ideal supports for different axial forces

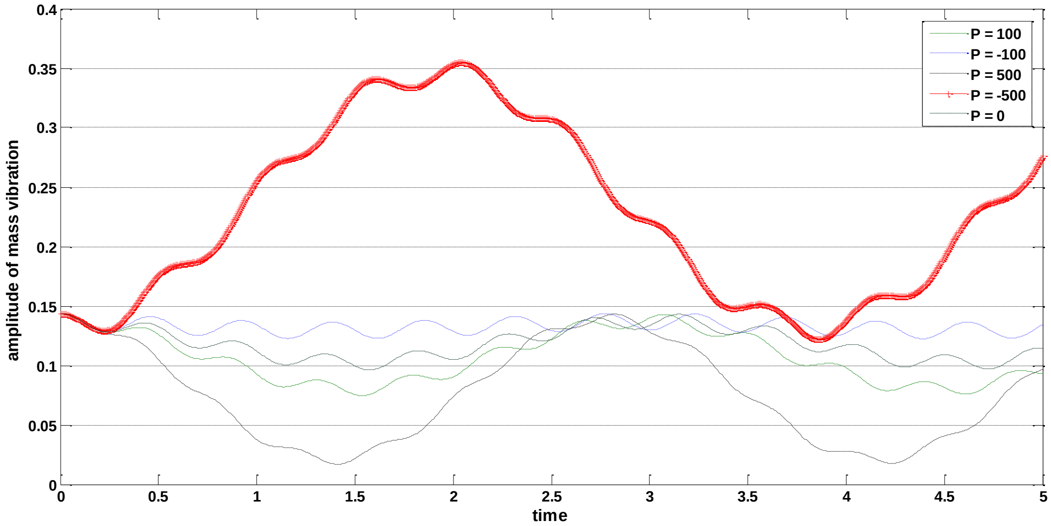

Figure 14. Comparison of vibration of the attached mass to beam with semi-ideal (ε = 0.1) supports for different axial forces

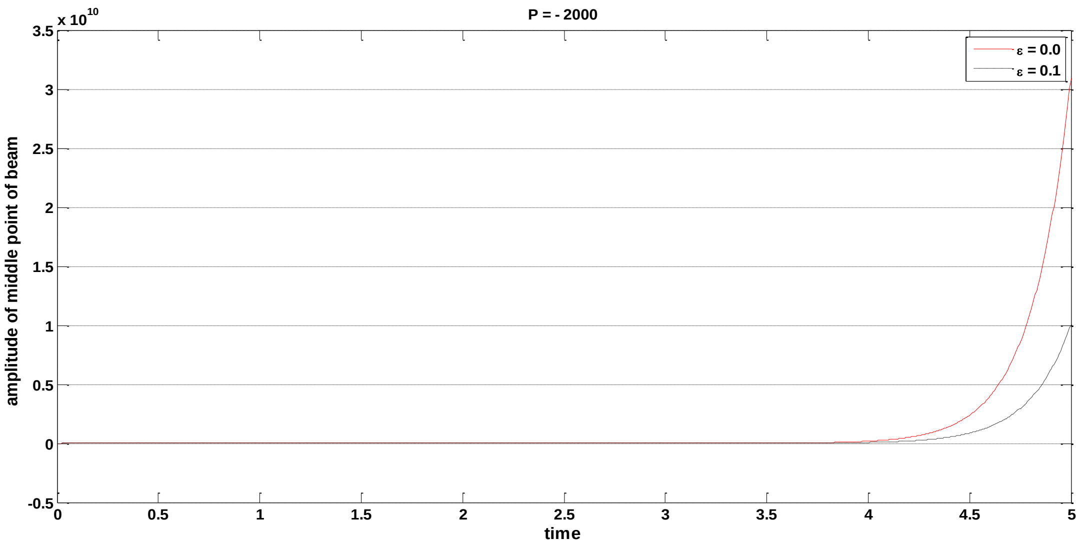

Figure 15. The effect of perturbation parameter (ε) on buckling of a beam.

The effect of the damping constant on the oscillation amplitude of the middle point of the beam for ideal ($\varepsilon = 0$) and non-ideal ($\varepsilon = 0.1$) supports is shown in Figure 16. It could be seen that the oscillation amplitude of the middle point of the beam with nonzero damping constant decreases with time. While, the oscillation amplitude of the beam without damping does not change.

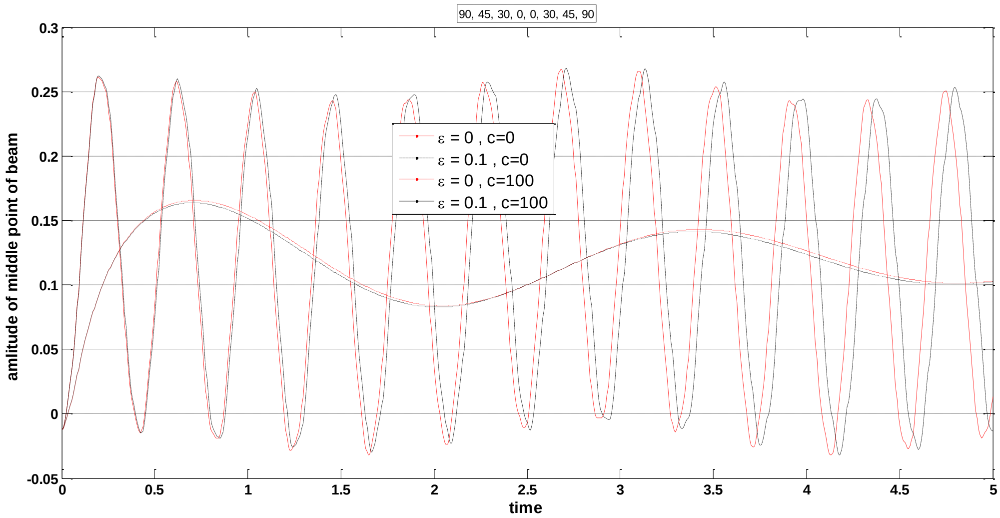

Figure 16. Comparison of vibration of the middle point of beam with ideal and non-ideal support for different damping constant

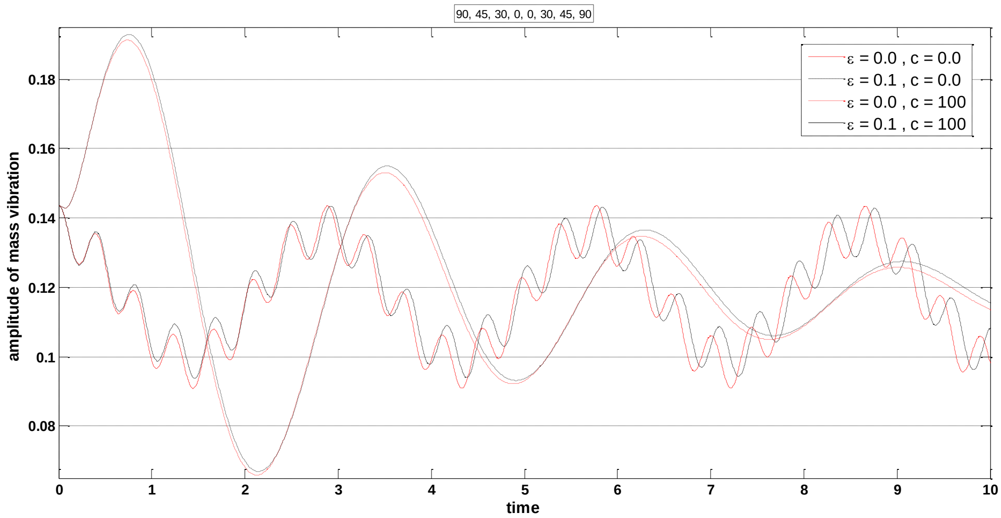

Figure 17. Comparison of vibration of attached mass to the beam with ideal and non-ideal support for different damping constant

The effect of the damping constant on the oscillation amplitude of the attached mass to beam for ideal (ε = 0) and non-ideal (ε = 0.1) supports is shown in Figure 17. It could be seen that the oscillation amplitude of the attached mass to the beam with nonzero damping constant decreases with time. It is shown that at the start of the oscillation, the amplitude of the attached mass to beam without damping is smaller than the amplitude of the attached mass to the beam with damping. The oscillation amplitude of the attached mass to the beam with nonzero damping constant decreases with time.

We know that as the degree of freedom increases, the natural frequency decreases. For example, for a beam with a specified geometry and physical property, natural frequencies based on Euler-Bernoulli beam theory are higher than the natural frequencies based on Timoshenko beam theory. This is because of the degree of freedom which, in Timoshenko beam theory, is more than Euler-Bernoulli beam theory. In the Timoshenko beam theory, the effect of shear deformation, in addition to the effect of rotary inertia, is considered. In the present investigation, according to the obtained results, with increasing perturbation parameter (i.e., ε), the natural frequency decreases and the oscillation amplitude increases. With noting the foregoing expression, this is because of the increasing degree of freedom due to increasing perturbation parameter.

8. Conclusions

The effect of a non-ideal support on free vibrations of an Euler-Bernoulli laminated composite beam carrying an attached mass-spring-damper system under axial force was investigated. The effect of non-ideal support on the oscillation frequency and the amplitude of the beam was studied. The Galerkin method is employed in the displacement field in conjunction with the average acceleration method in the time domain to solve the governing equations of the problem. The results show that the non-ideal boundary conditions may affect the oscillation frequency as well as the amplitude of the beam and the attached mass. The results could be classified as follows:

- The oscillation amplitude and phase difference between the oscillation amplitudes of the composite beam increases as the perturbation parameter (ε) increases. This behavior is independent of the fiber directions of the beam. Increasing the perturbation parameter, the average of the beam oscillation amplitude decreases.
- Increasing the perturbation parameter, the average of the attached mass oscillation amplitude decreases.
- The oscillation amplitude of the beam with ideal supports reduces in some fiber directions. However, the effect of the fiber directions in the oscillation amplitude of the attached mass is only a phase difference.
- When the fiber directions of the beam are symmetric, the fundamental frequency of the beam reaches to its maximum value. Increasing the perturbation parameter results in a decrease in the fundamental frequency of the beam, regardless of the fiber directions of beam.
- The more increase in the tensile axial force results in a less oscillation amplitude of the beam for symmetric fiber directions with ideal supports and vice versa. It means that by increasing the compressive axial force at the same conditions, the oscillation amplitude of the beam increases. The more increase in compressive axial force results in a more increase in the average value of the oscillation amplitude.
- For a specified fiber direction regardless of the kind of axial force, the oscillation amplitude of the beam increases for a semi-ideal supports case ($\varepsilon = 0.1$).
- The oscillation amplitude of the attached mass to the beam is affected from the value and the direction of the axial force and the amount of perturbation parameter.
- Using a non-ideal support postpones the buckling probability of the beam near the first mode of the buckling load. Therefore, the beams having fully-ideal supports would be buckled sooner than the beams with semi-ideal supports.

References

[1] J.W.S. Rayleigh, “The Theory of Sound”. 2rd ed. New York: Dover; 1945.

[2] S. Timoshenko, D.H.Young, W. “Weaver, Vibration Problems in Engineering”. 4rd ed. New York: Wiley; 1974

[3] Ö. Turhan, “On The Fundamental Frequency of Beams Carrying a Point Mass: Rayleigh Approximations Versus Exact Solutions”. Journal of Sound and Vibration, Vol. 230 (2000) No. 2, 449-459.

[4] H. Matsunaga, “Free Vibration and Stability of Thin Elastic Beams Subjected to Axial Forces”. Journal of Sound and Vibration, Vol. 191 (1996) No. 5, 917-933.

[5] J.R. Banerjee, “Free vibration of axially loaded composite Timoshenko beams using the dynamic stiffness matrix method”. Computers and Structures, Vol. 69 (1998) 197-208.

[6] S. Naguleswaran, “Transverse vibration of an uniform Euler–Bernoulli beam under linearly varying axial force”. Journal of Sound and Vibration, Vol. 275 (2004) 47-57.

[7] S. Naguleswaran, “Vibration and stability of an Euler–Bernoulli beam with up to three-step changes in cross-section and in axial force”. International Journal of Mechanical Sciences, Vol. 45 (2003) 1563-1579.

[8] Y. Yesilce, O. Demirdag, “Effect of axial force on free vibration of Timoshenko multi-span beam carrying multiple spring-mass systems”. International Journal of Mechanical Sciences, Vol. 50 (2008) 995-1003.

[9] M. Pakdemirli, H. Boyaci, “Effect of non-ideal boundary conditions on the vibrations of continuous systems”. Journal of Sound and Vibration, Vol. 249 (2002) No. 4, 815-823.

[10] M. Pakdemirli, H. Boyaci, “Non-linear vibrations of a simple–simple beam with a non-ideal support in between”. Journal of Sound and Vibration, Vol. 268 (2003) 331-341.

[11] H. Boyaci, “Beam vibrations with non-ideal boundary conditions”. Springer Proceedings in Physics, Vol. 111 (2007) 97-102.

[12] K. Malekzadeh, S.M.R. Khalili, P. Abbaspour, “Vibration of non-ideal simply supported laminated plate on an elastic foundation subjected to in-plane stresses”. Composite Structures, Vol. 92 (2010) 1478-1484.

[13] S.M.R. Khalili, P. Abbaspour, K. Malekzadeh, “Buckling of non-ideal simply supported laminated plate on Pasternak foundation”. Applied Mathematics and Computation, Vol. 219 (2013) 6420-6430.

[14] L. Jinhee, “Free vibration analysis of beams with non-ideal clamped boundary conditions ”. Journal of Mechanical Science & Technology, Vol. 27 (2013) 297-303.

[15] M. Ghadiri, M. Hosseini, “Vibration Analysis of A Composite Beam with Non-Ideal Boundary Conditions”. International Journal of Basic Sciences & Applied Research, Vol. 3 (2014) 103-118.

[16] S. Rao, Mechanical vibrations. 3rd ed. Wesley: Addison; 1995.

[17] D. Shu, C.N. Della, “Free vibration analysis of composite beams with two non-overlapping delaminations”. International Journal of Mechanical Sciences, Vol. 46 (2004) 509–526.

[18] R.M. Jones, Mechanics of composite materials. 2rd ed. Taylor and Franci: Philadelphia; 1999.

[19] S.A. Siddiqui, M.F. Golnaraghi, G.R. Heppler, “Large free vibration of a beam carrying a moving mass”. International Journal of Non-Linear Mechanics, Vol. 38 (2003) No. 10, 1481-1493.

JJMIE

Volume 9 Number 3, June.2015
ISSN 1995-6665
Pages 209 - 216

Jordan Journal of Mechanical and Industrial Engineering

Investigation of Sweep Angle Effects on a Submarine Hydrodynamic Drag Using Computational Fluid Dynamics

Mohammad Hadipour, Ebrahim Goshtasbi rad*

Department of Aerospace and energy, School of mechanical engineering Shiraz University, Shiraz, Iran

Received 11 Jan 2015 *Accepted 1 June 2015*

Abstract

In the present paper, the effects of the increase in surfaces backward sweep angle of horizontal tail and the hydrofoil of a typical submarine on its hydrodynamic drag are investigated with Computational Fluid Dynamics (CFD). Results show that with the increase in the horizontal tail backward sweep angle about 50° in constant surface area, hydrodynamic drag can reduce 6% than zero backward sweep angle condition. This value is equal to 44 N reductions in hydrodynamic drag force and 180 watt of consumption power in 4 m/s speeds of this submarine. Also, with increasing 60° of this submarine hydrofoil backward sweep angle, the constant hydrofoil volume can reduce 14% from hydrodynamic drag rather than zero hydrofoil backward sweep angle. This hydrodynamic drag reduction of this typical submarine in cruising speed (4 m/s) is equal to 97 N force, saving 388 watt of the consumption power. In general, the 50° of horizontal tail backward sweep angle and 60° of hydrofoil backward sweep angle can reduce 19% of hydrodynamic drag rather than zero tail and hydrofoil backward sweep angles. These amounts of drag reduction and power saving in this typical submarine can increase the range and the endurance.

Keywords: *CFD, Hydrodynamic Drag, Sweep Angle, Drag Reduction*.

1. Introduction

One of the most important parameters in designing vehicles that move in fluids, such as aircrafts or submarines, is the proper aerodynamic or hydrodynamic design. In general, suitable aerodynamic or hydrodynamic design is increasing in lift coefficient and moves toward the minimum value of drag coefficient [1]; but in ships and submarines, the main subject is hydrodynamic drag force reduction regardless of lift coefficient [2-5]. In the present paper, an investigation of the drag reduction is done on a special type of small scale unmanned submarine. The main purpose is to reduce the hydrodynamic drag using the implementation of proper geometrical shape changes, whereas the hydrofoil volume and the horizontal tail surface area remain fixed (hydrofoil surface area and horizontal tail volume are set as fixed parameters) because the main systems of this unmanned submarine and water tank located in the hydrofoil and its volume reduction can cause problems in necessary systems packaging. Figures 1 and 2 show the shape of this unmanned submarine and its dimensions.

Nature has always been the best inspiration for engineers and designers in all industrial fields, especially in aerospace and marine industries [2]. For drag reduction in this vehicle, the idea is to apply a backward sweep angle in submarine hydrofoil and horizontal tail, like fish bodies. This idea, proposed by the present authors, is unique and does not in any other report. Implementation of backward and forward sweep angles in near sonic and supersonic aircraft wings can reduce wings wave drag due to the reduction in the normal velocity component on wing leading edge and can decrease the local Mach number (increase in critical Mach number) [6]. The present study is part of a study on a multi-mission vehicle [7], concentrated on the investigation of the backward sweep angle effects of hydrofoil and horizontal tail in incompressible subsonic (very low speed) regime and dense environment of water. At first, with fixed hydrofoil shape (zero sweep angle), horizontal tail sweep angle changes from 0° to 50°. Figure 3 illustrates the variation in the horizontal tail sweep angle. Tail airfoil and main hydrofoil have a standard section of NACA0012 and NACA0019, respectively.

* Corresponding author. e-mail: goshtasb@shirazu.ac.ir.

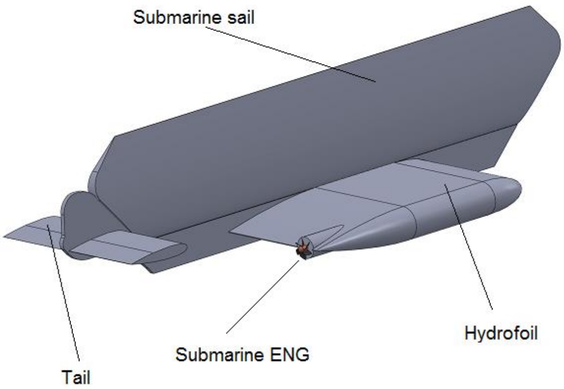

Figure 1. Components of studying submarine in basic shape (zero hydrofoil and horizontal tail sweep angle)

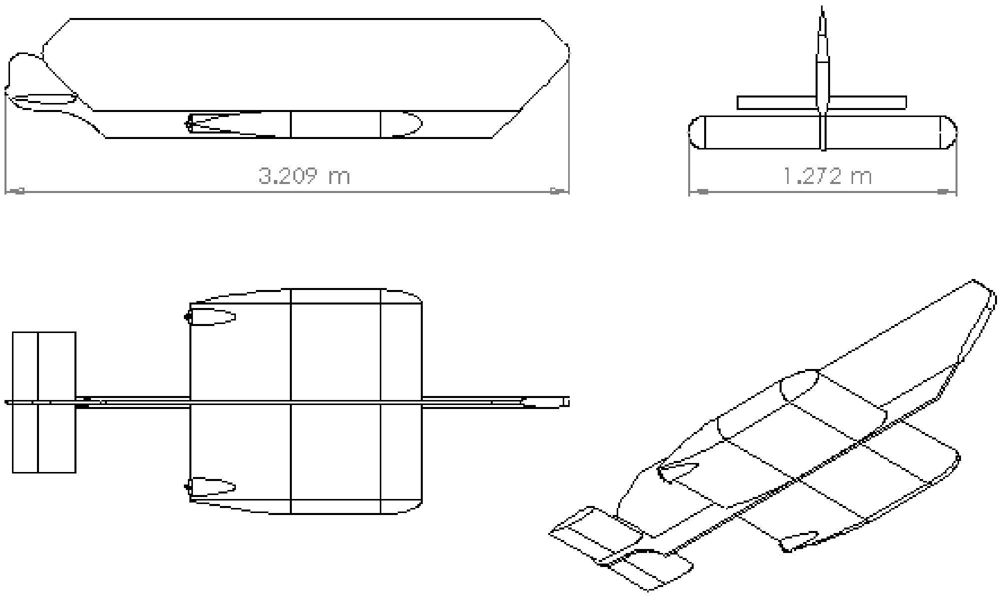

Figure 2. Standard views of studying submarine in basic shape (zero hydrofoil and horizontal tail sweep angle)

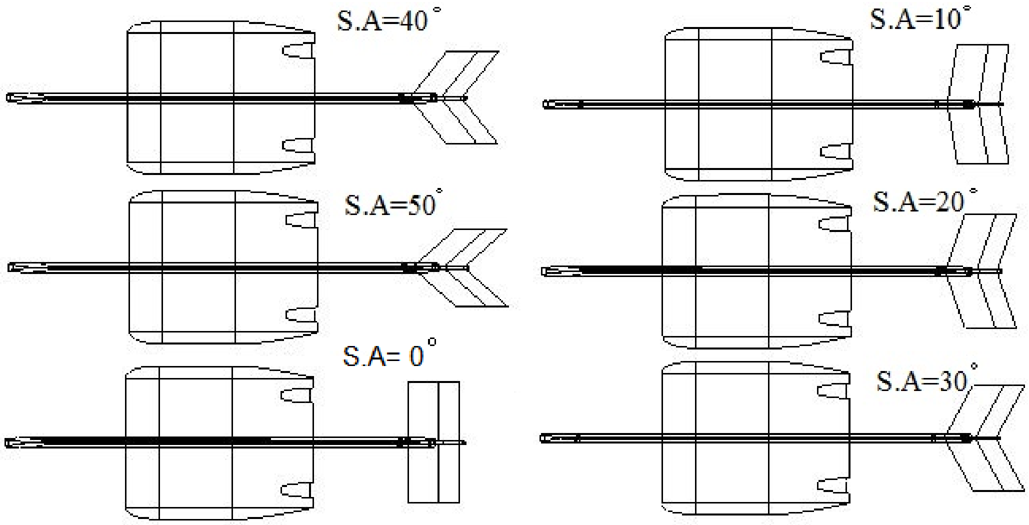

Figure 3. Submarine with fixed hydrofoil and swept horizontal tail that change from $0°$ to $50°$

In the first step, the hydrofoil sweep angle is zero (constant) and the tail sweep angle increases from 0° to 50°; then, in the next step, with a constant horizontal tail sweep angle, the effects of applying hydrofoil sweep angle, that changes from 0° to 60° degrees, is investigated. Figure 4 illustrates how the hydrofoil sweep angle changes with the fixed (50°) horizontal tail sweep angle:

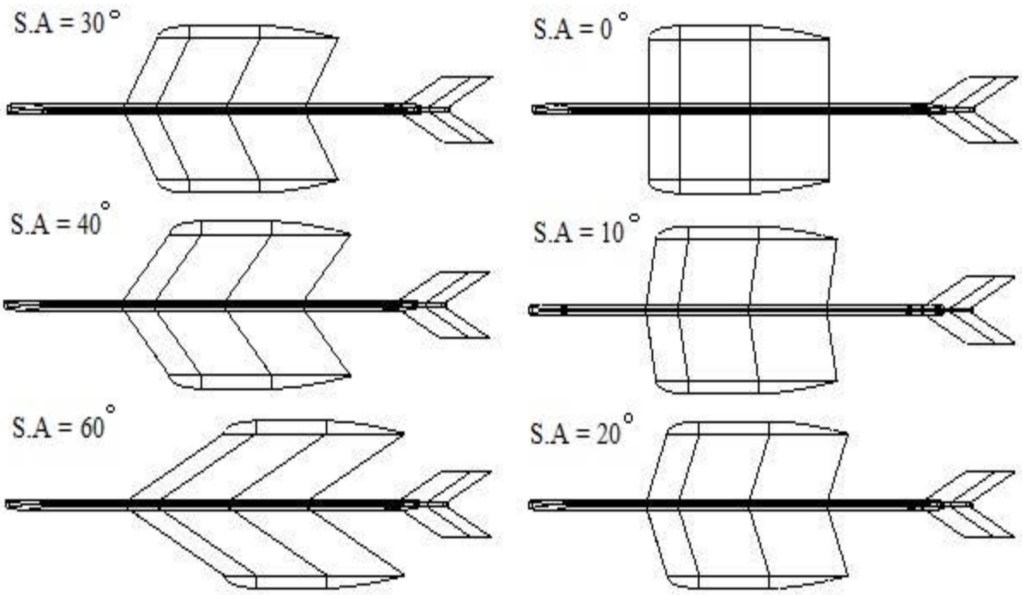

Figure 4. Submarine with fixed horizontal tail and swept hydrofoil that change from 0° to 60°

When the sweep angles of the hydrofoil and the tail are changed (in Mechanical Design Software), the orthogonal span is also changed. Therefore, authors decided to maintain the volume of the hydrofoil and the tail surface as a fixed parameter because of their missions and only to show the infuence of the sweep angles on drag reduction. Figure 5 shows the elongation of span to fix the hydrofoil volume:

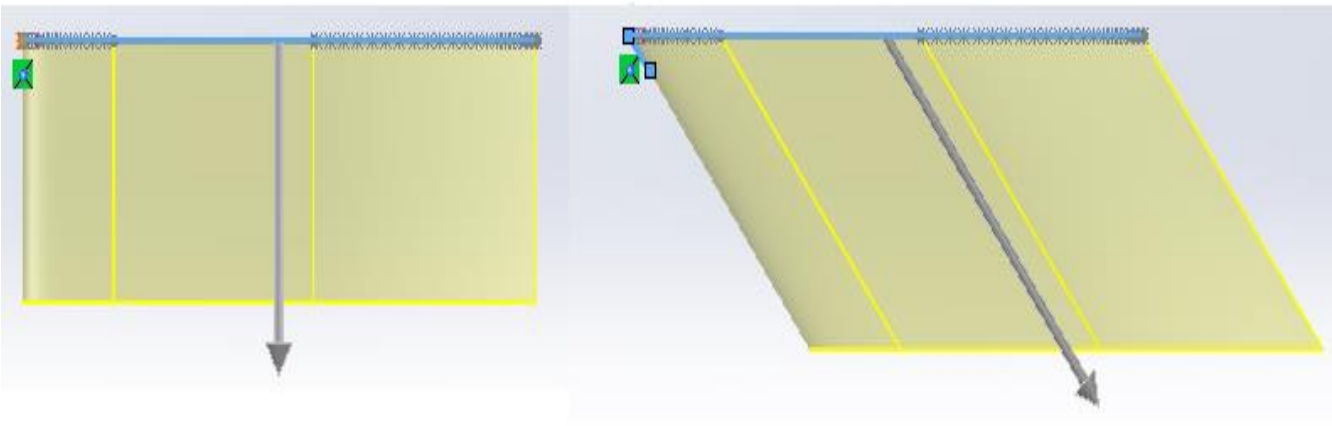

Figure 5. Increase extrude length of hydrofoil in non zero sweep angles to maintain constant hydrofoil volume

The present study is built of the bases that submarines usually move with zero angle of attack and that 4m/s (7.8 knots) is the maximum cruise speed of the proposed submarine.

2. Numerical Approach

The CFD method is convenient and time saving. To ensure reliable results and since experimental data were not available for this submarine, ANSYS Fluent and ANSYS CFX software were used. Different computational grids were generated with various quality and characteristics to ensure the independence of the model from computational grid. In addition, mesh density control was applied in order to save computational power and time by setting coarse grids at the boundaries of the domain and fine grids near area of interests and where the geometries are more complex. Mesh density near the walls and at the boundary layer can properly predict a viscous force on submarine surfaces. The Computational domain in both CFX and FLUENT has the same extent and size but has different boundary layer mesh due to differences in these solvers (Table.1).

Table 1. Comparison of boundary layer mesh characteristics in CFX and FLUENT

CFD Software	Transition Ratio	Maximum Layer	Growth Rate 3	Collision Avoidance
FUENT	0.272	5	1.2	Layer Compression
CFX	0.77	5	1.2	Stair Stepping

In addition, to avoid generating any highly skew mesh, mesh control is also needed to ensure that the transition from fine to coarse mesh is smooth. After the implementation of the computational grid and the domain study methods, mesh refinements are done in five steps. The total number of cells in the chosen computational grid is approximately 4.5 million. This is thought, by the authors, to be rough to give accurate results but proper to capture the characteristics of the flow properties; see Figure 6.

For the computational domain, the inflow was placed 6*c* upstream of the submarine nose, the outflow 15*c* downstream and 6*c* in height (c is hydrofoil mean chord), as shown in Figure 7. The side boundary was placed 6*c* away from hydrofoil tip. The y+ value at the wall is around 200, which is suitable for wall function applied in numerical simulation. A velocity inlet boundary condition prescribed a uniform velocity of 4m/s. At the outflow boundary, a pressure outlet boundary condition specified a gauge pressure of zero. A slip boundary condition (symmetry) was specified on the top and side far boundaries. A no-slip boundary condition was specified on the submarine surfaces. Domain is mono-phase and water has a constant density of 998.2 kg/m^3 and its viscosity set to 0.001003 kg/ms.

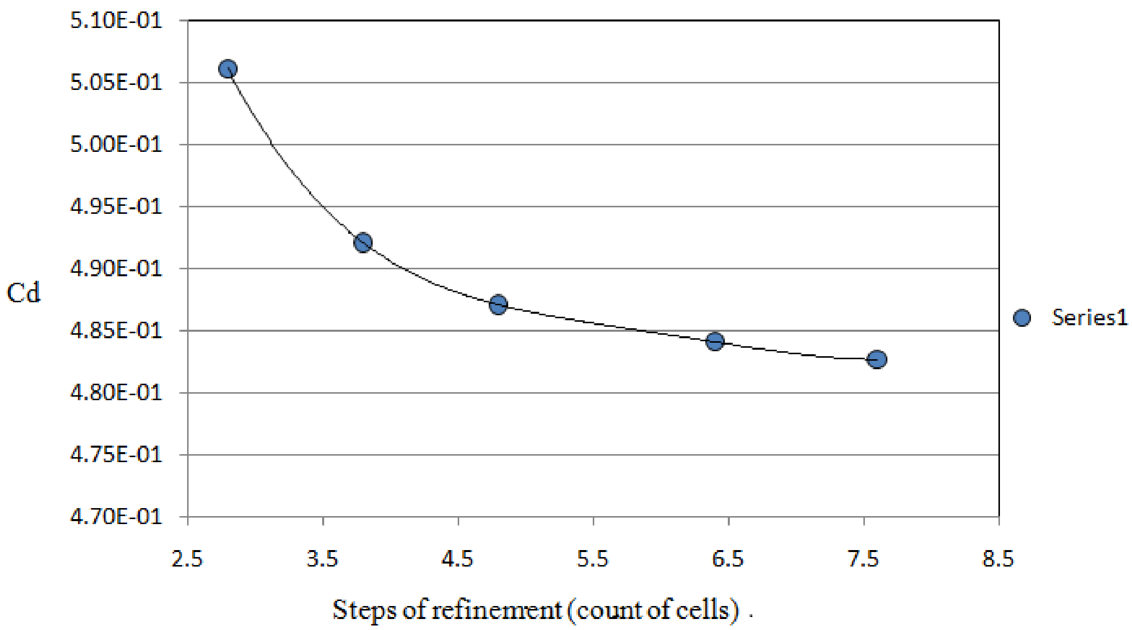

Figure 6. Hydrodynamic drag coefficient versus number of meshes(million grids).

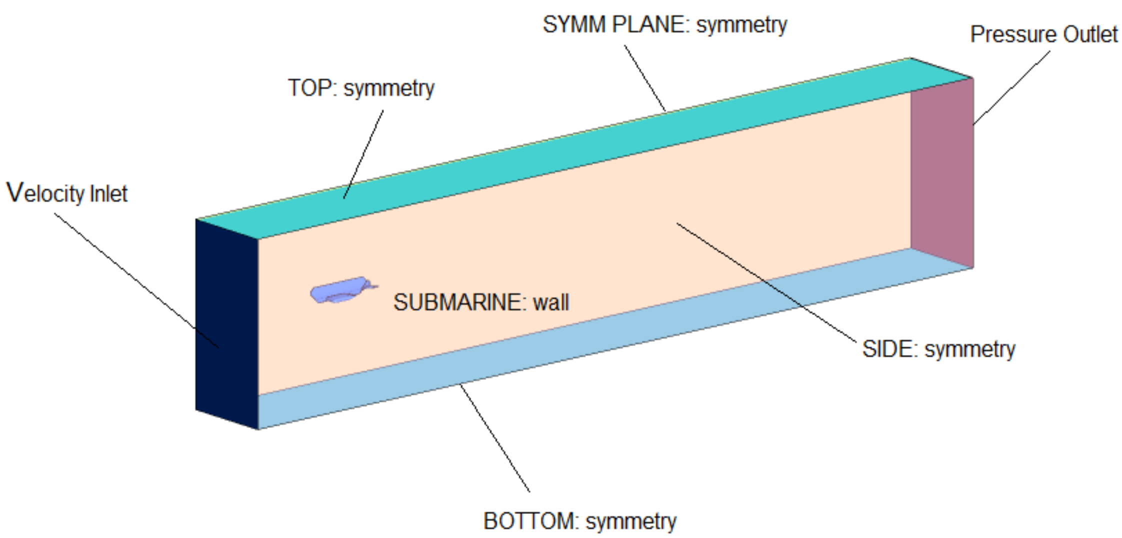

Figure 7. Applied boundary conditions on computational domain

Unstructured boundary layer mesh was used for simulations due to its good adaption ability to complex geometries and its reliability. Unstructured boundary layer mesh was generated in ANSYS Mesher and CFD analysis was carried out using FLUENT and ANSYS CFX commercial codes. Results show good agreements between FLUENT and CFX data that confirmed each other. Various turbulent models were used in both software but the best results in FLUENT was realizable *k-ε* model and in CFX was standard *k-ε* model.

2.1. Governing Equations

In the present study, flow regime is simulated by solving the incompressible Reynolds-averaged Navier-Stokes equations with the realizable $k-\varepsilon$ turbulence model in FUENT at the Reynolds number of 12.72×10^9 (based on the length of submarine).

The governing equations are written as:

$$\frac{\partial U_i}{\partial x_i} = 0 \tag{1}$$

$$\frac{\partial U_i}{\partial x_i} + \frac{\partial (U_i U_J)}{\partial x_j} = -\frac{1}{\rho}\frac{\partial p}{\partial x_i} + v\frac{\partial^2 U_i}{\partial x_j \partial x_j} + \frac{\partial}{\partial x_j}(\overline{-\acute{u}_i \acute{u}_j}) \tag{2}$$

where $(\overline{-\acute{u}_i \acute{u}_j})$ is the Reynolds stress term.

The transport equations of k and ε are written as:

$$\frac{\partial}{\partial t}(\rho k) + \frac{\partial(\rho k u_j)}{\partial x_j} = \frac{\partial}{\partial x_j}\left[\left(\mu + \frac{\mu_t}{\sigma_k}\right)\frac{\partial k}{\partial x_j}\right] + G_k + G_b - \rho\varepsilon - Y_M + S_k \tag{3}$$

$$\frac{\partial}{\partial t}(\rho \varepsilon) + \frac{\partial(\rho \varepsilon u_j)}{\partial x_j} = \frac{\partial}{\partial x_j}\left[\left(\mu + \frac{\mu_t}{\sigma_\varepsilon}\right)\frac{\partial \varepsilon}{\partial x_j}\right] + \rho C_1 S\varepsilon - \rho C_2 \frac{\varepsilon^2}{k + \sqrt{v\varepsilon}} + C_{1\varepsilon}\frac{\varepsilon}{k}C_{13\varepsilon}G_b + S_\varepsilon \tag{4}$$

The realizable κ-ε model is a more advanced version of a two-equation turbulence model. This turbulence model was extensively validated and well behaved for a wide range of flows, including rotating homogeneous shear flows, free flows including jets and mixing layers, channel and boundary layer flows, and separated flows [8, 9]. The incompressible Navier-Stokes equations (eq. (1) and eq. (2)) are solved by the SIMPLE [10] algorithm with a second-order upwind scheme applied to the convection terms. Also, in the operating condition panel, the operating pressure was set at 1 atmosphere and gravity was activated. Near wall treatment was set as a scalable wall function that is a new method and has a better convergence in two solvers. A default set of under-relaxation factor was suitable for a solver convergence.

To ensure the proper convergence of the solutions, a study is made on the tolerance value needed for the convergence criteria. Since the drag is the most important parameter needed, the solutions of this parameter is observed with a different tolerance value. When the fluctuation of the drag is sufficiently small in the next successive steps of iterations, the solutions are said to have converged sufficiently.

3. Results

In the first step of simulations, results show that the increase in the horizontal tail sweep angle with constant zero hydrofoil backward sweep cause hydrodynamic drag reduces about 6% in 50° tail backward sweep angle. This reduction of hydrodynamic drag in 4m/s speeds of this submarine is equal to 44 N; therefore, the consumption power decreases about 180 watt; see Figure 8.

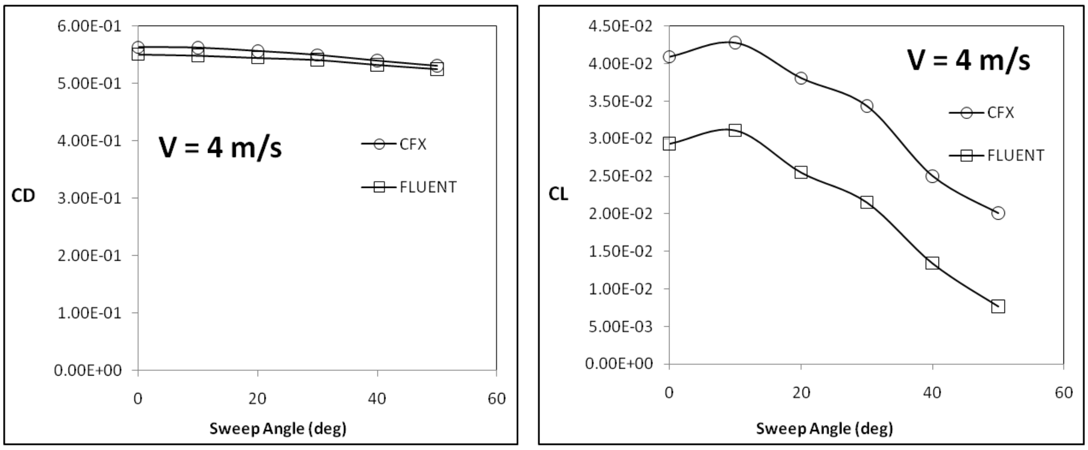

Figure 8. Hydrodynamic drag and lift coefficient versus horizontal tail sweep angle (constant zero hydrofoil sweep angle)

In the next step, hydrofoil sweep angle that has a larger cross section and a wetted area and subsequent has more contribution in the hydrodynamic drag graduate from 0° to 60° but the horizontal sweep angle remains 50° fixed.

Figure 9 illustrates how the increase in the hydrofoil sweep angle decreases the hydrodynamic drag. CFX and FLUENT results are in agreement with each other.

Figure 9 shows that in 4m/s of the submarine speed, with 60° increasing in hydrofoil sweep angle, hydrodynamic drag coefficient decreases about 14% rather than zero hydrofoil sweep angle. This amount of drag reduction is equal to 97 N and 388 watt of consumption power in maximum cruising speed causing an increase in the submarine range and endurance.

Figures 10 and 11 illustrate velocity contours behind the submarine in parallel section planes and Figures 12 and 13 show the velocity contours in longitudes plan (top view) in two conditions consisting of hydrofoils zero and 60° sweep angles. Contours show how the hydrofoil sweep angle desirably alters the pressure and velocity contribution to decrease the wake and hydrodynamic drag force. Therefore, the overall drag reduction without any reduction in the hydrofoil volume and the horizontal tail surface area, as shown in Figure 14, reaches about 19% rather than zero sweep angle condition of tail and hydrofoil. This hydrodynamic drag is equal to 141 N and 564 watt of consumption power in cruise (4m/s) speed.

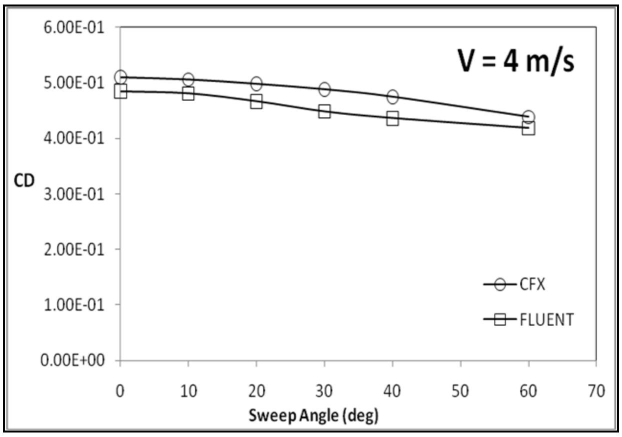

Figure 9. Hydrodynamic drag coefficient versus hydrofoil sweep angle (constant 50° horizontal tail sweep angle)

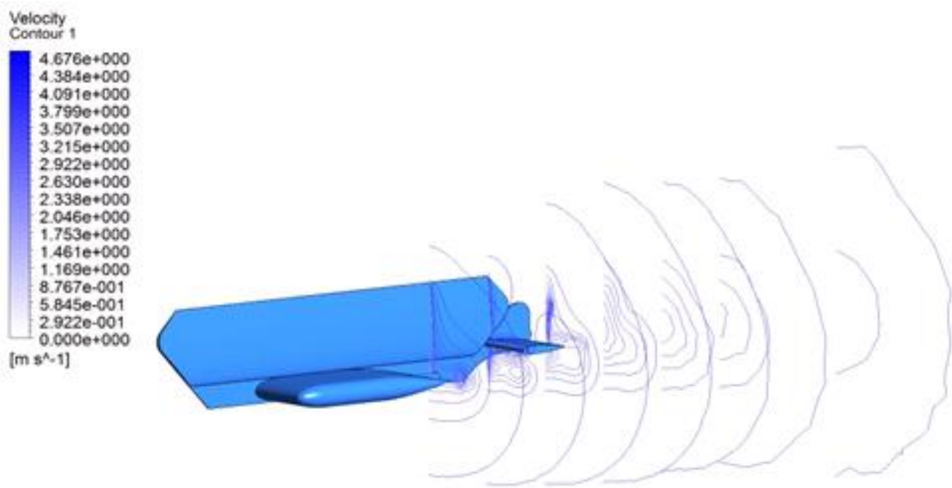

Figure 10. Velocity contours in parallel section planes with zero hydrofoil and tail sweep angle

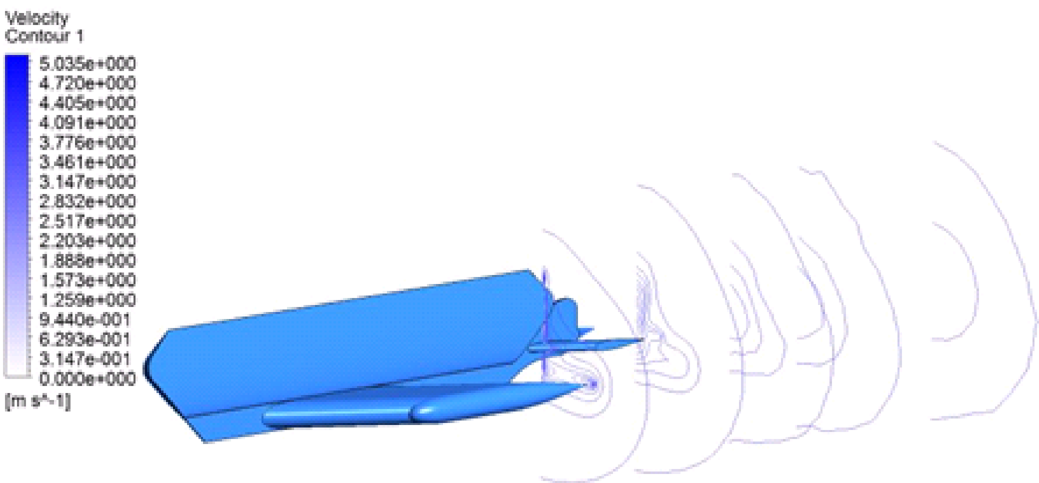

Figure 11. Velocity contours in parallel section planes with 60° hydrofoil and 50° tail sweep angle

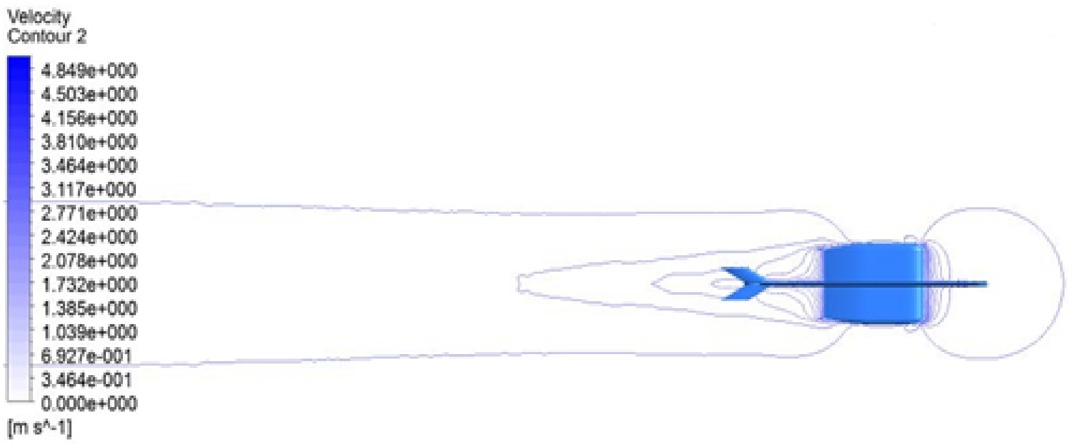

Figure 12. Velocity contours in longitude plane (top view) with zero hydrofoil and 50° tail sweep angle

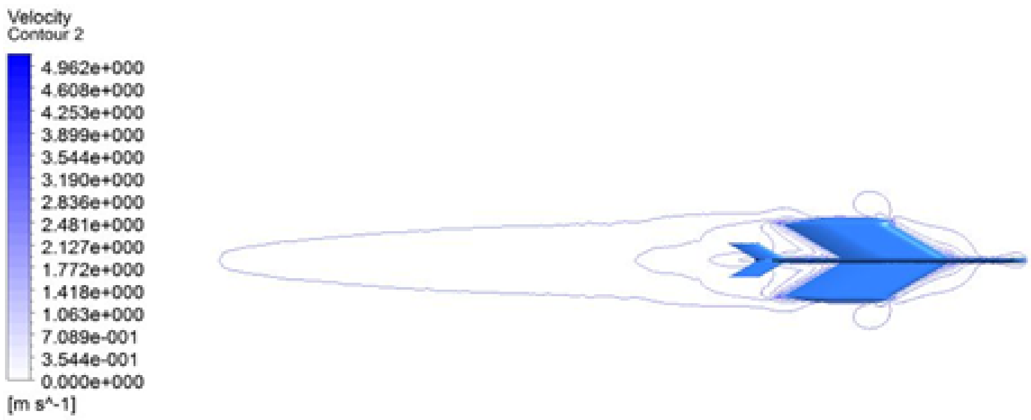

Figure 13. Velocity contours in longitude plane (top view) with 60° hydrofoil and 50° tail sweep angle

4. Conclusion

Results show that the implementation of backward sweep angle on control surfaces and hydrofoil (main body) of small scale submarine with a new design that has a non-cylindrical shape and shapes like as airplanes unlike classic submarine cylindrical body, same as wave drag reduction in supersonic aircrafts flight can be effective in reducing the hydrodynamic drag in low speed dense fluid regime like water.

It's clear that applying a backward sweep angle on control surfaces and hydrofoil with a reduction in the maximum normal to chord cross section in constant volume even in more surface area of hydrofoil results in significant changes in pressure contribution in the front of the hydrofoil and a reduction in the wake area behind of the submarine. Wake zone reduction due to sweep of hydrofoil can increase the secrecy of this submarine that is an important parameter in such a vehicle design. Therefore, with applying a backward sweep angle on this submarine surface, and similar cases, can reduce the engine consumption power and save fuel and cost.

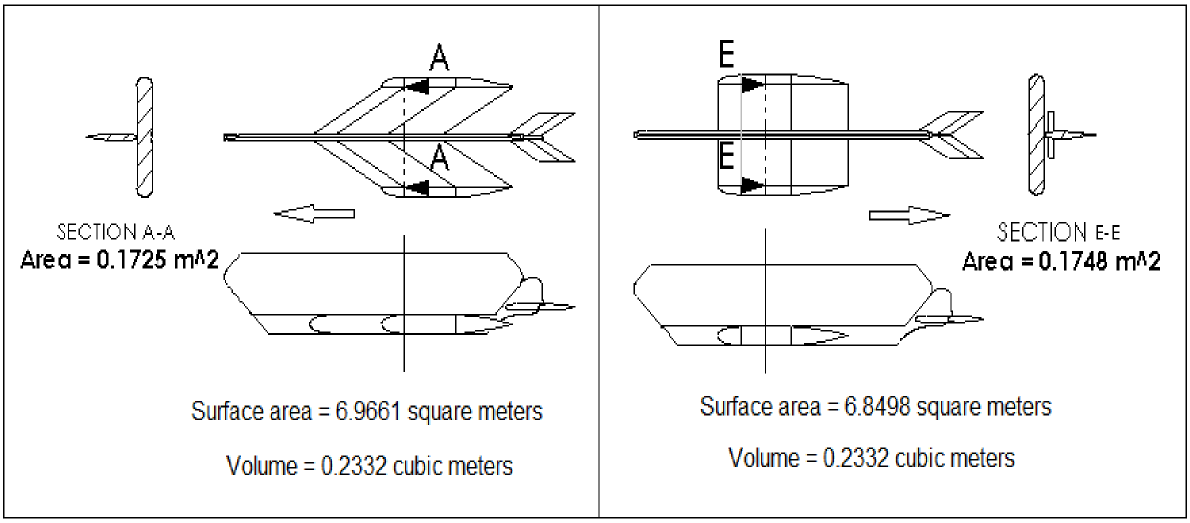

Figure14. comparing of wetted area, overall volume and maximum cross section area of submarine in zero and 60° hydrofoil sweep angles

References

[1] Hossain, P.R. Arora, A. Rahman, A.A. Jaafar and A.K.M. Parves Iqbal, “Analysis of longitudinal aerodynamic characteristics of an aircraft model with and without winglet”. Jordan Journal of Mechanical and Industrial Engineering Vol. 2 (2008), No. 3, pp 143 - 150

[2] F.E. Fish, “Imaginative solutions by marine organisms for drag reduction”. Department of biology, West Chester University, West Chester, PA 19383 USA, (2012), www.researchgate.net

[3] Zobeiri, “Effect of hydrofoil trailing edge geometry on the wake dynamics”. PhD. Theses No. 5218. Ecole Polytechnique Federal de Laussanne, (2012)

[4] M.H. Djavareshkian, A. Esmaeili and A. Parsania, “Numerical simulation of smart hydrofoil in marine systems”. Ocean Engineering 73 (2013) pp 16-24

[5] Ashrafi, M. Ketabdari and H. Ghassemi, “Numerical study on improvement of hydrofoil performance using vortex generators”. IJE Transaction B: Application, Vol. 28 (2015) No.2 pp 305-313

[6] Roskam, J., and Edward Lan C.T. “Airplane aerodynamics and performance”. Kansas, Lawrence, DARcorporation, (1997), pp. 112-114

[7] M. Hadipour and E. Goshtasbi Rad, "Investigation and comparing between two air propulsion systems used in a multipurpose vehicle using computational fluid dynamics" Journal of Science and Engineering, Vol. 5 (2014), No. 1, pp. 11-23

[8] T.H. Shih, W.W. Liou, A. Shabbir, and Z. Yang, “A new *k*-*ε* Eddy-viscosity model for high Reynolds number turbulent flows - model development and validation” Computers Fluids, Vol. 24 (1995) ,No. 3: pp. 227-238.

[9] M.P. Bulat and P.V. Bulat, “Comparison of turbulence models in the calculation of supersonic separated flows”. World Applied Science Jour. 27 (2013), Issue 10, pp 1263-1266.

[10] Patankar, S.V., Numerical heat transfer and fluid flow, McGraw-Hill, 1980, pp.126-130.

JJMIE

Jordan Journal of Mechanical and Industrial Engineering

Volume 9 Number 3, June.2015
ISSN 1995-6665
Pages 217 - 221

The Influence of the Addition of 4.5 wt.% of Copper on Wear Properties of Al-12Si Eutectic Alloy

Shivaprasad Channappagoudar [a *], Kiran Aithal [b], Narendranath Sannayallappa [a] Vijay Desai [a] , Pudukottah Gopaliengar Mukunda[b]

[a] *Dept. of Mechanical Engineering, National Institute of Technology, Surathkal, India*
[b] *Dept. of Mechanical Engineering, Nitte Meenakshi Inst. of Tech. Bangalore, India*

Received 7 Dec 2014 *Accepted 14 May 2015*

Abstract

The influence of 4.5 wt.% copper addition on wear behavior of as-cast Al-12Si alloy prepared by gravity casting is investigated in dry sliding against a steel counterface using a pin-on-disk apparatus. The microstructures of test alloys and worn surfaces were examined by scanning electron microscopy and energy dispersing X-ray spectroscopy. The addition of copper to the binary Al-12Si alloy led to the precipitation of CuAl2 phase. Copper addition resulted in a refinement of α-Al and a minor modification of eutectic Si. The Al-12Si-4.5Cu alloy showed a higher wear resistance as compared to Al-12Si binary eutectic alloy.

Keywords: *Eutectic alloy; Effect of Cu addition; Microstructure; Wear*.

1. Introduction

Al-Si alloys are widely used in automotive industry as they offer a high wear resistance, a low thermal expansion and a good corrosion resistance [1]. These alloys are used in manufacturing Cylinder blocks, cylinder heads, pistons and valve filters [2]. These applications require excellent wear properties of the alloys. The effect of adding Si content on wear characteristics of Al-Si alloys were studied [3]. The wear characteristics of the material depend on the structural features of the material, such as shape, size and distribution of micro constituents in the matrix apart from operating conditions, such as sliding speed, load, temperature and distance [4]. Many authors investigated the influence of alloying elements on tribological properties of Al-Si alloys [5,6]. Studies conducted to investigate the influence of adding Al-1Ti-3B (grain refiner) and Al-10Sr (modifier) master alloys to eutectic Al-Si alloys reported an improved wear resistance after the modification and grain refinement [7]. The studies on the wear behavior of Al-12Si alloy reinforced with TiB_2 particles showed that these particles played a vital role in reducing the size of Si particles and minimizing the subsurface crack propagation resulting in an improved wear resistance [8]. The addition of grain refiner (Al-1Ti-3B), modifier (Sr) and modifier (P) to Al-15Si-4Cu cast alloys resulted in an improvement in the wear resistance due to grain refinement, and fine $CuAl_2$ particles found in the interdendritic region [9]. The wear behavior of hypereutectic Al–Si–Cu–Mg casting alloys with 6 wt % and 10 wt% Mg was investigated using a dry sand rubber wheel and it was found that alloys with high Mg content showed an improved wear resistance [10]. Microstructural investigations indicated that the intermetallic Mg_2Si particles in alloys with 6% and 10% Mg addition are more solidly bonded to the matrix compared to the coarse primary silicon particles. The effects of pressurized solidification on copper containing Al-Si alloy were studied. The micro structural studies indicated that microstructure of non-pressurised specimen contained course dendrites and the pressurized specimen showed a fine microstructure with modified eutectic Si particles. These structural changes resulted in an improved wear behavior of the pressurized cast samples [11]. The studies were carried out to understand the evaluation of the microstructure and dry sliding wear behavior of thixoformed A319 aluminium alloy [12]. The thixoforming process resulted in uniformly distributed Si and intermetallic compounds of the test alloy. The enhanced microstructure was found to play a major role in improving wear performance.

Copper is another important alloying element in aluminium alloys among the elements used in production. It imparts heat treatability to castings through the formation of Al_2Cu and enhances the mechanical properties remarkably [13]. Al–Si–Cu alloys, with up to 4.5 wt.% copper, are satisfactory for the ordinary

* Corresponding author. e-mail: hivaprasad.hma@gmail.com.

conditions of service. The addition of just 1% copper in these alloys increases the transition load by 3-4 times by increasing the strength and stability of protective surface layer [14]. The effect of adding 1, 2 and 4 wt.% Cu to Al-12Si-20Mg cast alloys on their wear and corrosion properties were studied [15]. Studies showed that the addition of Cu led to the formation of $CuAl_2$ phase. Adding Cu to Al-12Si-20Mg alloy increased hardness values. The role of adding copper in optimizing the tensile properties of Al-11Si-0.3Mg alloy was studied [16]. Studies reported a slight coarsening of α-Al dendrites due to the addition of copper. However, copper addition had an insignificant effect on the size and morphology of eutectic Si particles. The effect of adding Cu on the wear behavior of Al-18Si-0.5Mg alloys was investigated [5]. The study showed that the wear rate is not appreciably affected with the addition of Cu. However, the addition of copper increased the transition load at 2.0 m/s sliding speed. Further addition of Cu (more than 2%) did not show any effect on the transition load. The study that investigated the influence of the combined action of grain refiner and modifier on dry sliding wear of Al-12Si alloy and Al-12Si-3Cu alloy showed that the treated Al-12Si-3Cu alloy offered the best wear resistance at higher loads [17]. The experimental studies on the effect of copper addition on dry sliding wear behavior of A356 alloy reported an increase in wear resistance due to the increase in the strength and hardness of the alloy after copper addition . The formation of oxide layers on the surface is found to be one of the causes of improving the sliding wear performance [18].

The objective of the present work is to investigate the influence of the addition of 4.5 wt.% Cu on wear properties of as cast Al-12Si alloy in dry sliding using pin-on-disk wear tests.

2. Experimental Work

The chemical compositions of Al-12Si and Al-12Si-4.5Cu alloys, as determined by optical emission spectrometer, are given in Table 1.

Table 1. Chemical composition of experimental alloys

Alloy	Composition (wt.%)					
	Si	Cu	Fe	Mn	Mg	Al
Al-12Si	12.09	0.04	0.16	0.02	0.01	Balance
Al-12Si-4.5Cu	12.06	4.46	0.18	0.04	0.03	Balance

The eutectic Al-Si alloys were melted in clay-graphite crucible at 720±5°C. Before pouring the melt into steel moulds, 1 wt% of hexachloroethane (C_2Cl_6) was added to degas the melt. For Al-12Si alloy, pre determined amount pure copper was added for getting Al-12Si-4.5Cu alloy. For optical microscopy, the samples were mechanically polished and etched with Keller's reagent (1.5 ml HNO_3, 2.5 ml HCl, 1.0 ml HF, and 95 ml H_2O). SEM was carried out using FEI Netherlands make Quanta-200 SEM.

Dry sliding wear studies were carried out following ASTM-G-99 standard and using pin-on-disc apparatus at a speed of 2m/s using variable loads. The wear pins were cylindrical rods (10 mm diameter and 25mm long) with flat ends. The specimens of the experimental alloys were held against a rotating steel disc of 98 BHN. The sliding wear tests were conducted on pin-on-disc (TR-20 LE, DUCOM, Bangalore) test machine. The wear test arrangement is shown in Figure 1.

Figure 1. Dry sliding wear test arrangement

3. Results and Discussions

3.1. Microstructure of the Alloys

SEM images of Al-12Si binary alloy and Al-12Si-4.5Cu alloy are shown below. The microstructure of Al-12Si alloy, as seen in Figure 2 (a), consists of large primary α-Al grains and eutectic Si with needle like morphology (actually, plate like or flake like in three dimension) well dispersed throughout the matrix. EDX of Si needle is shown in Figure 2 (b).

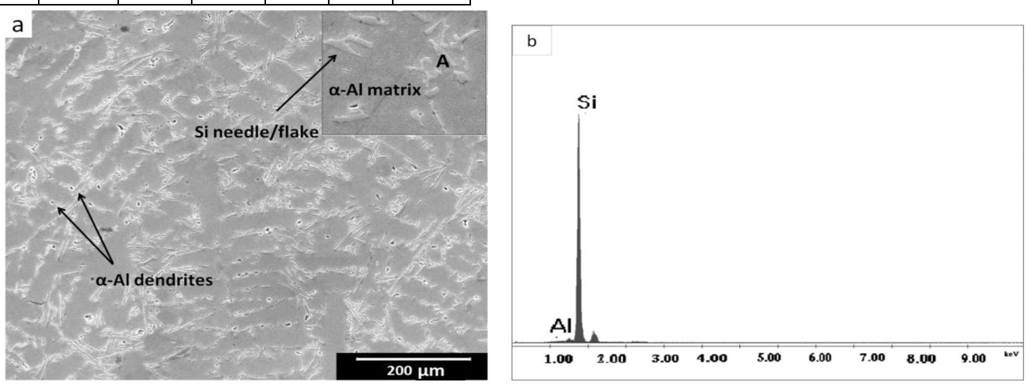

Figure 2. (a) SEM image of Al-12Si alloy (b) EDX of Si needle (marked 'A')

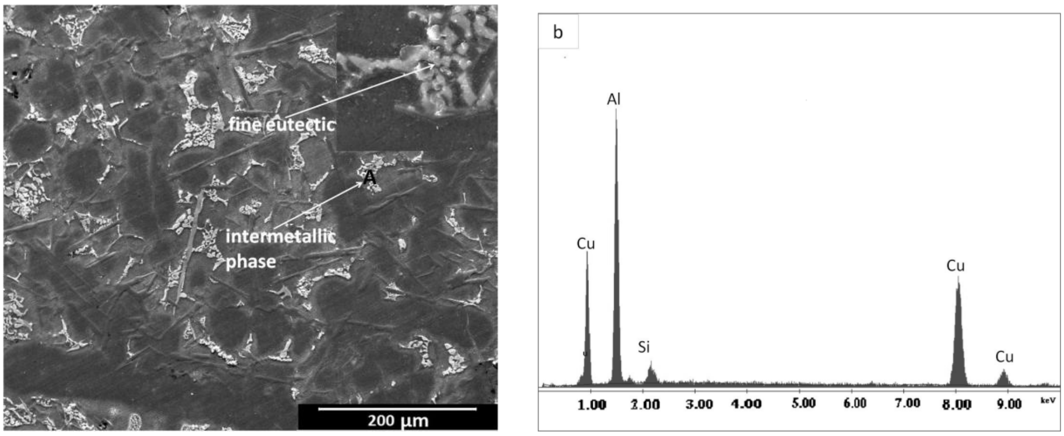

Figure 3. (a) SEM image of Al-12Si-4.5Cu alloy (b) EDX of $CuAl_2$ (marked 'A')

The change in microstructure with the addition of 4.5 wt. % of Cu is shown in Figure 3 (a). It can be seen that the eutectic Si is seen as coarse needles and orientation and morphology of α-Al grains is non uniform. In the inter-dendritic region $CuAl_2$ intermetallic particles are found. EDX of $CuAl_2$ intermetallic is shown in Figure 3 (b).

The effect of changes in microstructure due to the addition of 4.5 wt.% of Cu on wear behavior of the alloy was studied.

3.2. Wear Behaviour

Figure 4 shows the sliding wear of Al-12Si and Al-12Si-4.5 Cu alloys at different normal loads of (10, 20, 30, 40 and 50N) with a constant sliding speed of 2.0 m/s and a constant sliding distance of 1500 m. As the normal load on the test specimen is increased, the actual area of the contact increases resulting in an increased frictional force between the sliding surfaces. The results demonstrate that the increase in the load is responsible for the wear loss of the investigated samples. The addition of 4.5% Cu to Al-12Si alloy shows a lower wear rate when compared to that of Al-12Si alloy.

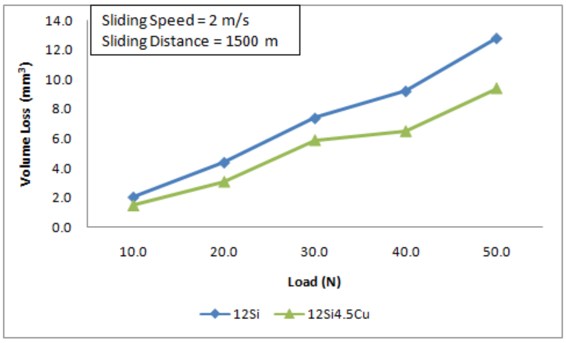

Figure 4. Variation of Volume loss with different loads

Figure 5(a) shows SEM image of the worn surface of Al-12Si alloy. A number of long, deep unidirectional ploughing grooves can be observed. A unidirectional action during sliding takes place and fragments come out of its surface and form debris. This depends on the critical shear stress of both mating surfaces. However, at 40 N load, Al-12Si base alloy witnessed a significant material removal or a high level of surface damage. These damages are mostly due to the low hardness of base alloy (64 HB).

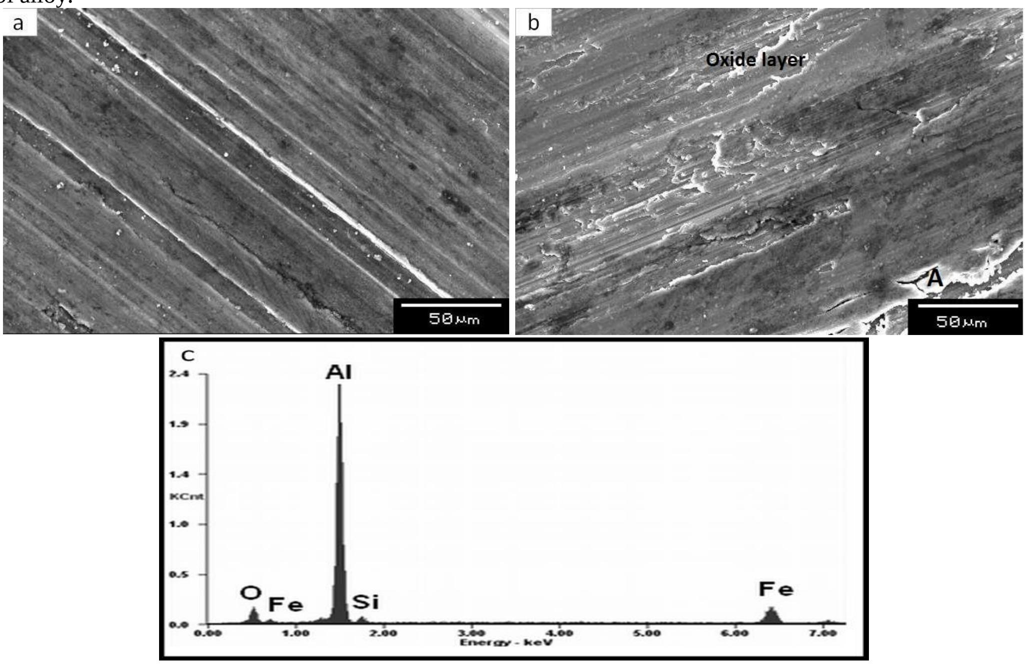

Figure 5. SEM of worn surface of Al-12Si alloy at load (a) 10 N (b) 40 N (c) EDX of oxide layer (Marked A)

From a close observation of Figure 5(b), it can be explained that the wear during sliding is mostly oxidation and metallic in nature. The tensile stress at the asperity increases with the increase in friction and results in the formation of oxide layer [19]. EDX, shown in Figure 5(c), confirms presence of the oxide layer.

Figure 6 (a) shows the wear track observed for Al-12Si-4.5Cu alloy. It can be observed that the wear grooves are smooth and not much deeper as compared to Figure 5 (a). This clearly demonstrates that the copper addition to the Al-12Si alloy results in a better sliding wear performance. Further, the presence of copper in Al-12Si makes the material hard (85 HB) and, as a result, it makes the depth of the sliding abrasive grooves low.

These results can be compared with Figure 4 where the wear loss for the Al-12Si-4.5Cu alloy exhibited low wear rates as compared to the Al-12Si base alloy.

Wear debris were collected at 50 N load at a sliding speed of 2m/s and Figure 7 shows the SEM of the wear debris of the experimental alloy. Figure 7 (a) depicts the wear debris of Al-12Si, whereas Figure 7 (b) depicts the debris of Al-12Si-4.5Cu alloy. Various shapes and sizes of wear debris were formed as a result of a dry sliding test. The shape and sizes of wear debris varied from fine particles to coarse flakes. The average size of wear debris of Al-12Si alloy and Al-12Si-4.5Cu alloy are about 300 microns and 80 microns, respectively. The higher size of wear debris of Al-12Si alloy was due to the delamination of particles from the wear surface. Fine wear debris of Al-12Ai-4.5Cu was due to a mild oxidative wear. Changes in the morphology of the wear debris were found to be consistence with the severity of the worn surface.

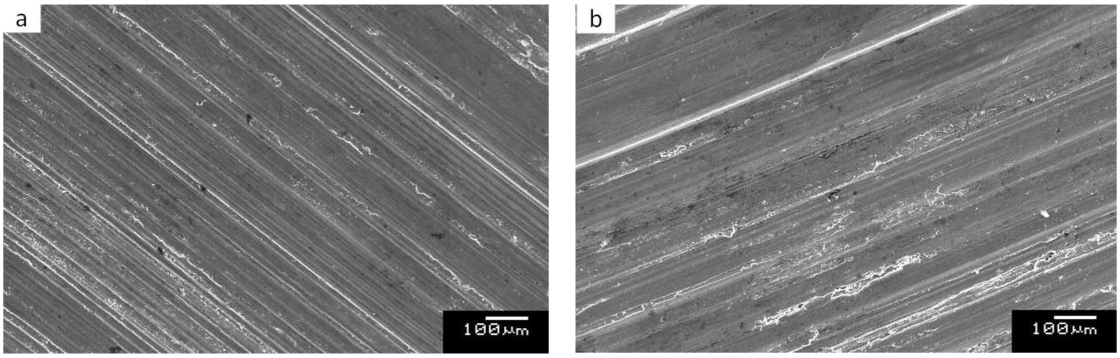

Figure 6. SEM of worn surface of Al-12Si-4.5Cu alloy at Load (a) 10 N (b) 40 N

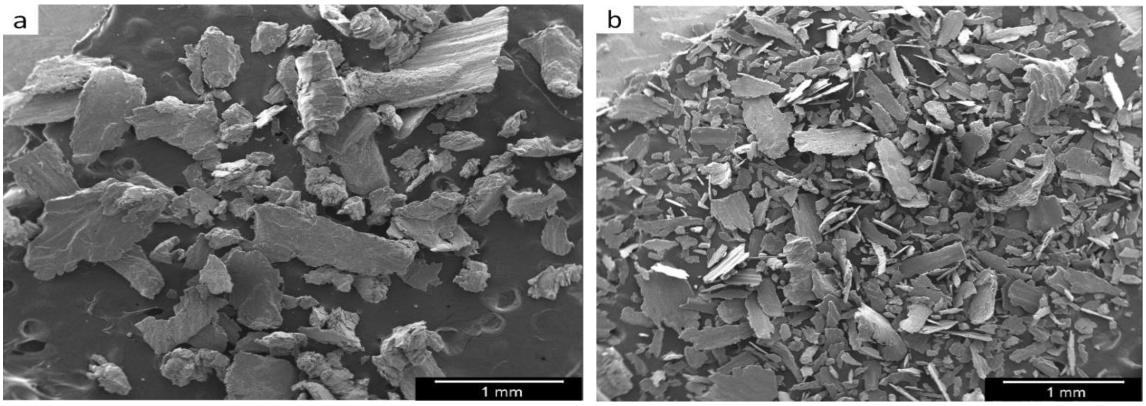

Figure 7. SEM of wear debris of (a) Al-12Si alloy (b) Al-12Si-4.5Cu alloy

4. Conclusions

Al-12Si alloys are widely used for automobile applications. A large number of experiments are made for the enhancement of the wear properties of these alloys. The present investigation aimed at improving the wear performance of Al-12Si alloy by the addition of 4.5 wt.% Cu. The copper addition resulted in the refinement of α-Al and a minor modification of eutectic Si. From the results obtained, the following conclusions are drawn:

- The microstructure details of as cast Al-12Si alloy clearly depict large primary α-Al and plate like eutectic Si. These structural details were responsible for the inferior sliding wear properties.
- The addition of 4.5 wt.% Cu to Al-12Si alloy resulted in improved hardness and sliding wear properties. The presence of $CuAl_2$ particles in Al-12Si-4.5Cu alloy was responsible for the improved wear properties.
- In general, the increase in the wear is observed with an increase in the load and sliding distance for both the test alloys.

References

[1] S.A Kori, B.S. Murty, M. Chakraborty, "Development of an efficient grain refiner for Al-7Si alloy". Materials Science and Engineering A, Vol. 280 (2000), 58-61.

[2] A.K. Prasada Rao, Karabi Das, B.S Murty, M. Chakraborty, "Effect of grain refinement on wear properties of Al and Al-7Si alloy". Wear, Vol. 257 (2004), 148-153.

[3] H. Torabian H, J.P. Pathak, S.N. Tiwari, "Wear characteristics of Al-Si alloys". Wear, Vol. 172 (1994), 49-58.

[4] T.M. Chandrashekharaiah, S.A. Kori, "Effect of grain refinement and modification on the dry sliding wear behaviour of eutectic Al-Si alloys". Tribology International, Vol. 42 (2009), 59-65.

[5] D.K. Dwivedi, T.S. Arjun, P. Thakur, H.Vaidya, K.Singh, "Sliding wear and friction behaviour of Al–18% Si–0.5% Mg alloy". J. Mater. Process. Techno., Vol. 152 (2004), 323–328.

[6] D.E. Lozano, R,D. Mercado-Solis, A.J. Perez, J. Talamantes, F. Morales, M.A.L. Hernandez-Rodriguez, "Tribological behaviour of cast hypereutectic Al–Si–Cu alloy subjected to sliding wear". Wear, Vol. 267 (2009), 545–549.

[7] T.M. Chandrashekharaiah, S.A. Kori, "Effect of grain refinement and modification on the dry sliding wear behaviour of eutectic Al– Si alloys". Tribology International, Vol. 42 (2009), 59-65.

[8] A. Mandal, B.S. Murty, M.Chakraborty, "Wear behaviour of near eutectic Al–Si alloy reinforced with in-situ TiB_2 particles". Mater. Sci. Eng. A, Vol. 506 (2009), 27-33.

[9] P.V.Chandra Sekhar Rao, A. Satya Devi, K.G. Basava Kumar, "Influence of Melt Treatments on Dry Sliding Wear Behavior of Hypereutectic Al-15Si-4Cu Cast Alloys". Jordan Journal of Mechanical and Industrial Engineering, Vol. 6 (2012), No. 1, 55-61.

[10] A. Hekmat-Ardaka, X. Liua, F. Ajerscha, G. Chen, "Wear behaviour of hypereutectic Al-Si–Cu–Mg casting alloys with variable Mg contents". Wear, Vol. 269 (2003), No. 9-10, 684-692

[11] R. Ashiri, B. Niroumand, F. Karimzadeh, "Physical, mechanical and dry sliding wear properties of an Al–Si–Mg–Ni–Cu alloy under different processing conditions" J. Alloys Compd, Vol. 582 (2014), 213-222.

[12] K.S. Alhawari, M.Z. Omar, M.J. Ghazali, M.S. Salleh, M.N. Mohammed, "Evaluation of the microstructure and dry sliding wear behaviour of thixoformed A319 aluminium alloy", Mater. Des., In press.

[13] C.H. Caceres, I.L. Svensson, J.A. Taylor, "Strength- ductility behaviour of Al-Si-Cu-Mg casting alloys in T6 temper". Int. J. Cast. Met. Res. Vol. 15 (2003), 531–543.

[14] S. Das, S.V. Prasad, T.R. Ramchandran, "Microstructure and wear of cast (Al–Si alloy)–graphite composites". Wear. Vol. 133 (1989), No. 1, 173–87.

[15] A. Palta, Y. Sun, H. Ahlatci, "Effect of copper addition on wear and corrosion behaviours of Mg_2 Si particle reinforced composites", Mater. Des., Vol. 36 (2012), 451–458.

[16] Tao Lu, Jili Wu, Ye Pan, Shiwen Tao, Yu Chen, "Optimizing the tensile properties of Al–11Si–0.3Mg alloys: Role of Cu addition". J. Alloys Compd, Vol. 631 (2015), 276-282.

[17] K.G. Basavakumar, P.G.Mukunda, M.Chakraborty, "Dry sliding wear behaviour of Al–12Si and Al–12Si–3Cu cast alloys". Mater. Des. Vol. 30 (2009), 1258–1267.

[18] M.S Prabhudev, V. Auradi, K. Venkateswarlu, N.H. Siddalingswamy, S.A. Kori, "Influence of Cu Addition on Dry Sliding Wear Behaviour of A356 Alloy". Procedia Engineering, Vol. 97 (2014), 136-1367.

[19] R. L. Deuis, C. Subramanian, J. M. Yellup, "Dry sliding wear of aluminium composites – A review". Composites Science and Technology, Vol. 57 (1997), 415-435

JJMIE

Volume 9 Number 3, June.2015
ISSN 1995-6665
Pages 223 - 240

Jordan Journal of Mechanical and Industrial Engineering

A Numerical Study on Deterministic Inventory Model for Deteriorating Items with Selling Price Dependent Demand and Variable Cycle Length

Prasad Patnaik,VVS. [a *] , Durga Prasad Patnaik, [a]. Srinivasa Rao K. [b]

[a]Department of Mathematics, M.R.College (Autonomous) Vizianagaram 535 002, A.P.
[b]Department of Statistics, Andhra University, Waltair - 530 003, A.P.

Received 9 January 2014 Accepted 25 May 2015

Abstract

In the present paper, an inventory replenishment model for deteriorating items is developed with the assumptions that demand is a function of selling price and the cycle length of successive replenishments is a variable in the planning period. It is assumed that the cycle length in each cycle decreases in Arithmetic Progression. Shortages are allowed and are completely backlogged. The instantaneous state of inventory with shortages is derived. The total cost function of the horizon is obtained with suitable costs. The optimal pricing and ordering policies of the model are derived. The objective is to determine a replenishment policy that minimizes the total inventory cost. The model is illustrated with some numerical results. The sensitivity of the model with respect to the parameters and cost is also discussed. This model includes some of the earlier models as particular cases.

Keywords: *Perishable Inventory, Cycle Length, Demand Rate and Cost Function, Optimal Ordering Policies and Sensitivity Analysis*.

1. Introduction

Inventory control deals with the determination of the optimal stock levels of items to meet future demand. According to Nadoor [3], starting from the development of the first lot size inventory model in 1912, a wide variety of models have been developed for inventory control with various assumptions. In order to analyze the practical situations arising at places, like business, production, material handling, resource sharing etc., inventory models are essential. The nature of the inventory model varies depending upon the items under consideration. In general, the items can be classified as deteriorating and non-deteriorating. In deteriorating items, the life time of the commodity is finite and it is lost after a certain period of time. Inventory of deteriorating items was first developed and analysed by Within [1], who considered the deterioration of fashion goods at the end of a prescribed storage period. Ghare and Schrader [2] extended the classical EOQ formula with exponential decay of inventory due to deterioration, developing a mathematical model of inventory of deteriorating items. Dave and Patel [6] developed the first deteriorating inventory model with a linear trend in demand. They considered demand as a linear function of time. Goyal and Giri [15] explained the recent trends of modeling in deteriorating items inventory. They classified inventory models on the basis of demand variations and other various conditions or constraints. Ouyang *et al.* [16] developed an inventory model for deteriorating items with exponential declining demand and partial backlogging. Alamri and Balkhi [17] studied the effects of learning and forgetting on the optimal production lot size for deteriorating items with time varying demand and deterioration rates. Dye and Ouyang [18] found an optimal selling price and lot size with a varying rate of deterioration and exponential partial backlogging. They assumed that a fraction of customers who backlog their orders increases exponentially as the waiting time for the next replenishment decreases.

Ajanta Roy [19] studied a model in which the deterioration rate is time proportional, demand rate is function of selling price and holding cost is time dependent. Much work has been reported in deteriorating inventory models developed by many researchers, like Goyal *et al.* [13], Haipingxu *et al.* [10], Nahmias [7], and Sachan [8]. For modeling the inventory system, the prominent factors are demand and replenishment of items. Datta and Pal [12], Dave [9], Donaldson [4], Gioswami and Chaudhury [11] developed deterministic lot size

* Corresponding author. e-mail: prasad_vvs07@yahoo.co.in.

inventory models with shortages and a linear trend in demand. In many of these models, they assumed that the cycle length, i.e., the time between two replenishments, is fixed or constant. In several inventory systems, the cycle length is to be made as a variable in order to have optimal operating policies. For example, in case of the production of edible oils, food products etc., the cycle length is to be reduced gradually in the planning period (Horizon). Nahamias [7] reviewed the perishable inventory models. Bhunia and Maiti [14] and Dave and Patel [6] developed inventory models with shortages with the assumptions that the successive replenishment cycles were diminished by constant amounts of time without considering the deterioration of items. Haipingxu *et al.* [10] and Sachan [8] developed the inventory models for deteriorating items with time dependent demand. Mondal *et al.* [20] investigated the finite replenishment inventory models of a single product with imperfect production process. In this process, a certain fraction or a random number of produced items are defective. Skouri *et al.* [21] studied inventory models with ramp type demand rate, partial backlogging and Weibull deterioration rate. Chung and Huang [22] studied ordering policy with permissible delay in payments to show the convexity of total annual variable cost function. Shah and Mishra [23] studied an EOQ model when units in inventory deteriorate at a constant rate and demand is stock dependent. The salvage value is associated to deteriorated units.

Wou [24] developed an inventory model with a stochastic demand. Jaggi Chandra and Priyanka Verma [25] developed and analyzed a two-warehouse inventory model for deteriorating items with linear trend in demand and shortages under inflationary conditions. Uma Maheswara Rao *et al.* [26] developed and analyzed a production inventory model for deteriorating items by assuming that the demand is a function of both on-hand inventory and time. It is also assumed that the lifetime of the commodity is random and follows a Weibull distribution. A case study is carried out to determine the production schedules in a pickle manufacturing industry.

Hung [27] made a continuous review of inventory models under time value of money and crashable lead time. Lin [28] analyzed inventory models with managerial policy independent of demand. Lin *et al.* [29] studied an inventory model with ramp type demand under stock dependent consumption rate. Roy and Chaudhuri [30] developed and analyzed an EPLS model for a variable production rate with stock price sensitive demand and deterioration. Khana *et al.* [31] developed a model which investigates an Economic Order Quantity (EOQ) model over a finite time horizon for an item with a quadratic time dependent demand by considering shortages in inventory under permissible delay in payments. They derived the model under three different circumstances depending on the time of occurrence of shortages, credit period, and cycle time. Karmakark and Dutta Choudhury [32] gave an inventory model with ramp-type demand for deteriorating items with partial backlogging and time-varying holding cost. Bhunia *et al.* [33] made an attempt to develop two inventory models for deteriorating items with a variable demand dependent on the selling price and the frequency of the advertisement of items. In the first model, shortages are not allowed, whereas in the second, they are allowed and partially backlogged with a variable rate dependent on the duration of the waiting time up to the arrival of the next lot. In both models, the deterioration rate follows a three-parameter Weibull distribution and the transportation cost is considered for explicitly replenishing the order quantity. Vipin Kumar *et al.* [34] studied a two-Warehouse partial backlogging inventory model for deteriorating items with ramp type demand. Srinivasa Rao *et al.* [35] developed and analyzed an EOQ model for deteriorating items with permissible delay in payments under inflation. They assumed that the demand is a function of both time and selling price. Further, they assumed that the lifetime of the commodity is random and follows a generalized Pareto distribution. Bhunia *et al.* [36] developed a paper which deals with a deterministic inventory model for the linear trend in demand under inflationary conditions with different rates of deterioration in two separate warehouses (owned and rented warehouses). Goel and Aggarwal [5] considered perishable inventory models with a selling price dependent demand. In many research papers, the researchers assumed that the cycle length is constant for successive replenishments; [10-13,15-17], etc. are examples for this type of models, except the works of Bhunia and Maiti [14] in which they developed an inventory model for deteriorating items with infinite rate of replenishment and time dependent linearly increasing demand over a finite time horizon. Shortages are allowed and are fully backlogged. The model is formulated by assuming that the successive replenishment cycle lengths are in arithmetic progression.

However, very few studies reported regarding the inventory models for deteriorating items having a variable cycle length of successive replenishments with selling price dependent demand, which are more useful in analyzing the inventory situation of deteriorating items. In the present paper, we develop and analyze an inventory model for deteriorating items having selling price dependent demand with variable cycle lengths for successive replenishments. Using the total cost function, the optimal selling price and cycle lengths are derived and the sensitivity of the parameters are analyzed.

2. Assumptions and Notations

We have considered an inventory model with the following assumptions and notations:

1. Replenishment is instantaneous.
2. The system operates for a prescribed period of H units of time (planning Horizon) inventory level is zero at times $t = 0$ and $t = H$
3. The demand rate at any instant "t" is a linear function of the selling price s and is of the form $\lambda(s) = a + b.s$ where $a > 0, b < 0$.
4. Lead time is zero.
5. Shortages are allowed and are fully backlogged. Shortages are not allowed in the final cycle.
6. T_i is the total time that elapses up to and including the i^{th} cycle (i = 1,2, ..., m), where, m denotes the total number of replenishments to be made during the prescribed time horizon H. Hence $T_0 = 0, T_m = H$
7. t_i is the time at which the inventory in the i^{th} cycle reaches zero ($i = l,2,...,m - l$).

8. T is the length of the first replenishment cycle and w is the rate of reduction of the successive cycle lengths.
9. The on hand inventory deteriorates at a constant rate of θ $(0 < \theta < 1)$ per unit time and there is neither repair nor replacement of the deteriorated inventory during H.
10. The inventory holding cost C_1 per unit per unit time, the shortage cost C_2 per unit time, the unit cost C and the replenishment cost (ordering cost) C_3 per replenishment are known and constant during the planning time horizon H.

3. The Inventory Model

The schematic diagram of the inventory model is given in Figure 1:

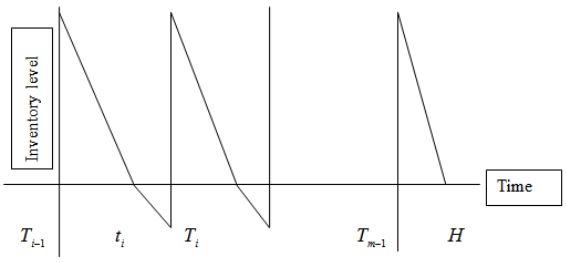

Figure 1. The schematic diagram of the inventory model

$I_i(t)$ denote the amount of inventory at time t, during the i^{th} cycle $T_{i-1} \le t \le t_i (i=1,2.....,m)$ The rate of change in inventory at time t during the i^{th} cycle is due to deterioration which amounts to $\theta.I_i(t)$ and demand rate $\lambda(s)=a+b.s$. Therefore, the differential equation governing the system during i^{th} cycle is:

$$\frac{d}{dt}I_i(t)+\theta I_i(t)=-\lambda(s);\ T_{i-1} \le t \le t_i \left(i=1,2.....,m\right) \quad (1)$$

The rate of change in inventory at time t during the cycle $t_i \le t \le T_i$ $i = 1,2, ..., (m-1)$) is due to unfulfilled demand as a consequence of backlogged shortages. Therefore, the differential equation governing the system during i^{th} cycle is:

$$\frac{d}{dt}I_i(t)=-\lambda(s);\ t_i < t < T_i \ \left(i=1,2.....,m-1\right) \quad (2)$$

with the initial conditions $I_i(t) = 0$ at $t = t_i$ and $\lambda(s) = (a+bs)$; where $a > 0, b < 0$.

Solving the equation (1) we get:

$$I_i(t)=\left(\frac{a+bs}{\theta}\right)\left(e^{\theta\left(t_i-1\right)}-1\right), \quad (3)$$

$T_{i-1} \le t \le t_i;\ i=1,2.....,m$

From equation (2) we get:

$$I_i(t)=\left(a+bs\right)\left(t_i-t\right); \quad (4)$$
$$t_i \le t < T_i, \left(i=1,2........,\ m\text{-}1\right)$$

The $(i+1)^{th}$ replenishment time T_i can be expressed as:

$$T_i=iT\text{-}i\left(i\text{-}1\right)\frac{w}{2},\ i=0,1,2......,m\text{-}1 \quad (5)$$

The length of the i^{th} cycle is

$$T_i - T_{i-1} = T-(i-1)w \quad i = 1,2, ..m \quad (6)$$

Hence $$T=\left(m\text{-}1\right)\frac{w}{2}+\frac{H}{m} \quad (7)$$

The total cost of the system during the planning horizon H is:

$$K(m,t_i,T_i)=m.C_3+\sum_{i\text{-}1}^{m\text{-}1}\left[\left(C_1+C\theta\right)\int_{T_{i\text{-}1}}^{t_i}I_i\left(t\right)dt+C_2\int_{t_i}^{T_i}I_i\left(t\right)dt\right]+\left(C_1+C\theta\right)\int_{T_{m\text{-}1}}^{H}I_m\left(t\right)dt+C_2\sum_{i=1}^{m}\int_{t_i}^{T_i}I_i(t)\,dt \quad (8)$$

$$=m.C_3+\sum_{i\text{-}1}^{m\text{-}1}\left[\left(C_1+C\theta\right)\int_{T_{i\text{-}1}}^{t_i}\frac{a+bs}{\theta}\left(e^{\theta\left(t_i\text{-}t\right)}\text{-}1\right)dt\right]+\left(C_1+C\theta\right)\int_{T_{m\text{-}1}}^{H}\frac{a+bs}{\theta}\left(e^{\theta\left(H\text{-}1\right)}\text{-}1\right)dt+C_2\sum_{i=1}^{m}\int_{t_i}^{T_i}\left(a+bs\right)\left(t_i\text{-}t\right)dt$$

To ensure the convexity of the total cost function formulate the Hessian matrix and the determinant of the said matrix is observed as positive. That is:

$$\begin{vmatrix}\frac{\partial^2 K}{\partial t_i^2} & \frac{\partial^2 K}{\partial t_i\,\partial T}\\ \frac{\partial^2 K}{\partial t_i\,\partial T} & \frac{\partial^2 K}{\partial T_i^2}\end{vmatrix} > 0$$

Hence, the parameters and costs are assumed such that the Hessian matrix associated with the decision variables t_i and T_i is a positive definite.

For a fixed m, the corresponding optimal values of t_i are the solutions of the system of $(m\text{-}1)$ equations

$$\frac{\partial K\left(m,t_i,T_i\right)}{\partial t_i}=0;\left(i=1,2,.....m\text{-}1\right)$$

For a fixed i,

$$K\left(m.t_i,T_i\right)=m.C_3+\left(C_1+C\theta\right)\int_{T_{i\text{-}1}}^{t_i}\frac{a+bs}{\theta}\left(e^{\theta\left(t_i\text{-}t\right)}\text{-}1\right)dt$$

$$+C_2\int_{t_i}^{T_i}(a+bs)(t_i-t)dt+(C_1+C\theta)\int_{T_{m-1}}^{H}\frac{a+bs}{\theta}\left(e^{\theta(H-t)}-1\right)dt$$

This implies

$$\frac{\partial K(m,t_i,T_i)}{\partial t_i}=\frac{\partial}{\partial t_i}\left[\begin{array}{l}(C_1+C\theta)\int_{T_{i-1}}^{t_i}\left(\frac{a+bs}{\theta}\right)\left(e^{\theta(t_i-t)}\theta\right)dt+\\ C_2\int_{t_i}^{T_i}(a+bs)dt\end{array}\right]$$

$$=\frac{(C_1+C\theta)(a+bs)}{\theta}\left(1-e^{\theta(t_i-T_{i-1})}\right)+C_2(a+bs)(T_i-t_i)$$

Using the power series expansion of and neglecting higher powers of θ,, we get:

$$\frac{\partial K(m,t_i,T_i)}{\partial t_i}=\frac{(C_1+C\theta)(a+bs)}{\theta}\left[\theta(T_{i-1}-t_i)\right]+C_2(a+bs)(T_i-t_i)$$

Solving $\frac{\partial K(m,t_i,T_i)}{\partial t_i}=0$ we get

$$t_i=\frac{T_i+V.T_{i-1}}{1+V},\ i=1,2.....,m-1 \qquad (9)$$

Where $V=\frac{C_1+C.\theta}{C_2}$

Using equation (8), neglecting the terms of θ^3 and higher powers of θ, we obtain

$$K(m,t_i,T_i)=m.C_3+\frac{(C_1+C\theta)(a+bs)}{6}\left\{3(H-T_{m-1})^2+\theta(H-T_{m-1})^3\right\}+\sum_{i-1}^{m-1}\left[\begin{array}{l}\frac{(C_1+C\theta)(a+bs)}{6}\left\{3(t_i-T_{i-1})^2+\theta(t_i-T_{i-1})^3\right\}\\ -C_2(a+bs)\frac{(t_i-T_i)^2}{2}\end{array}\right] \qquad (10)$$

Using equation (9) in (10) and substituting:

$$T_i=i\ T-i\ (i-1)\frac{w}{2}\ \text{ and }\ T_i-T_{i-1}=T-(i-1)w \qquad (11)$$

$$\begin{aligned}K(m,t_i,T_i)&=m.C_3+\frac{(C_1+C\theta)(a+bs)}{6(1+V)^2}\sum_{i-1}^{m-1}3(1-V)\left(T^2-2T(i-1)w+w^2(i-1)^2\right)\\&+\frac{(C_1+C\theta)(a+bs)}{6(1+V)^3}\sum_{i-1}^{m-1}\theta\left(T^3-(i-1)^3w^3-3(i-1)^2+3T(i-1)w^2\right)\\&+\frac{(C_1+C\theta)(a+bs)}{6}\left\{3\left(H-(m-1)T+(m-1)(m-2)\frac{w}{2}\right)^2+\theta\left(H-(m-1)T+(m-1)(m-2)\frac{w}{2}\right)^3\right\}\end{aligned} \qquad (12)$$

Substituting $T=(m-1)\frac{w}{2}+\frac{H}{m}$ from the equation (7) in the equation (12), the cost function K reduced to a function of three variables m, s and w only of which m is a discrete, s and w are continuous variables. Let it be $\overline{K}(m.s.w)$.

For given value m_0 (>1) of m, the optimal value of w and s are obtained by minimizing the total cost i.e.

$$\frac{d\overline{K}}{dw}(m_0,s,w)=0 \qquad (13)$$

$$\frac{d\overline{K}}{ds}(m_0,s,w)=0 \qquad (14)$$

Solving the equations (13) and (14) by using the numerical methods, the optimal value of w (say, $w(m_0)$) and s (say, s^*) can be obtained. The corresponding optimal value of $\overline{K}(m_o,s^*,w(m_o))=K^*(m_0)$, which can be calculated from equation (12). Putting $m_0 = 2, 3, 4$ ... we can calculate $K^*(2)$, $K^*(3)$ and so on.

For $m = 1$, the system reduces to a single period with finite time horizon. In such case the total cost for the period H is fixed and is:

$$K^*(1)=C_3+\frac{(C_1+C\theta)(a+bs^*)}{6}\left(3H^2+\theta H^3\right) \qquad (15)$$

The values of $K^*(l)$, $K^*(2)$, $K^*(3)$ are the optimal costs and the corresponding values of m_0 $(=m^*)$ and w $(=w^*)$are their optimal values. The optimal values of T $(=T^*)$ and T_i $(=T_i^*,\ i=1,2,\ ...\ m-1)$ can be obtained from equations (7) and (5), respectively.

As we have the total cost of the system for fixed m, it is to be noted that

$$K(s,t_i,T_i)=m.C_3+\sum_{i=1}^{m-1}(C_1+C\theta)\int_{T_{i-1}}^{t_i}\frac{a+bs}{\theta}\left(e^{\theta(t_i-t)}-1\right)dt+C_2\int_{t_i}^{T_i}(a+bs)(t_i-t)dt+(C_1+C\theta)\int_{T_{m-1}}^{H}\left(\frac{a+bs}{\theta}\right)\left(e^{\theta(H-t)}-1\right)dt \qquad (16)$$

(Since total cost is a function of selling price "s", it is denoted by $K(s,t_i,T_i)$ Total Revenue = $s.\lambda(s).H$

$$s(a+bs)H \qquad (17)$$

The total profit function is:

$$P(s,t_i,T_i) = s\,(a+bs)H - \left\{ m.C_3 + \sum_{i=1}^{m-1} \left(C_1 + C\theta\right) \int_{T_{m-1}}^{t_i} \frac{a+bs}{\theta} \left(e^{\theta(H-t)} - 1\right) dt + C_2 \int_{t_i}^{T_i} \left(a+bs\right) \left(t_i - t\right) dt \right] \tag{18}$$

$$+ \left(C_1 + C\theta\right) \int_{T_{m-1}}^{H} \left(\frac{a+bs}{\theta}\right) \left(e^{\theta(H-t)} - 1\right) dt \Bigg\}$$

Regarding the concavity of the Profit function one can verify that $\begin{vmatrix} \dfrac{\partial^2 P}{\partial t_i^{\,2}} & \dfrac{\partial^2 P}{\partial t_i\, \partial T_i} \\ \dfrac{\partial^2 P}{\partial t_i\, \partial T_i} & \dfrac{\partial^2 P}{\partial T_i^{\,2}} \end{vmatrix} < 0$ Which means that the Hessian Matrix is a negative definite.

4. Numerical Illustration

As an illustration of the above model consider the values of the parameters as:

$a = 25, b = -1, c = 2, c_1 = 0.1, c_2 = 5, c_3 = 9, H = 12.$

Substituting these values in equations (14) and (15) and solving the equations iteratively by using "MAT CAD", we obtained the optimum values of selling price (s^*), optimum w^*. Optimum cycle length (T_1^*, T_2^*, T_3^*) for various values of θ and given in the following Table 1.

Table 1. Optimal values of the parameters of the model with shortages and with fixed selling price *a*=25, *b*=-1, *H*=12

θ	M	C_1	C_2	C_3	C	s	w*	T_1*	Q_1*	T_2*	Q_2*	T_3*	Q_3*	T_4*	Q_4*	K*	P*
0.01	3	0.1	5	9	2	3	1.1434	5.1434	278.1074	9.1434	320.4827	12	342.8228	-	-	189.1761	602.8239
0.01	3	0.1	5	9	2	4	1.7499	5.7499	268.3892	9.7499	305.8548	12	314.5645	-	-	90.535	701.465
0.01	3	0.1	5	8	2	5	2.5	6.5	248.1172	10.5	293.1746	12	310.4464	-	-	50.5625	741.4299
0.01	3	0.1	5	9	2	3	1.1434	5.1434	278.1074	9.1434	420.4827	12	442.8228	-	-	89.1761	702.8239
0.02	2	0.1	5	9	2	3	11.25	11.625	567.7659	12	272.3085	-	-	-	-	76.0333	715.9667
0.02	3	0.1	5	9	2	3	1.7391	5.7391	266.2339	9.7391	380.3554	12	395.8698	-	-	91.4879	700.5103
0.02	4	0.1	5	9	2	3	0.0076	3.0114	136.2772	6.0152	202.1746	9.014	27.6425	12	337.1866	91.5429	700.4571
0.02	3	0.1	5	9	2	3	1.7391	5.7391	266.2339	9.7371	380.3554	12	395.8698	-	-	81. 4897	710.5103
0.02	3	0.1	5	10	2	3	1.7391	5.7391	266.2339	9.7371	380.3554	12	395.8698	-	-	84.4897	707.5103
0.02	3	0.1	5	11	2	3	1.7391	5.7391	266.2339	9.7371	380.3554	12	395.8698	-	-	87. 4897	704.5103
0.02	3	0.1	5	9	2	3	1.7391	5.7391	266.2339	9.7371	315.1127	12	317.0637	-	-	81. 4897	710.5103
0.02	3	0.1	5	9	3	3	1.8719	5.8119	279.7668	8.8119	316.9802	12	323.6075	-	-	118.7213	673.2787
0.02	3	0.1	5	9	4	3	1.8726	5.8726	283.4184	9.8726	380.3554	12	395.8698	-	-	127.7704	664.2296
0.1	3	0.1	5	9	2	3	1.8494	5.8494	264.5525	9.8494	308.0438	12	312.2836	-	-	95.2885	696.7115
0.2	3	0.2	5	9	2	3	0.6795	4.6795	324.0051	8.6795	343.7388	12	375.7254	-	-	342.8275	449.1725
0.2	3	0.5	5	9	2	3	1.3263	5.3263	282.7075	9.3263	335.0714	12	345.4114	-	-	521.8641	270.1359
0.2	3	0.1	2	9	2	3	0.4589	4.4589	252.1787	8.4589	319.1518	12	377.2152	-	-	252.8018	539.1982

For fixed values of m, C_1, C_2, C_3, C, s, H and θ the optimal values of w^*, $T_1^*(i=1,2,\ldots,m)$, $Q_1^*(i=1,2,\ldots,m)$, K^* and P^* are computed and presented in the Table 1. From Table 1, it is observed that the optimal ordering quantities, optimal cycle lengths and optimal total profit are significantly affected by the parameters and cost. It is observed that as the rate of deterioration increases the optimal value of the reduction in successive cycle length w^* increases when the other parameters and costs remain fixed and, hence, the optimal cycle length of the first cycle increases. It is also observed that the optimal ordering quantity decreases as "θ" increases. However, the total cost increases and profit decreases when "θ" increases for the fixed values of the other parameters and costs. It is also observed that as the number of cycles (orders) increases, the optimal values of w^* decrease and the optimal ordering quantity per a cycle also decreases, when the other costs and parameters remain fixed. It is also observed that as the number of orders increases, the total cost increases and, hence, the profit decreases when the other parameters are fixed. Since the demand is dependent on the selling price and we assume that the selling price increases, the demand decreases.

As the cost per a unit increases, the optimal value of w increases and, hence, the optimal ordering quantity of the first cycle increases since T_1^* increases when the other parameters and costs remain fixed. However, in the second and third cycles, the optimal ordering quantities decrease since their cycle lengths decrease when the cost per a unit increases.

The profit decreases when the cost per unit increases for the fixed values of the other parameters and costs. If the holding cost C_1 increases the optimal value of successive reduction of the cycle length increases when the other parameters and costs are fixed. The phenomenon has a vital influence on the ordering quantities; the optimal ordering quantity of the first cycle increases when C_1 increases because the first cycle length increases. The total profit decreases as the holding cost increases for fixed values of the other parameters and costs when the holding cost increases. The replenishment cost has no influence on the optimal value of the reduction of the cycle length and, hence, the optimal ordering quantities and cycle lengths are not affected by the changes in C_3, when the number of orders are fixed. But the total cost of the planning period increases, hence the reduction in the total profit when C_3 increases. It is also observed that the shortages have a vital influence on the reduction of the cycle length, when the other parameters and costs are fixed. The optimal value of w^* increases as the penalty cost (shortage cost) increases. The optimal ordering quantities also increase in each cycle. However, there is a decline in the profits when C_2 increases for fixed values of the parameters and costs. There is an increase in the optimal ordering quantities of the second and third cycle even though cycle lengths are less than the earlier cycle lengths because of fulfilling the backlogged demand in the earlier cycle. This may reduce the loss due to the deterioration and holding cost but increase the penalty cost. Hence, the optimal strategy for the inventory system under consideration is to choose the optimal ordering quantities and the optimal cycle lengths for the given values of the number of cycles, rate of deterioration, holding cost, penalty cost, cost per a unit, replenishment cost and selling price which maximizes profit.

5. Particular Cases

Case (i): For $m = 1$, the system reduces to a single period with finite time horizon without shortages. In such a case, the total cost for the period H is fixed and is:

$$K^*(1) = C_3 + \frac{\left(C_1 + C\theta\right)\left(a+bs\right)}{6}\left(3H^2 + \theta H^3\right) \tag{19}$$

and the optimal ordering quantity Q^* is:

$$Q^* = \frac{\left(a+bs\right)}{2}\theta H^2 \tag{20}$$

Hence, this model reduces to the usual inventory model for deteriorating items with fixed cycle length.

Case (ii) :

If the rate of deterioration $\theta \to 0$ in the above model, we obtain:

$$t_i = \frac{T_i + V.T_{i-1}}{1+V}\quad i = 1,2,3.....,m .$$

Where $$V = \frac{C_1}{C_2} \tag{21}$$

The total cost function for the entire horizon H can be obtained as:

$$K(m,w) = m.C_3 + \frac{C_1\left(a+bs\right)}{6\left(1+V\right)^2}\sum_{i=1}^{m-1} 3\left(1+V\right)$$
$$* \left(\left(m\text{-}1\right)\frac{w}{2} + \frac{H}{m} - \left(i\text{-}1\right)w\right)^2 + \frac{C_1\left(a+bs\right)}{6} \tag{22}$$
$$* \left\{\left(H\text{-}\left(m\text{-}1\right)\left(\left(m\text{-}1\right)\frac{w}{2} + \frac{H}{m}\right) + \left(m\text{-}1\right)\left(m\text{-}2\right) + \frac{w}{2}\right)^2\right\}$$

This gives the optimal total cost for the inventory model for non-deteriorating items with variable cycle lengths. The optimal ordering quantities are:

$$Q_i^* = t_i^* + t_{i-1}^*\left(a+bs\right) ;\ i = 1,2,3,...,m. \tag{23}$$

6. Sensitivity Analysis

A sensitivity analysis was carried out to explore the effect on the optimal policies by varying the value of each parameter at a time and all parameters together. The results obtained by changing parameters by -15%, -10%. -5%, +5% +10% and +15% are exhibited in Table 1(a) and Figure 2.

The values of the total cost K varies from 130.011 to 166.177 and the total profit varies from 693.103 to 693.366 for 15% under estimation and over estimation of all parameters under consideration.

7. Optimal Pricing and Ordering Policies under Variable Selling Price

In this section, we obtain the optimal pricing and ordering policies of the inventory system under a variable selling price. In the previous section, we considered the selling price "***s***" as fixed. However, in many situations the selling price is variable and can be fixed by developing an optimal pricing policy. To obtain the optimal selling price along with the optimal ordering quantity, we maximize the total profit of the inventory system with respect to the selling price and the time at which shortages occur in each cycle (i.e. t_i, $i = 1, ,.....,m\text{-}1$).

From equation (18) we have the total profit function as:

$$P(s,t_i,T_i) = s\ (a+bs)\ H - \left\{m.C_3 + \sum_{i=1}^{m-1}\left(C_1 + C\theta\right)\right.$$
$$\left.* \int_{T_{m-1}}^{t_i}\frac{a+bs}{\theta}\left(e^{\theta(H-t)} - 1\right)dt + C_2\int_{t_i}^{T_i}\left(a+bs\right)\left(t_i - t\right)dt\right] \tag{24}$$
$$\left. + \left(C_1 + C\theta\right)\int_{T_{m-1}}^{H}\left(\frac{a+bs}{\theta}\right)\left(e^{\theta(H-t)} - 1\right)dt\right\}$$

Table 1(a) Sensitivity of the model with fixed selling price and having Shortages

Variation Parameters		Percentage change in parameter						
		-15	**-10**	**-5**	**0**	**5**	**10**	**15**
C_3	**K**	144.691	146.041	147.391	148.741	150.091	151.441	152.791
	Q_1	98.542	98.542	98.542	98.542	98.542	98.542	98.542
	Q_2	98.541	98.541	98.541	98.541	98.541	98.541	98.541
	Q_3	98.541	98.541	98.541	98.541	98.541	98.541	98.541
	P	696.71	695.80	694.62	693.17	692.53	691.21	690.32
C_1	**K**	139.449	142.041	145.839	148.741	151.091	154.441	156.791
	Q_1	98.542	98.542	98.542	98.542	98.542	98.542	98.542
	Q_2	98.541	98.541	98.541	98.541	98.541	98.541	98.541
	Q_3	98.541	98.541	98.541	98.541	98.541	98.541	98.541
	P	702.171	699.680	696.62	693.17	690.253	687.21	684.732
C_2	**K**	58.373	88.51	117.975	148.741	176.615	201.697	231.908
	Q_1	98.623	98.389	98.205	98.542	98.94	98.848	98.673
	Q_2	98.597	98.417	98.276	98.541	98.074	98.001	98.942
	Q_3	98.700	98.568	98.466	98.541	98.323	98.272	98.231
	P	723.02	713.58	703.78	693.17	683.01	673.91	663.98
C	**K**	118.024	128.041	138.789	148.741	158.601	168.471	178.009
	Q_1	98.542	98.542	98.542	98.542	98.542	98.542	98.542
	Q_2	98.541	98.541	98.541	98.541	98.541	98.541	98.541
	Q_3	98.541	98.541	98.541	98.541	98.541	98.541	98.541
	P	708.317	703.960	698.862	693.17	688.753	683.21	678.572
θ	**K**	148.711	148.721	148.731	148.741	148.751	148.761	148.771
	Q_1	98.542	98.542	98.542	98.542	98.542	98.542	98.542
	Q_2	98.541	98.541	98.541	98.541	98.541	98.541	98.541
	Q_3	98.541	98.541	98.541	98.541	98.541	98.541	98.541
	P	696.366	695.149	694.114	693.17	692.258	691.891	690.005
All Parameters	**K**	130.011	136.921	142.731	148.741	154.651	160.376	166.177
	Q_1	98.542	98.542	98.542	98.542	98.542	98.542	98.542
	Q_2	98.541	98.541	98.541	98.541	98.541	98.541	98.541
	Q_3	98.541	98.541	98.541	98.541	98.541	98.541	98.541
	P	693.366	693.249	693.199	693.17	693.158	693.11	693.103

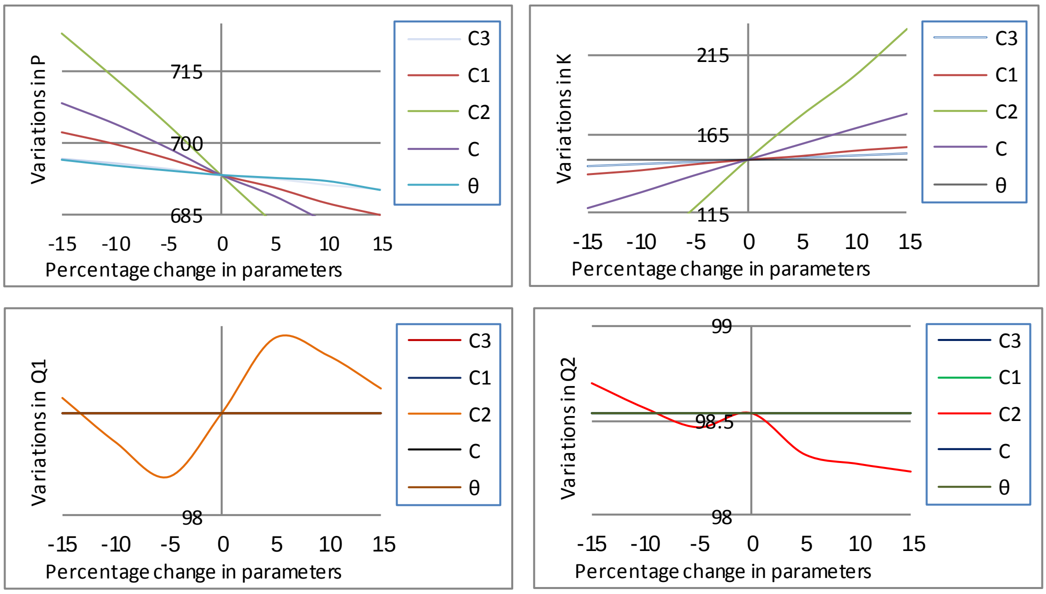

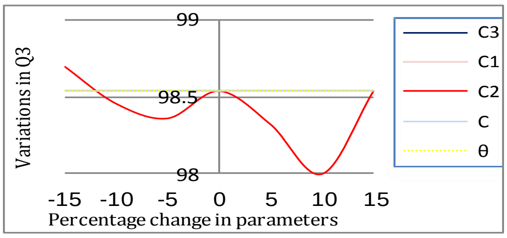

Figure 2. Graphical representation of the sensitivity with respect to the parameters of the model with fixed selling price and with shortages when *a = 25, b= -1, H= 12.*

To find the optimal value of t_i, we maximise the function $P(s,t_i,T_i)$ with respect to t_i

i.e $\frac{\partial}{\partial t_i}\left(P\left(s,t_i,T_i\right)\right)=0$ and

$$\frac{\partial^2}{\partial t_i^2}\left(P\left(s,t_i,T_i\right)\right)<0$$

Now $\frac{\partial}{\partial t_i}\left(P\left(s,t_i,T_i\right)\right)=0$ implies

$$\frac{\partial}{\partial t_i}\left(K\left(s,t_i,T_i\right)\right)=0$$

We have $t_i=\frac{T_i+V.T_{i-1}}{1+V}$

where $V=\frac{C_1+C\theta}{C_2}$

Hence, the total profit function $P\ (s,\ t_i,\ T_i)$ has maximum value when $t_i=\frac{T_i+V.T_{i-1}}{1+V}$ Substituting this value of t_i in equation (24), the total profit function will become a function of the variables "s" and T_i.

We have $T_i-T_{i-1}=T-(i-1)w$, and

$$T=(m\text{-}1)\frac{w}{2}+\frac{H}{m}$$

Substituting these values in the equation (24), the total profit function becomes a function of the variables "s" and "w" only. Hence we denote the profit function by $P(w,s)$

$$\begin{aligned}P(w,s)=&\ s(a+bs).Hm.C_3-\frac{(C_1+C\theta)(a+bs)}{6(1+V)^2}\sum_{i=1}^{m-1}3(1+V)(T-(i-1)w)^2-\frac{(C_1+C\theta)(a+bs)}{6(1+V)^2}\\&*\sum_{i=1}^{m-1}3(1+V)(T-(i-1)w)^2-\frac{(C_1+C\theta)(a+bs)}{6}\\&*\left\{3\left(H-(m-1)T+(m-1)(m-2)\frac{w}{2}\right)^2+\theta\left(H-(m-1)T+(m-1)(m-2)\frac{w}{2}\right)^3\right\}\end{aligned}\tag{25}$$

where $T=(m-1)\frac{w}{2}+\frac{H}{m}$. To find the optimal values of w and s, equate the first order partial derivatives of $P(w,s)$ with respect to w and s to zero and $\frac{\partial}{\partial s}\left(P(w,s)\right)=0$ implies

$$\begin{aligned}&a.H+2\,b\,s\,H-\frac{(C_1+C\theta)b}{2(1+V)}\sum_{i=1}^{m-1}(T(i\text{-}1)-w)^2-\frac{(C_1+C\theta)b\theta}{6(1+V)^3}\sum_{i=1}^{m-1}(T(i\text{-}1)-w)^3\\&-\frac{(C_1+C\theta)b}{6}\left\{3\left(H-(m\text{-}1)T+(m\text{-}1)(m\text{-}2)\frac{w}{2}\right)^2+\theta\left(H-(m\text{-}1)T+(m\text{-}1)(m\text{-}2)\frac{w}{2}\right)^3\right\}=0\end{aligned}\tag{26}$$

$\frac{\partial}{\partial s}\left(P(w,s)\right)=0$ implies

$$\begin{aligned}&\frac{(C_1+C\theta)(a+bs)}{2(1+V)^3}\sum_{i\text{-}1}^{m-1}2\left(T\text{-}(i\text{-}1)w\right)\left(\frac{m-1}{2}-(i\text{-}1)\right)-\frac{(C_1+C\theta)(a+bs)}{2(1+V)^3}\sum_{i\text{-}1}^{m-1}3\left(T\text{-}(i\text{-}1)w\right)\left(\frac{m-1}{2}-(i\text{-}1)\right)\\&-\frac{(C_1+C\theta)(a+bs)}{6}\left\{6\left(H\text{-}(m\text{-}1)T+(m\text{-}1)(m-2)\frac{w}{2}\right)\left(-(\mathrm{m}-1)\frac{(\mathrm{m}-1)(\mathrm{m}-2)}{2}\right)\right.\\&\left.+3\theta\left(H\text{-}(m\text{-}1)T+(m\text{-}1)(m-2)\frac{w}{2}\right)^2\left((\mathrm{m}-1)\frac{(\mathrm{m}-1)}{2}+\frac{(\mathrm{m}-1)(\mathrm{m}-2)}{2}\right)\right\}=0\end{aligned}\tag{27}$$

Where, $T = (m-1)\frac{w}{2} + \frac{H}{m}$ Implies $\frac{dT}{dw} = \frac{m-1}{2}$

Solving the equations (26) and (27) we get the optimal values w^* of w and s^* of s respectively. Substituting the values of w^* and s^* in (25) we get the optimal value of the profit function $P(w,s)$ as $P^*(w^*, s^*)$.

For various values of the parameters m, θ, C_1, C_2, C_3, C and H the optimal values of the selling price s and the rate of reduction in successive cycle periods w are computed by solving equations (26) and (27) iteratively using the Newton Raphson's Method and are given in Table (2).

Table 2. Optimal values of the parameters of the model with variable selling price and with shortages $a = 25$, $b= -1$, $H= 12$

θ	m	C_1	C_2	C_3	C	s*	w*	T_1*	Q_1*	T_2*	Q_2*	T_3*	Q_3*	T4*	Q_4*	K*	P*
0.01	3	0.1	5	9	2	12.628	1.138	5.138	148.81	9.1385	163.244	12	175.5811	-	-	65.2393	1839.5616
0.01	4	0.1	5	9	2	12.623	0.150	3.225	81.05	6.4000	119.699	9.22	150.0848	12	183.7	66.5438	1828.2746
0.02	3	0.1	5	9	2	12.716	1.140	5.140	151.63	9.1406	170.562	12	181.2659	-	-	73.5213	1821.8624
0.02	3	0.2	5	9	2	13.126	0.972	4.972	164.90	8.9727	184.324	12	195.7792	-	-	205.496	1664.79
0.02	3	0.5	5	9	2	13.336	0.614	4.614	143.31	8.6142	180.602	12	190.6658	-	-	261.026	1505.58
0.02	3	0.1	2	9	2	12.927	0.459	4.459	138.38	8.4590	175.137	12	206.9962	-	-	150.843	1721.9648
0.02	3	0.1	6	9	2	13.163	1.943	5.943	174.91	9.9430	197.309	12	211.9344	-	-	215.552	1654.1618
0.02	3	0.1	5	9	2	12.716	1.140	5.140	151.63	9.1406	170.562	12	181.2659	-	-	73.5213	1821.8624
0.02	3	0.1	5	10	2	12.716	1.140	5.140	151.63	9.1406	170.562	12	181.2659	-	-	73.5213	1821.8624
0.02	3	0.1	5	11	2	12.716	1.140	5.140	151.63	9.1406	170.562	12	181.2659	-	-	73.5213	1821.8624
0.02	3	0.1	5	9	2	12.668	1.276	5.276	127.53	9.2769	156.674	12	171.6926	-	-	76.8838	1877.0003
0.02	3	0.1	5	9	3	12.668	1.714	5.714	155.69	9.7146	175.116	12	177.4824	-	-	82.6161	1861.9589
0.02	3	0.1	5	9	4	13.438	1.75	5.75	168.29	9.75	176.192	12	178.2755	-	-	87.4324	1737.7755
0.1	3	0.1	5	9	2	12.807	1.147	5. 479	154.29	9. 4790	177.669	12	189.9128	-	-	116.916	1756.9043
0.2	3	0.1	5	9	2	12.716	1.140	5.140	151.63	9.1406	170.562	12	181.2659	-	-	73.5213	1821.8624

From Table 2, we observe that the selling price is much influenced by the values of the parameters and costs. As the number of the cycles increases, the optimal value of the selling price decreases when the other parameters and costs are fixed. Even though the optimal selling price decreases as the number of the cycles increases, the optimal total profit increases. It is also observed that as the decay rate (i.e., rate of deterioration) increases, the optimal value of the selling price also increases and the total profit decreases, when the other parameters and costs are fixed. This phenomenon is very close to the realistic situation with the perishable inventory system, since the rate of deterioration increases, the wastage is more, and the burden is to be balanced between the customer and the seller. It is also observed that as the shortage cost increases the optimal value of selling price increases and the total profit decreases, when the other parameters and costs are fixed. There is no influence of the ordering cost on the optimal value of the selling price. However, the total profit decreases when the other parameters and costs are fixed. As the cost per a unit increases, the optimal value of the selling price increases to maintain the profits at a maximum level. Hence, by the suitable choice of the parameters and costs for the commodity under consideration, one can have the optimal values of the selling price and the ordering quantities for each cycle.

8. Sensitivity Analysis

A sensitivity analysis was carried out to explore the effect on the optimal policies by varying the value of each parameter at a time and all parameters together. The results obtained by changing the parameters by -15%, -10%. -5%, +5% +10% and +15% are tabulated in Table 2(a) and Figure 3.

The values of the total cost K varies from 38.474 to 74.105 and the total profit varies from 435.423 to 735.736 for 15% under estimation and over estimation of all parameters under consideration.

9. Inventory Model With-out Shortages

In this section, we consider that the shortages are not allowed. When we assume that shortages are not allowed, it is not necessary to have a backlog fulfillment. Then, the parameter t_i becomes T_i $(i = 1, 2, \ldots, m-1)$ and the shortage cost C_2 is to be considered as $C_2 \to \infty$. Substituting these values in the corresponding equations given in the total cost function becomes:

Table 2(a). Sensitivity of the model with variable selling price and having Shortages

Variation Parameters		Percentage change in parameter						
		-15	-10	-5	0	5	10	15
C_3	K	50.461	52.741	54.147	56.424	58.801	60.441	62.051
	Q_1	304.420	304.420	304.420	304.420	304.420	304.420	304.420
	Q_2	311.198	311.198	311.198	311.198	311.198	311.198	311.198
	Q_3	319.711	319.711	319.711	319.711	319.711	319.711	319.711
	P	741.67	739.690	737.62	735.576	733.753	731.321	729.009
C_1	K	56.109	56.216	56.356	56.424	56.591	56.637	56.791
	Q_1	304.420	304.420	304.420	304.420	304.420	304.420	304.420
	Q_2	311.198	311.198	311.198	311.198	311.198	311.198	311.198
	Q_3	319.711	319.711	319.711	319.711	319.711	319.711	319.711
	P	702.171	699.680	696.62	735.576	690.253	687.21	684.732
C_2	K	139.449	142.041	145.839	56.424	151.091	154.441	156.791
	Q_1	287.115	290.300	297.669	304.420	311.324	318.742	315.130
	Q_2	311.198	311.198	311.198	311.198	311.198	311.198	311.198
	Q_3	319.711	319.711	319.711	319.711	319.711	319.711	319.711
	P	702.171	699.680	696.62	735.576	690.253	687.21	684.732
C	K	62.414	60.128	58.158	56.424	54.156	52.751	50.989
	Q_1	298.140	300.520	302.371	304.420	306.92	308.327	310.114
	Q_2	311.198	311.198	311.198	311.198	311.198	311.198	311.198
	Q_3	288.866	298.676	309.48	319.711	329.711	339.675	349.661
	P	732.817	733.790	734.486	735.576	736.012	737.621	738.752
θ	K	50.471	52.148	54.831	56.424	58.521	60.161	62.968
	Q_1	304.420	304.420	304.420	304.420	304.420	304.420	304.420
	Q_2	311.198	311.198	311.198	311.198	311.198	311.198	311.198
	Q_3	319.711	319.711	319.711	319.711	319.711	319.711	319.711
	P	796.347	776.349	756.114	735.576	715.692	691.891	670.545
All Parameters	K	38.474	44.797	50.731	56.424	62.567	68.676	74.105
	Q_1	304.420	304.420	304.420	304.420	304.420	304.420	304.420
	Q_2	311.198	311.198	311.198	311.198	311.198	311.198	311.198
	Q_3	319.711	319.711	319.711	319.711	319.711	319.711	319.711
	P	735.736	735.684	735.634	735.576	735.524	735.470	435.423

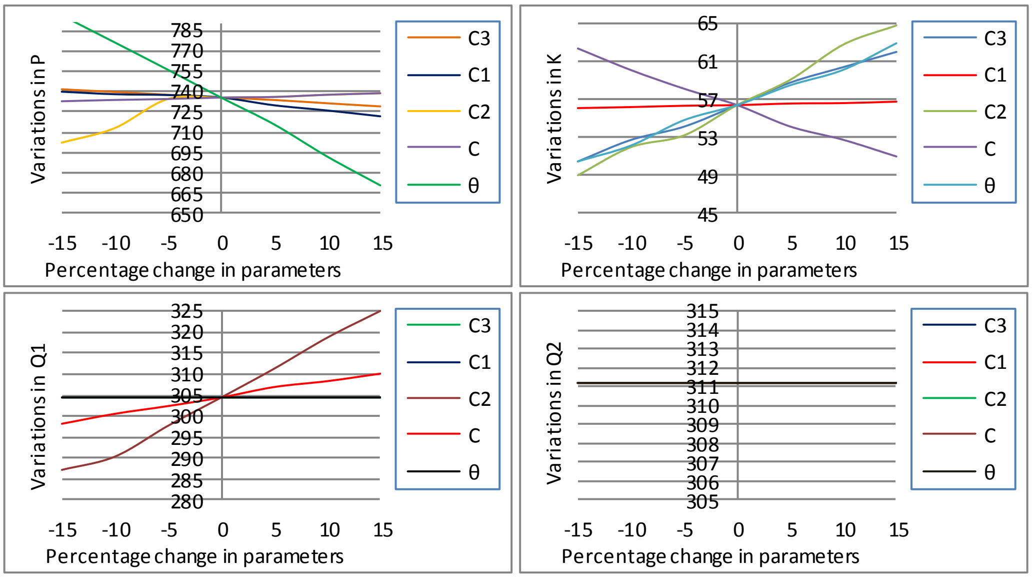

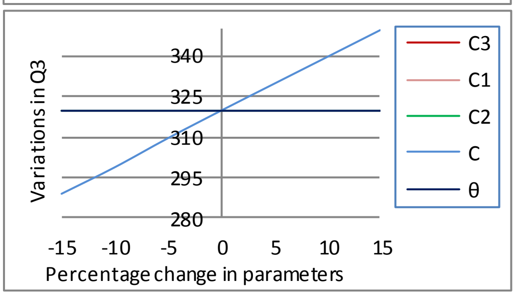

Figure 3. Graphical representation of the sensitivity with respect to the parameters of the model with variable selling price and with shortages when $a = 25$, $b = -1$, $H = 12$.

$$\overline{K}(m,w) = m.C_3 + \frac{(C_1+C\theta)(a+bs)}{6}\sum_{i-1}^{m-1} 3\left((m-1)\frac{w}{2}+\frac{H}{m}-(i\text{-}1)w\right)^2$$
$$+\frac{(C_1+C\theta)(a+bs)}{6}\sum_{i-1}^{m-1} 3\left((m-1)\frac{w}{2}+\frac{H}{m}-(i\text{-}1)w\right)^3$$
$$-\frac{(C_1+C.\theta)(a+bs)}{6}\left\{3\left(H\text{-}(m\text{-}1)\left((m\text{-}1)\frac{w}{2}+\frac{H}{m}\right)+(m\text{-}1)(m-2)\frac{w}{2}\right)^2\right.$$
$$\left.+\theta\left(H\text{-}(m\text{-}1)\left((m\text{-}1)\frac{w}{2}+\frac{H}{m}\right)+(m\text{-}1)(m-2)\frac{w}{2}\right)^3\right\} \quad (28)$$

for fixed m the optimal value w^* *of* w can be obtained by minimizing the cost function:

$$\frac{d\overline{K}(w)}{dw} = \frac{(C_1+C\theta)(a+bs)}{6}\sum_{i-1}^{m-1}\left\{\left((m-1)\frac{w}{2}+\frac{H}{m}-(i\text{-}1)w\right)(m+1\text{-}2i)\right\}$$
$$+\frac{(C_1+C\theta)(a+bs)}{4}\sum_{i-1}^{m-1}\left\{\left((m-1)\frac{w}{2}+\frac{H}{m}-(i\text{-}1)w\right)^2(m+1\text{-}2i)\right\}$$
$$+\frac{(C_1+C\theta)(a+bs)}{6}\left[6\left(H-(m-1)\left((m-1)\frac{w}{2}+\frac{H}{m}\right)+(m-1)(m\text{-}2)\frac{w}{2}\right)\right.$$
$$\left.+3\theta\left(H-(m-1)\left((m-1)\frac{w}{2}+\frac{H}{m}\right)+(m-1)(m\text{-}2)\frac{w}{2}\right)^2\right]$$

The optimal ordering quantity Q_i^* is:

$$Q_i^* = \frac{(a+bs)}{2}.\theta\left(T_i^*-T_{i\text{-}1}^*\right)^2 + \left(T_i^*-T_{i\text{-}1}^*\right)(a+bs) \quad (29)$$

For different values of the parameters and costs m, θ, C_1, C_2, C_3, C and s the optimal values of w^* (i.e., the reduction in successive cycle lengths) are computed. The optimal values of the ordering quantities for the i^{th} cycle *(i = 1, 2,..., m)* and cycle lengths are presented in Table 3 along with total cost and profits.

From Table 3, we observe that the consideration of not allowing shortages has a significant effect on the optimal ordering policies of the model. It is also observed that the optimal profit of the model, without shortages, is less when compared with the optimal profits of the model with shortages when all parameters and costs are fixed. It is also observed that the optimal ordering quantities in the first cycle, second cycle and third cycle are more for this model than those of the model with shortages. However, the first cycle length increases; the rate of reduction in each cycle length also increases for this model in comparison with the model with shortages when all the parameters and costs are fixed. This phenomenon clearly indicates that it is better to have the strategy of allowing shortages and fully back-logging than without shortages in order to maximize profits even though there is a penalty cost for allowing shortages.

10. Sensitivity Analysis

A sensitivity analysis was carried out to explore the effect on the optimal policies by varying the value of each parameter at a time and all parameters together. The results obtained by changing parameters by -15%, -10%. -5%, +5% +10% and +15% are tabulated in Table 3(a) and Figure 4.

The values of the total cost K varies from 150.871 to 172.111 and the total profit varies from 825.423 to 829.550 for 15% under estimation and over estimation of all parameters under consideration.

Table 3. Optimal values of the parameters of the model with out shortages and with fixed selling price *a = 25, b= -1, H= 12*

θ	m	C_1	C_3	C	s	w^*	T_1^*	Q_1^*	T_2^*	Q_2^*	T_3^*	Q_3^*	T_4^*	Q_4^*	K^*	P^*
0.01	3	0.1	9	2	3	1.886	5.886	266.643	9.886	294.982	12	297.314	-	-	93.8653	698.1347
0.01	3	0.1	9	2	3	1. 886	5.886	242.402	9.886	280.936	12	283.157	-	-	90.7349	701.2651
0.01	3	0.1	9	2	3	1. 886	5.888	335.258	9.886	340.709	12	345.314	-	-	229.590	562.4099
0.02	3	0.1	9	2	3	2	6	279.84	10	315.040	12	319.760	-	-	112.099	681.6975
0.02	4	0.1	9	2	3	1.586	5.379	248.722	9.172	291.219	11.379	300.919	12	307.82	110.302	681.6975
0.02	3	0.2	9	2	3	0.909	4.909	322.037	8.909	374.030	12	376.400	-	-	405.880	386.1191
0.02	3	0.5	9	2	3	0.065	4.065	251.622	8.065	335.845	12	358.660	-	-	526.714	265.0858
0.02	3	0.1	9	2	3	2	6	279.84	10	315.040	12	319.760	-	-	112.099	679.9007
0.02	3	0.1	9	2	3	2	6	279.84	10	315.040	12	319.760	-	-	115.099	679.9007
0.02	3	0.1	9	2	3	2	6	279.84	10	315.040	12	319.760	-	-	118.099	679.9007
0.02	3	0.1	10	2	3	2	6	279.84	10	315.040	12	319.760	-	-	112.099	679.9007
0.02	3	0.1	11	4	3	1.769	5.769	275.806	9.769	313.480	12	316.364	-	-	118.297	673.7027
0.02	3	0.1	9	2	3	2	6	279.84	10	315.040	12	319.76	-	-	112.099	679.9007
0.1	3	0.1	9	2	3	2.124	6. 20	271.199	10.120	311.198	12	319.012	-	-	56.4240	735.576

Table 3(a). Sensitivity of the model with Fixed selling price Without Shortages

Variation Parameters		Percentage change in parameter						
		-15	-10	-5	0	5	10	15
C_3	K	161.645	162.872	163.991	164.099	165.549	166.365	167.745
	P	833.154	830.895	828.999	827.755	825.675	823.175	821.447
C_1	K	163.465	163.689	163.991	164.099	164.579	164.965	165.075
	P	833.565	831.220	829.013	827.755	825.871	821.475	820.755
C	K	158.777	160.489	162.888	164.099	165.771	166.115	167.871
	P	830.111	829.544	828.443	827.755	826.471	825.695	824.235
θ	K	163.465	163.689	163.991	164.099	164.579	164.965	165.075
	P	824.115	825.730	826.336	827.755	828.681	829.846	830.114
All Parameters	K	150.871	154.221	159.002	164.099	167.258	169.996	172.111
	P	829.550	829.007	828.589	827.755	826.158	526.094	825.423

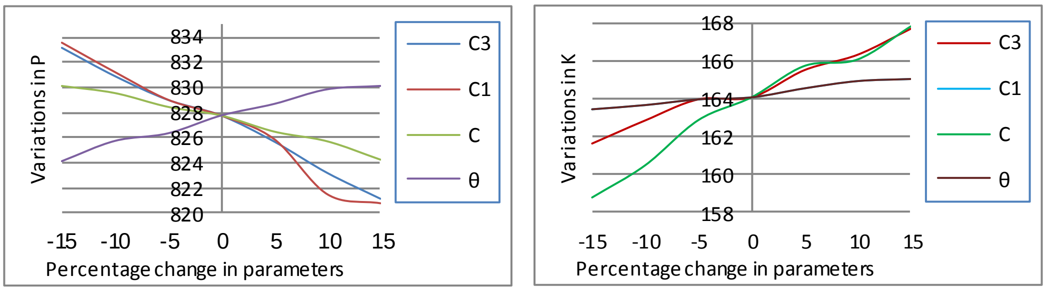

Figure 4. Graphical representation of the sensitivity with respect to the parameters of the model with fixed selling price and without shortages when *a = 25, b= -1, H= 12.*

Now the Profit function of the model is given by:

$$P(w,s)=a(a+bs)H-m.C_3-\frac{(C_1+C.\theta)(a+bs)}{6}\sum_{i=1}^{m-1}3\left(T-(i-1)w\right)^2-\frac{(C_1+C\theta)\theta(a+bs)}{6}\sum_{i=1}^{m-1}\left(T-(i-1)w\right)^3$$

$$-\frac{(C_1+C\theta)(a+bs)}{6}\left\{3\left(H-(m-1)T+(m-1)(m-2)\frac{w}{2}\right)^2+\theta\left(H-(m-1)T+(m-1)(m-2)\frac{w}{2}\right)^3\right\}$$

where $T=(m-1)\frac{w}{2}+\frac{H}{m}$

To find the optimal values of ***w*** and ***s***, equate the first order partial diversities of ***P (w,s)*** with respect to ***w*** and ***s*** to zero than solve the equations $\frac{\partial}{\partial w}\left(P(w,s)\right)=0$ and $\frac{\partial}{\partial s}\left(P(w,s)\right)=0$

$\frac{\partial}{\partial w}\left(P(w,s)\right)=0$ implies.

$$\frac{\left(C_1+C\theta\right)\left(a+bs\right)}{6}\left\{\sum_{i=1}^{m-1}6\left(T-(i-1)w\right)\left(\frac{m-1}{2}-(i-1)\right)-\sum_{i=1}^{m-1}3\left(T-(i-1)w\right)^2\left(\frac{m-1}{2}-(i-1)\right)\right\}$$
$$-\frac{\left(C_1+C\theta\right)\left(a+bs\right)}{6}\left\{6\left(H-(m-1)T+(m-1)(m-2)\frac{w}{2}\right)-(m-1)\frac{m-1}{2}+\frac{(m-1)(m-2)}{2}+3.\theta\left(H-(m-1)T+(m-1)(m-2)\frac{w}{2}\right)^2\right.$$
$$\left.-\frac{\left(C_1+C\theta\right)\left(a+bs\right)}{6}\left(-(m-1)\frac{m-1}{2}+\frac{(m-1)(m-2)}{2}\right)\right\}=0 \tag{30}$$

Here $T=(m-1)\frac{w}{2}+\frac{H}{m}\Rightarrow\frac{dT}{dw}=\frac{m-1}{2}$

Again $\frac{\partial}{\partial s}\left(P(w,s)\right)=0$ implies

$$a.H+2bH-\frac{b\left(C_1+C\theta\right)}{6}\sum_{i=1}^{m-1}3\left(T-(i-1)w\right)^2\frac{b\left(C_1+C\theta\right)}{6}\sum_{i=1}^{m-1}3\left(T-(i-1)w\right)^3$$
$$-\left\{3\left(H-(m-1)T+(m-1)(m-2)\frac{w}{2}\right)^2-\theta^3\left(H-(m-1)T+(m-1)(m-2)\frac{w}{2}\right)^3\right\}=0 \tag{31}$$

For different values of the parameters and costs, the optimal values of T_1*, T_2*, T_3*, . . . , T_m*, Q_1*, Q_2*, . . . Q_m*, *K**, *P** and optimal selling price *s** are computed from the equations using the Newton Raphson's method and given in Table 4.

From Tables 2 and 4, it is observed that allowing shortages has a tremendous effect on the optimal selling price and the operating policies of the system.

11. Sensitivity Analysis

A sensitivity analysis was carried out to explore the effect on the optimal policies by varying the value of each parameter at a time and all parameters together. The results obtained by changing parameters by -15%, -10%. -5%, +5% +10% and +15% are tabulated in Table 4(a) and Figure 5.

The values of the total cost *K* varies from 836.112 to 896.777 and the total profit varies from 1463.870 to 1493.869 for 15% under estimation and over estimation of all parameters under consideration.

12. Conclusion

In the present model, when there is no shortage, it is observed that the net profit decreases when the deterioration parameter decreases and the selling price varies slightly. In the real market, the selling price of an item is the main factor for its demand and it optimizes the net profit. The other important factor for net profit is the replenishment time interval and the retailer's lot size is affected by the demand of the product and the demand of the product is dependent on the selling price of the product. Therefore, in order to optimize the net profit, we either reduce the price of the product or increase the replenishment cycle time. Hence, this model becomes more practicable and very useful in the business organizations dealing with domestic goods especially the perishable products. Also, it is observed that the optimal value of the selling price is more in the model without shortages than that in the model with shortages when the parameters and the costs are fixed. Even though the optimal value of the selling price is less with shortages, the optimal profit increases more than that of the model without shortages. Hence, it is observed that allowing shortages fully backlogging is a better strategy for both the customer and the stock keeper. This coincides with the natural phenomenon of increasing the productivity by allowing shortages even though some penalty is to be paid for back orders.

Acknowledgements

The authors wish to express their gratitude towards the referees for their valuable and helpful suggestions on an earlier version of the paper.

 © 2015 Jordan Journal of Mechanical and Industrial Engineering. All rights reserved - Volume 9, Number 3 (ISSN 1995-6665)

Table 4. Optimal values of the parameters of the model with variable selling price and without shortages a = 25, b= -1, H= 12

Θ	m	C_1	C_3	C	s*	w*	T_1*	Q_1*	T_2*	Q_2*	T_3*	Q_3*	T_4*	Q_4*	K*	P*
0.01	3	0.1	9	2	12.625	1.600	5.600	174.038	9.600	184.519	12	189.761	-	-	132.121	1800.400
0.02	2	0.1	9	2	12.721	1.201	6.100	107.526	12	166.035	12	-	-	-	83.1327	1791.281
0.02	3	0.1	9	2	12.860	1.626	5.626	147.648	9.626	170.569	12	178.554	-	-	154.506	1741.316
0.02	4	0.1	9	2	16.622	0.147	3.220	54.7894	6.294	79.2328	9.220	102.448	12	124.425	68.2741	1602.805
0.02	3	0.2	9	2	13.667	0.909	4.909	180.522	8.909	210.996	12	216.671	-	-	76.6083	1598.054
0.02	3	0.5	9	2	14.576	0.909	4.909	167.216	8.909	184.024	12	194.224	-	-	322.099	1438.999
0.02	3	0.1	9	2	12.860	1.626	5.626	147.648	9.626	167.549	12	172.585	-	-	154.506	1718.165
0.02	3	0.1	10	2	12.860	1.626	5.626	147.648	9.626	167.549	12	172.585	-	-	157.506	1718.165
0.02	3	0.1	9	2	12.860	1.626	5.626	147.648	9.626	167.549	12	172.585	-	-	160.605	1718.165
0.02	3	0.1	10	2	12.669	1.5	5.5	146.864	9.5	172.426	12	172.585	-	-	77.5432	1797.125
0.02	3	0.1	11	2	12.698	1.785	5.785	158.819	9.785	177.460	12	180.572	-	-	84.9028	1789.625
0.02	3	0.1	9	2	13.940	1.786	5.786	167.648	9.786	187.549	12	181.245	-	-	154.506	1718.165
0.1	3	0.1	9	2	12.940	1.786	5. 786	143.165	9. 786	167.549	12	172.585	-	-	164.409	1718.165

Table 4(a). Sensitivity of the model with variable selling price and without shortages a = 25, b= -1, H= 12

Variation Parameters		Percentage change in parameter						
		-15	-10	-5	0	5	10	15
C_3	K	878.158	874.666	870.227	866.232	862.113	858.232	854.787
	P	1466.888	1470.934	1474.222	1478.448	1482.513	1486.666	1490.982
C_1	K	863.123	864.332	865.111	866.232	867.787	868.147	869.824
	P	1481.412	1480.118	1479.404	1478.448	1477.668	1476.874	1475.006
C	K	863.132	864.006	865.418	866.232	867.555	868.999	869.542
	P	1481.209	1480.176	1479.021	1478.448	1478.121	1477.333	1477.078
θ	K	878.158	874.666	870.227	866.232	862.113	858.232	854.787
	P	1466.888	1470.934	1474.222	1478.448	1482.513	1486.666	1490.982
All Parameters	K	836.112	846.437	856.999	866.232	876.487	886.335	896.777
	P	1493.869	1488.555	1483.148	1478.448	1473.682	1468.111	1463.870

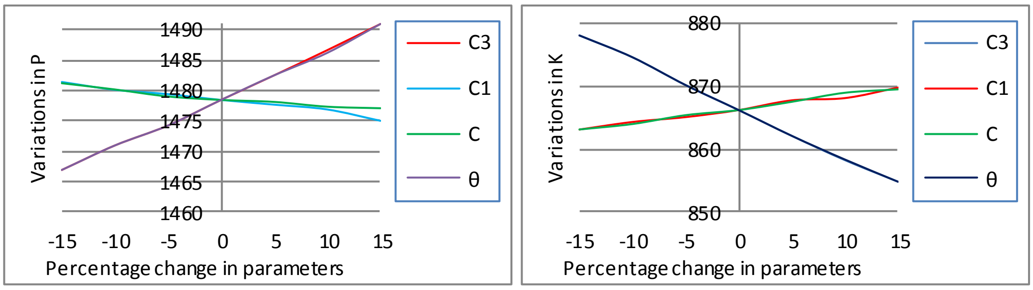

Figure 5. Graphical representation of the sensitivity with respect to the parameters of the model with variable selling price and with-out shortages when *a = 25, b= -1, H= 12.*

References

[1] T.M. Whitin, "The Theory of Inventory Management". 2nd ed. Princeton, NJ: Princeton University Press ;1957.

[2] P.M. Ghare,G.F. Schrader, "A model for an exponentially decaying inventory". Journal of Industrial Engineering, Vol. 14 (1963), 238-243.

[3] Nadoor, "Inventory systems", John Wiley and Sons, New Delh; 1975.

[4] W.A .Donaldson, "Inventory replenishment policy for a linear trend in demand -An analytical solution". Operational Research Quarterly, Vol. 28 (1977) 663-670.

[5] V.P. Goel, S.P. Aggarwal "Pricing and ordering policy with general weibull rate of deteriorating inventory". Indian J Pure. Appl. Math, Vol. 11 (1980) No. 5, 618-627.

[6] U. Dave, L.K. Patel, " (T, Si) - policy inventory model for deteriorating items with time proportional demand".Journal of Operational Research Society, Vol. 32 (1981), 137-142.

[7] S.Nahmias,"Perishable inventory theory: A review", Oper. Res. Vol. 30 (1982) No. 4, 680-708.

[8] R.S.Sachan. "(T, Si) policy inventory model for deteriorating items with proportional demand". Journal of the Operational Research Society, Vol. 35 (1984) 1013-1019.

[9] U.Dave, "A deterministic lot size inventory model with shortages and a linear trend in demand". Naval Research Logistics, Vol. 36 (1989) 507-514.

[10] Haipingxu , Hsu Pin, Ben Wang. "An economic ordering policy model for deteriorating items with time proportional demand", European Journal of Operational Research Vol. 46 (1990) 21-27.

[11] Gioswami ,K.S.Chaudhury "An EOQ model for deteriorating items with shortages and a linear trend in demand". Journal of the Operational Research Society Vol. 42 (1991) 1105-1110.

[12] T.K.Datta ,A.K. Pal "A note on a replenishment policy for an inventory model with linear trend in demand and shortages". Journal of the Operations Research Society, Vol. 43, (1992) 993-1001.

[13] S.K. Goyal , D. Morin and F.Nebebe"The finite horizon trend inventory replenishment problem with shortages". Journal of the Operational Research Society, Vol. 43 (1992) 1173-1178.

[14] A.K. Bhunia, M.Maiti. "A deterministic inventory replenishment problem for deteriorating items with time - dependent demand and shortages for the finite time Horizon", Operational Research Society of India, Vol. 34 (1997) No. l, 51-61.

[15] Goyal, S.K., & Giri, B.C." Recent trends in modeling of deteriorating inventory" European Journal of Operational Research, 134 (2001), 1-16.

[16] L.Y.Ouyang, L.-Y., Wu, K.-S., & Cheng, M.-C. "An inventory model for deteriorating items with exponential declining demand and partial backlogging" Yugoslav Journal of Operations Research, Vol. 15 (2005) No. 2, 277-288,.

[17] A.A.Alamri, & Z.T. Balkhi,"The effects of learning and forgetting on the optimal production lot size for deteriorating items with time varying demand and deterioration rates". International Journal of Production Economics, Vol. 107 (2007), 125-138.

[18] C.Y.Dye, L.Y.Ouyang, & T.P. Hsieh, "Deterministic inventory model for deteriorating items with capacity constraint and time-proportional backlogging rate". European Journal of Operational Research, Vol. 178 (2007) No. 3, 789-807.

[19] Ajanta. Roy,"An inventory model for deteriorating items with price dependent demand and time varying holding cost".Advanced Modeling and Optimization, Vol. 10 (2008), 25-37.

[20] B.Mondal, A.K. Bunia, M.Maitti, " Inventory models for defective items incorporating marketing decisions with variable production cost", Applied Mathematical Modelling Vol. 33 (2009) No. 6, 2845-2852

[21] K.Skouri, I.Konstantaras, S.Papachristos,I.Ganas,"Inventory models with ramp ype demand rate, partial backlogging and Weibull deterioration rate", European Journal of Operational Research, 192 (2009) 79-92.

[22] K.J.Chung, Huang, "An ordering policy with allowable shortage and permissible delay in payments", Appl. Math. Model. 33 (2009) 2518-2525.

[23] Nita H. Shah, Poonam Mishra **"**An EOQ model for Deteriorating items under supplier credits when demand is stock dependent" Yugoslav Journal of Operations Research Vol. 20 (2010), No. 1, 145-156 .

[24] Y.W.Wou, "Note on Inventory Model with a Stochastic Demand", Part I, LNAI 6421, Springer-Verlag, Berlin Heidelberg, (2010) 260-264.

[25] K.Jaggi Chandra,Priyanka Verma, "Two-warehouse inventory model for deteriorating items with linear trend in demand and shortages under inflationary conditions", International Journal of Procurement Management (IJPM), Vol. 3 (2010), No. 1, pp. 54-71.

[26] S.V.Uma aheswara Rao,K.Srinivasa Rao,K.Venkata Subbaiah, "Production Inventory Model for Deteriorating Items with On- Hand Inventory and Time Dependent Demand" Jordan Journal of Mechanical and Industrial Engineering, Vol. 4 (2010) No. 6, pp 739- 756

[27] K.C.Hung, "Continuous review inventory models under time value of money and crashable lead time consideration", Yugoslav Journal of Operations Research, Vol. 21 (2011) No. 2 293-306.

[28] S.W.Lin,"Inventory models with managerial policy independent of demand", European Journal of Operational Research, 211 (2011) 520-524.

[29] J.Lin,H.C.J.Chao,P. Julian, "Improved solution process for inventory model with ramp type demand under stock dependent consumption rate", Journal of the Chinese Institute of Industrial Engineers, Vol. 29 (2012) No. 4, 2219-225.

[30] T.Roy,K.S. Chaudhuri, "An EPLS model for a variable production rate with Stock price sensitive demand and deterioration", Yugoslav Journal of Operations Research, Vol. 22 (2012) No. 1, 19-30.

[31] S. Khanra , Buddhadev Mandal, Biswajit Sarkar, "An inventory model with time dependent demand and shortages under trade credit policy" Economic Modelling**,** Vol. 35, (2013) pp 349–355

[32] Karmakark, Dutta Choudhury, "Inventory models with ramp-type demand for Deteriorating items with partial Backlogging and time-varying holding cost", Yugoslav Journal of Operations Research(2013)23

[33] Asoke Kumar Bhuniaa,Ali Akbar Shaikh, "A deterministic inventory model for deteriorating items with selling price dependent demand and three-parameter Weibull distributed deterioration" , International Journal of Industrial Engineering Computations, Vol 5 (2014), pp. 497–510.

[34] Vipin Kumar, Anupma Sharma , C.B.Gupta , "Two-Warehouse Partial Backlogging Inventory Model For Deteriorating Items With Ramp Type Demand", Innovative Systems Design and Engineering ,Vol. 6 (2015) No.2.

[35] K.S.Rao and S.E.Rao,"Inventory model under permissible delay in payments and inflation with generalised Pareto lifetime", International Journal of Procure Management, Vol.8 (2015) No. 1-2.

[36] A.K. Bhunia, A.A. Shaikh ,R.K. Gupta "A study on two-warehouse partially backlogged deteriorating inventory models under inflation via particle swarm optimization" International Journal of Systems Science, Vol. 46 (2015) No. 6, pp 1036-1050

Annexure

In the study of inventory models for deteriorating items, it is observed that the conventional method is to consider invariable cycle time for all cycles in the horizon, but in many situations viz., edible oil & food processing industries, market yards etc. the commodity under consideration may be influenced by seasonality. Due to the influence of season, the cycle lengths decrease and results unequal. To have effective control and monitoring of the inventory system with deteriorating items in particular, it is needed to decrease the cycle length in an arithmetic progression subject to the minimization of the cost.

Thus successive replenishment cycle times can be obtained by

$T_1 = T,\ T_2 = 2T - w,\ T_3 = 3T - 3w$ and in general $T_i = iT - [1+2+3+...+(i-1)]w$

This implies

$$T_i = iT - \frac{i(i-1)}{2}w,\ i = 1,2,...,(m-1)$$

The length of the i^{th} cycle = $T_i - T_{1-1}$ =

$$T - \frac{i(i-1)}{2}w,\ i = 1,2,3,...,(m-1)$$

But the total horizon is H which implies

$$\sum_{i=1}^{m}\left[T-(i-1)w\right] = H$$

$$\Rightarrow T + (T-w) + ... + \left[T-(m-1)w\right] = H$$

Therefore $T = (m-1)\frac{w}{2} + \frac{H}{m}$

Inventory model

Let $I_i(t)$ denote the amount of inventory at time t, during the i^{th} cycle ($(T_{i-1} \le t \le t_i;\ i-1,2,3,...,m)$. The rate of change in inventory at time t during the i^{th} cycle is due to deterioration which amounts to $\theta I_i(t)$) and demand rate $\lambda(s) = a + bs$. Therefore the differential equation governing the system during i^{th} cycle is

$$\frac{d}{dt}I_i(t) + \theta I_i(t) = -(a+bs);\ T_{i-1} \le t \le t_i\ (i=1,2.....,m) \quad \text{(i)}$$

The rate of change in inventory at time t during the cycle $(t_i \le t \le T_i;\ i-1,2,3,...,m-1)$ is due to unfulfilled demand as a consequence of backlogged shortages.. Theretore the differential equation governing the system during i^{th} cycle is

$$\frac{d}{dt}I_i(t) = -(a+bs);\ t_i < t < T_i\ (i=1,2.....,m-1) \quad \text{(ii)}$$

with the initial conditions $I_i(t) = 0$ at $t = t_i$ and $a > 0, b < 0$.

Solution of the equation (i)

Consider the equation (i) as

$$\frac{d}{dt}I_i(t) + \theta I_i(t) = -(a+bs);$$

$$T_{i-1} \le t \le t_i\ (i=1,2.....,m).$$

This is a linear ordinary differential equation of first order and first degree.

Therefore $I_i(t)e^{\int\theta dt} = \int -(a+bs)e^{\int\theta dt}dt$

$$\Rightarrow I_i(t)e^{\theta t} = \int -(a+bs)e^{\theta t}dt$$

$$\Rightarrow I_i(t)e^{\theta t} = -\frac{(a+bs)e^{\theta t}}{\theta} + C_1$$

Using the initial condition $I_i(t) = 0$ at $t = t_i$ we have

$$0 = -\frac{(a+bs)e^{\theta t_i}}{\theta} + C_1$$

Implies

$C_1 = \frac{(a+bs)e^{\theta t_i}}{\theta}$ .Using the value we have

$$\Rightarrow I_i(t)e^{\theta t} = -\frac{(a+bs)e^{\theta t}}{\theta} + \frac{(a+bs)e^{\theta t_i}}{\theta}$$

$$\Rightarrow I_i(t) = \frac{(a+bs)}{\theta}\left(e^{\theta(t_i - t)} - 1\right);$$

$$T_{i-1} \le t \le t_i\ (i=1,2.....,m) \quad \text{(iii)}$$

Again consider the equation

$$\frac{d}{dt}I_i(t) = -(a+bs);\ t_i < t < T_i\ (i=1,2.....,m-1).$$

This is an ordinary differential equation of first order and first degree.

Therefore $I_i(t) = -(a+bs)t + C_2$

Using the initial condition $I_i(t) = 0$ at $t = t_i$ we have

$0 = -(a+bs)t_i + C_2$.

This implies $C_2 = (a+bs)t_i$

Substituting the value of C_2 then

$I_i(t) = -(a+bs)t + (a+bs)t_i$

$$\Rightarrow I_i(t) = (a+bs)(t_i - t), t_i \le t < T_i, (i=1,2........, m\text{-}1) \quad \text{(iv)}$$

Calculation of the cost function

To find the total cost function, we consider various costs like Ordering Cost C_3, Holding Cost C_1, Unit Cost or Purchasing Cost $C$and Shortage Cost C_2.

Ordering cost: According to the assumptions of the model Ordering Cost per replenishment is C_3. Hence for all the 'm' cycles the ordering cost = $m.\ C_3$ **… (A)**

Holding cost: To find the holding cost we calculate

Inventory during the i^{th} cycle = $\int_{T_{i-1}}^{t_i} I_i(t)dt$

$$= \int_{T_{i-1}}^{t_i} \frac{(a+bs)}{\theta}\left(e^{\theta(t_i - t)} - 1\right)dt$$

Inventory during the last cycle = $\int_{T_{m-1}}^{H} I_i(t)dt$

$$= \int_{T_{m-11}}^{H} \frac{(a+bs)}{\theta}\left(e^{\theta(H-t)} - 1\right)dt$$

By making use of these equations we have

The holding cost during the i^{th} cycle = C_1

$$\left[\int_{T_{i-1}}^{t_i} \frac{(a+bs)}{\theta}\left(e^{\theta(t_i - t)} - 1\right) dt\right]$$

And the holding cost during the last cycle = C_1

$$\left[\int_{T_{m-1}}^{H} \frac{(a+bs)}{\theta}\left(e^{\theta(H - t)} - 1\right) dt\right]$$

Hence the total holding cost of the inventory is given by

$$\sum_{i=1}^{m-1} C_1\left[\int_{T_{i-1}}^{t_i} \frac{(a+bs)}{\theta}\left(e^{\theta(t_i - t)} - 1\right) dt\right] + \left[\int_{T_{m-1}}^{H} \frac{(a+bs)}{\theta}\left(e^{\theta(H - t)} - 1\right) dt\right] \quad \text{(B)}$$

Unit cost: To find the unit cost, we calculate the ordering quantity Q_i in the i^{th} cycle. It is given by

Q_i = Deterioration in the i^{th} cycle +Demand in the i^{th} cycle + Backlog demand in the $(i-1)^{st}$ cycle

$$= \theta \int_{T_{i-1}}^{t_i} I_i(t)\,dt + \int_{T_{i-1}}^{t_i}(a+bs)\,dt + \int_{t_{i-1}}^{T_{i-1}}(a+bs)\,dt$$

Hence the total unit cost of the inventory is given by

$$\sum_{i=1}^{m}\left[\theta \int_{T_{i-1}}^{t_i} I_i(t)\,dt + \int_{T_{i-1}}^{t_i}(a+bs)\,dt + \int_{t_{i-1}}^{T_{i-1}}(a+bs)\,dt\right] \quad \text{(C)}$$

The shortage cost in the i^{th} cycle $C_2 \int_{t_i}^{T_i} I_i(t)\,dt$

$$= C_2 \int_{t_i}^{T_i} (a+bs)(t_i - t)\,dt$$

Hence the total shortage cost of the inventory is given by

$$\sum_{i=1}^{m-1} C_2 \int_{t_i}^{T_i} (a+bs)(t_i - t)\,dt \quad \text{(D)}$$

By adding all the costs given in equations (A), (B), (C) and (D) the total Cost function is given by

$$k(m,t_i,T_i) = m.C_3 + \sum_{i-1}^{m-1}\left[(C_1 + C\theta)\int_{T_{i-1}}^{t_i} I_i(t)\,dt + C_2\int_{t_i}^{T_i} I_i(t)\,dt\right] + (C_1 + C\theta)\int_{T_{m-1}}^{H} I_m(t)\,dt + C_2 \sum_{i=1}^{m}\int_{t_i}^{T_i} I_i(t)\,dt$$

$$= m.C_3 + \sum_{i-1}^{m-1}\left[(C_1 + C\theta)\int_{T_{i-1}}^{t_i} \frac{a+bs}{\theta}\left(e^{\theta(t_i - t)} - 1\right) dt\right] + (C_1 + C\theta)\int_{T_{m-1}}^{H} \frac{a+bs}{\theta}\left(e^{\theta(H-1)} - 1\right) dt + C_2 \sum_{i=1}^{m}\int_{t_i}^{T_i}(a+bs)(t_i - t)\,dt \quad \text{(v)}$$

المملكة الأردنية الهاشمية

الجامعة الهاشمية

المجلة الأردنية
للهندسة الميكانيكية والصناعية

JJMIE

مجلة علمية عالمية محكمة

تصدر بدعم من صندوق البحث العلمي

http://jjmie.hu.edu.jo/

ISSN 1995-6665

المجلة الأردنية للهندسة الميكانيكية والصناعية

مجلة علمية عالمية محكمة

المجلة الأردنية للهندسة الميكانيكية والصناعية: مجلة علمية عالمية محكمة تصدر عن الجامعة الهاشمية بالتعاون مع صندوق دعم البحث العلمي في الأردن

ترسل البحوث إلى العنوان التالي

رئيس تحرير المجلة الأردنية للهندسة الميكانيكية و الصناعية

الجامعة الهاشمية

كلية الهندسة

قسم الهندسة الميكانيكية

الزرقاء - الأردن

هاتف : 3903333 5 00962 فرعي 4537

Email: jjmie@hu.edu.jo

Website: www.jjmie.hu.edu.jo